PARALLEL COORDINATES : *VISUAL* Multidimensional Geometry and its Applications

Alfred Inselberg(©1992, 2004)[1]

School of Mathematical Sciences
Tel Aviv University, Israel
aiisreal@post.tau.ac.il

[1]Senior Fellow San Diego SuperComputing Center & Multidimensional Graphs Ltd, Raanana 43556, Israel

Chapter 1

Planes, p-flats & Hyperplanes

1.1 Planes in $\mathbb{R}^3$

1.1.1 Vertical Line Representation

$\mathcal{A}$ hyperplane in $\mathbb{R}^N$ can be translated to one which contains the origin, that is an $N-1$-dimensional linear subspace of $\mathbb{R}^N$. Since $\mathbb{R}^{N-1}$ can be represented in $\|$-coords by $N-1$ vertical lines and a polygonal line representing the origin of the $\|$-coordinate system, it is reasonable to expect a similar representation for hyperplanes in $\mathbb{R}^N$.

$\mathcal{W}$e start with an intuitive discusion for $\mathbb{R}^3$. Consider a plane π as shown in Fig. 1.1,

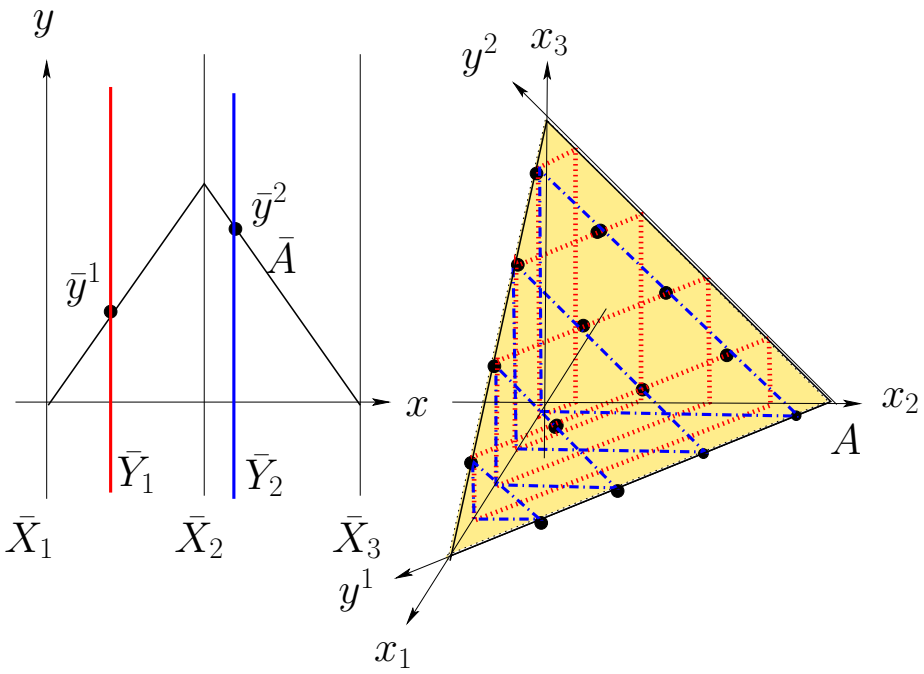

Figure 1.1: A plane π in $\mathbb{R}^3$ represented by two vertical lines and a polygonal line. This is a planar coordinate system with the polygonal line representing the origin.

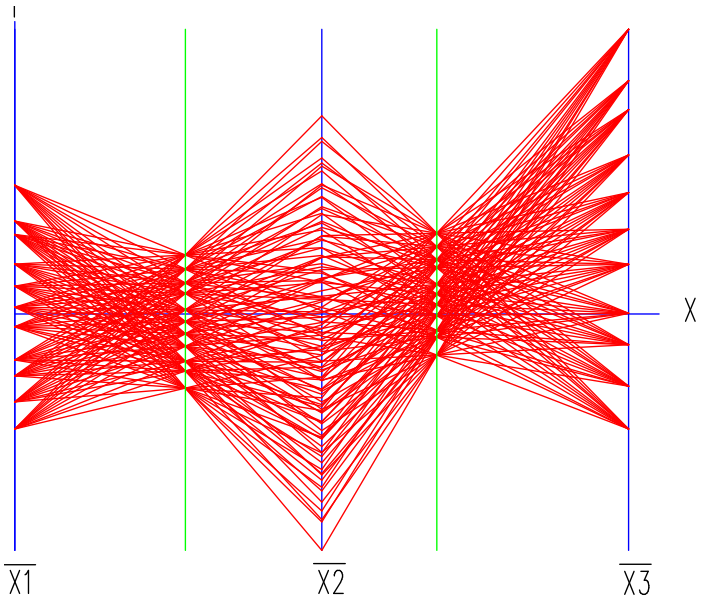

Figure 1.2: A set of coplanar points in $\mathbb{R}^3$ with the two vertical lines pattern.

intersecting the x_1x_2-plane at the line y^1 and the x_2x_3-plane at the line y^2 with $A = y^1 \cap y^2$. The lines y^i , $i = 1, 2$ being lines in $\mathbb{R}^3$ are represented by two points, $\bar{y}^i_{12}$, $\bar{y}^i_{23}$ each as shown. Next we construct a non-orthogonal coordinate system on π using the y^i as axes, consisting of the lines parallel to y^1 and the lines parallel to y^2. Any point $P \in \pi$ can be specified as the intersection of two lines one parallel to y^1 and the other to y^2. The family of lines parallel to y^1 are represented by a vertical line $\bar{Y}_1$ containing the point $\bar{y}^1_{12}$. Similarly the vertical line $\bar{Y}_2$ containing the point $\bar{y}^2_{23}$ represents the lines parallel to y^2. Strictly speaking the vertical lines $\bar{Y}_i$ represent the *projections* on the x_1x_2 and x_2x_3 planes, respectively, of the two families of parallel lines. Therefore, the vertical lines represent two such families of parallel lines on **any** plane parallel to π. By choosing a point, say A, as the origin we obtain a coordinate system specific to π. So the plane can be represented by two vertical lines and a polygonal line. Clearly the same argument applies in any dimension and, therefore, a hyperplane in $\mathbb{R}^N$ can be represented by a N-1 vertical lines and a polygonal line representing one of its points [3]. Conversely, a set of coplanar points chosen on a grid such as the one formed by lines parallel to a coordinate system, is represented by polygonal lines with a pattern specifying two vertical lines as shown in Fig. 1.2.

About the time these patterns were being discovered, word got around and we were requested to visually explore for relations that may exist in a set of industrial data consisting of several thousand records with 8 variables. This dataset is plotted in parallel coordinates and shown in Fig. 1.3. The pattern between the R111 and R112 axes, which for clarity is magnified and shown in Fig. 1.4, resembles one of vertical lines formed in Fig. 1.2. Yet for this pattern to represent a set of coplanar points at least **two** and not one vertical lines are needed, for even the plane with minimal dimensionality is in R^3. Still the variables R111 and R112 are linearly interelated, and there must be another variable say X also linearly related to R111 and R112 as is clear from Fig. 1.4 (see also the first exercise below). All this suggested that an important variable was not being measured. With these hints a search was

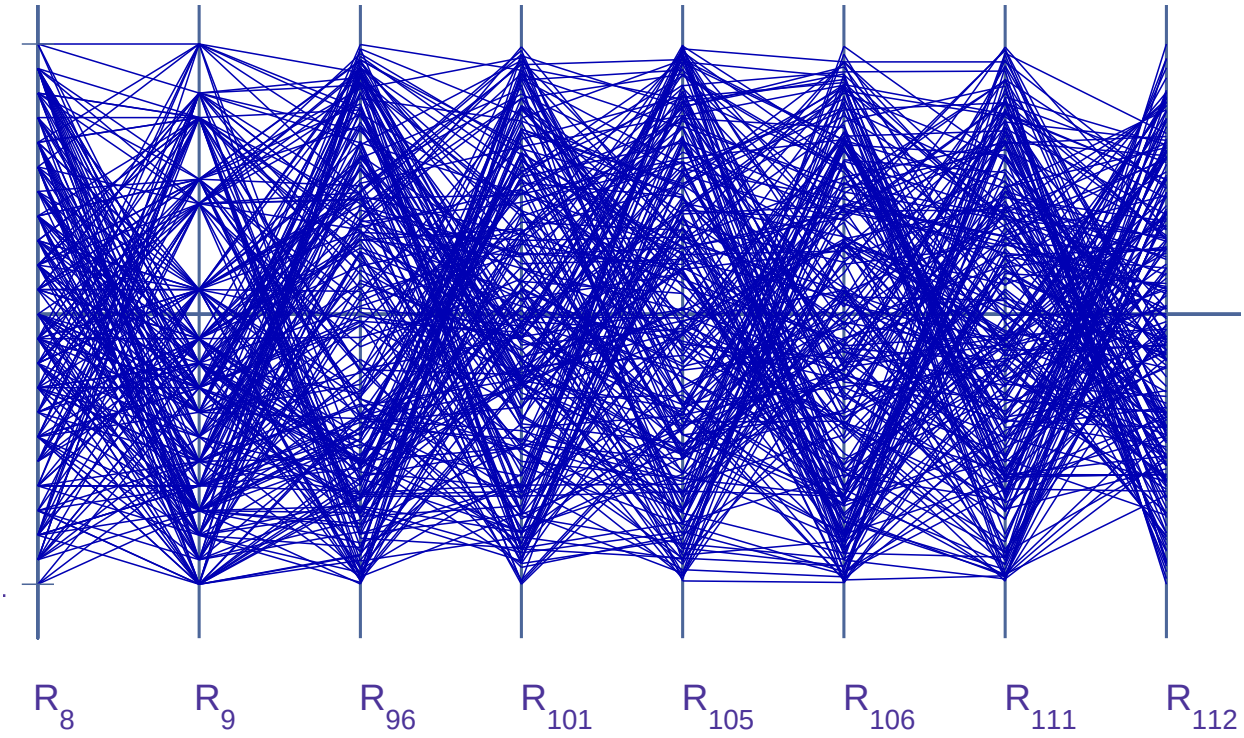

Figure 1.3: Industrial data with a "vertical line" pattern between R111 and R112 axes.

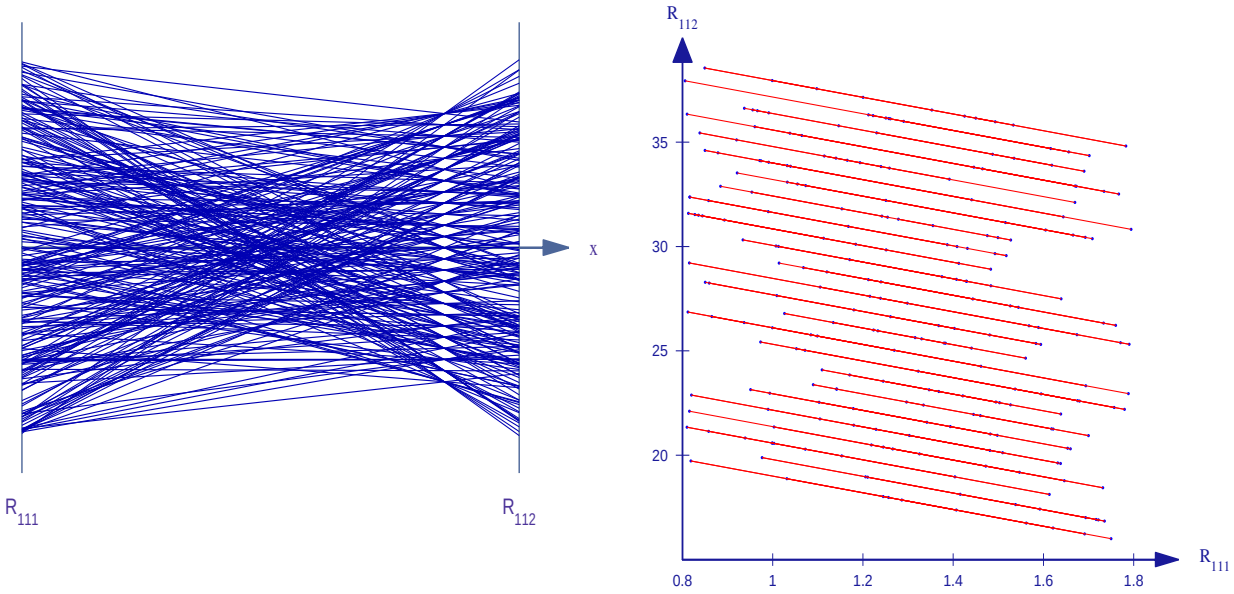

Figure 1.4: The portion between the R111 and R112 axes is magnified (left).

This suggest that there is linear relation between R111, R112 and an unknown parameter as is also indicated on the Cartesian coords plot on the right.

mounted and the missing variable was found. This, of course, was a stroke of good fortune and an instance of a favorite stochastic theorem i.e. "You can't be unlucky all the time". Let us return from our digression. Before this is done, it is worth distinguishing the vertical line pattern between the R8 and R9 axis with that between the R111 and R112. On the R8 axis and lower part of R9 axis the data is equally-spaced, while this is not the case with the last two axes. We can also obtain this representation using the theory of envelopes, starting with the description:

$$\pi : c_1x_1 + c_2x_2 + c_3x_3 = c_0 \tag{1.1}$$

Rather than proceeding completely formally, here we can find the envelope in a way which provides more insight. To determine a point $P \in \pi$ two coordinates must be specified. If one coordinate, say $x_3 = \alpha$ which specifies a plane π' parallel to the x_1x_2-plane, a particular line, $\ell'(\alpha) = \pi \cap \pi'$, on the plane π is fixed and is in fact one of the lines parallel to y^1 – see Fig. 1.5. It has the representation:

$$\bar{\ell}'(\alpha) : \left\{ \begin{array}{rcl} \bar{\ell}'_{23}(\alpha) & = & (2\,,\,\alpha) \\ \bar{\ell}'_{12}(\alpha) & = & (\frac{c_2}{c_1+c_2}\,,\,\frac{c_0-c_3\alpha}{c_1+c_2}) \end{array} \right. \tag{1.2}$$

since

$$\ell'(\alpha) : \left\{ \begin{array}{rcl} \ell'_{23}(\alpha) & : & x_3 = \alpha \\ \ell'_{12}(\alpha) & : & c_1x_1 + c_2x_2 = c_0 - c_3\alpha \end{array} \right. \tag{1.3}$$

where as usual the distance between the parallel axes is one unit. Returning to Fig. 1.2, each vertical line is formed by a set of points. On the $\bar{Y}_1$-axis these points are the $\bar{\ell}'_{12}(\alpha)$. The polygonal lines intersecting at such a point represent points on the corresponding line $\ell'_{12}(\alpha)$. Together these intersections provide one of the two vertical lines in the representation of π. As we know from Chapter **??**, for each α, $\bar{\ell}'_{12}(\alpha)$ is the *envelope* of a set of polygonal lines representing points on a line. As α varies the $\bar{\ell}'_{12}(\alpha)$ form the vertical line $\bar{Y}_1$ since, as one

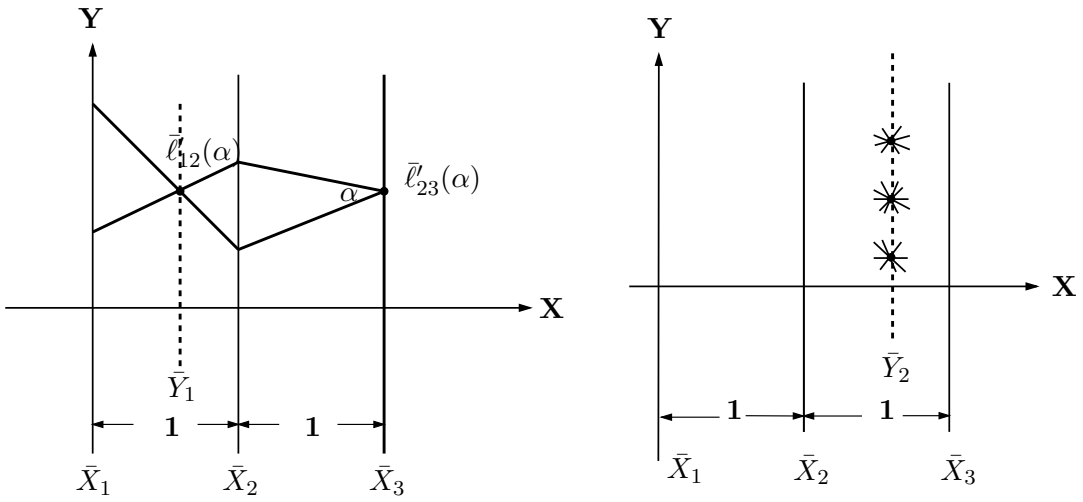

Figure 1.5: The construction of $\bar{Y}_1$ (left) the first and $\bar{Y}_2$ (right) second vertical axes.

Start with a line on π parallel to the y^1 and y^2 axes respectively.

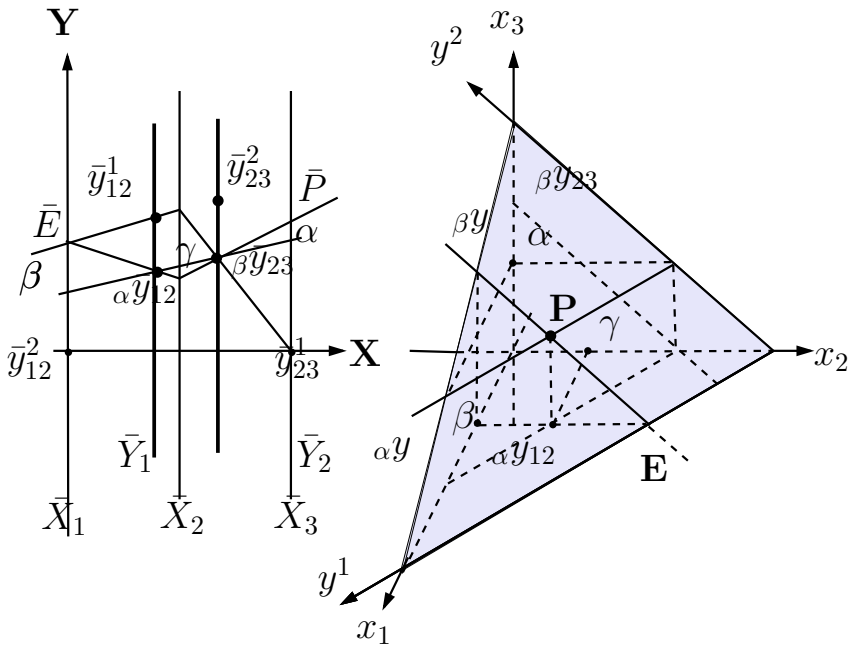

Figure 1.6: Constructing a point on a plane.

can see from eq. (1.2), their x-coordinate is a constant (independent of α). Strictly speaking, the points $\bar{\ell}'_{23}(\alpha)$ also vary with α and fall on the $\bar{X}_3$-axis. Since this would also occur for any other plane and the $\bar{X}_3$-axis already exists, it does not contribute any information on the specific plane π, so typically it is not considered as part of the representation of a particular plane. This takes care of the lines on π parallel to the y^1-axis. In exactly the same way it is found that the vertical line $\bar{Y}_2$ represents the lines parallel to the y^2-axis.

1.1.2 Planar Coordinates

$\mathcal{W}$hat has effectively happened is that a coordinate system is constructed on the plane π consisting of two vertical lines and a polygonal line as an origin. The plane π is after all a *2-flat* – i.e. it can be determined by 3 points. In general an *n-flat* is a linear manifold (translate of a linear space) that is determined by n+1 points. For an excellent short book on N-dimensional Geometry see [5]. Now we would like to use this coordinate system to specify points on the π. With reference to Fig. 1.7, consider a point $P \in \pi$. From it's $(x_1\,, x_2\,, x_3)$ coordinates we want to find it's y^1 and y^2 coordinates or equivalently to express $P = \ell^1 \cap \ell^2$ where $\ell^1\,, \ell^2$ are lines on π and parallel to the y^1 and y^2 axes respectively. So we look at P_{12}, the projection of P on the x_1x_2-plane and construct the line through P_{12} parallel to y^1. This line is represented by the point $\bar{\ell}^1_{12} = \bar{P}_{12} \cap \bar{Y}_1$ on the $\bar{Y}_1$ axis. Similarly we obtain $\bar{\ell}^2_{23} = \bar{P}_{23} \cap \bar{Y}_2$ on the $\bar{Y}_2$ axis, where P_{23} is the projection of P on the x_2x_3-plane. Notice how careful tracking of the indices is already helpful in the construction. The pair $(\bar{\ell}^1_{12}\,,\, \bar{\ell}^2_{23})$ are the *planar coordinates* of $\bar{P}$ in terms of the $\bar{Y}_1$ and $\bar{Y}_2$ axes. An interesting consequence is that a line $\ell \subset \pi$ can be represented by a single point $\bar{\eta}$ in terms of the $\bar{Y}_1$,$\bar{Y}_2$ coordinate system. Of course it is still represented by two points, the $\bar{\ell}$s, in terms of the original $\bar{X}_i$ $i = 1, 2, 3$ Fig. 1.7.

Theorem 1.1.1 For a line $\ell \subset \pi \subset \mathbb{R}^3$ the points $\bar{\ell}_{12}\,,\, \bar{\ell}_{23}$ and $\bar{\eta}$ are collinear.

Proof: Step 1 With reference to the figure below, let P_1 , $P_2 \in \ell$. The two lines AB and $A'B'$ joining the planar coordinates of $\bar{P}_1$ and $\bar{P}_2$ intersect at $\bar{\eta} = AB \cap A'B'$.

Step 2 The two $\triangle$s ABC and $A'B'C'$ formed between $\bar{Y}_1$ and $\bar{Y}_2$ are in perspective with respect to the ideal point in the vertical direction.

Step 3 The sides AB and CB are portions of $\bar{P}_2$ and corresponding to $A'B'$ and $C'B'$ which are portions of $\bar{P}_1$.

Step 4 By Step 3, $\bar{\ell}_{12} = AC \cap A'C'$ and $\bar{\ell}_{23} = BC \cap B'C'$.

Step 5 By Step2 through Step 4 and Desargues Theorem $\bar{\ell}_{12}$, $\bar{\ell}_{23}$ and $\bar{\eta}$ are all on the same line $\bar{L}$. ■

Of course, by the *3 point collinearity property* of Chapter **??** the point $\bar{\ell}_{13}$ is also on $\bar{L}$.

Corollary 1.1.2 *The rotation of a plane in $\mathbb{R}^3$ about a line corresponds to a translation of a point on a line.*

Proof: With reference to the Fig. 1.8 let $\ell \subset \pi \subset \mathbb{R}^3$. Rotate π about ℓ to a new position $\pi*$. Let $\bar{\ell}_{12}$, $\bar{\ell}_{23}$ represent ℓ in the $\bar{X}_1$, $\bar{X}_2$, $\bar{X}_3$ - coords and $\bar{\eta}$, $\bar{\eta}*$ in the $\bar{Y}_1$, $\bar{Y}_2$ and $\bar{Y}_1*$, $\bar{Y}_2*$ - coordinate systems respectively. By the theorem, $\bar{\ell}_{12}$, $\bar{\ell}_{23}$ and $\bar{\eta}$ are on a line $\bar{L}$. Also, $\bar{\ell}_{12}$, $\bar{\ell}_{23}$ and $\bar{\eta}*$ are on the line $\bar{L}$. That is the rotation of π about ℓ corresponds in $\|$-coords a translation of the point $\bar{\eta}$ on $\bar{L}$. ■

This is the 3-D analogue of *(rotation of a line around a point)* $\rightarrow$ *(translation of a point along a line)* in 2-D and corresponds to the *point* $\leftrightarrow$ *plane* duality in $\mathbb{P}^3$. Let us explore the

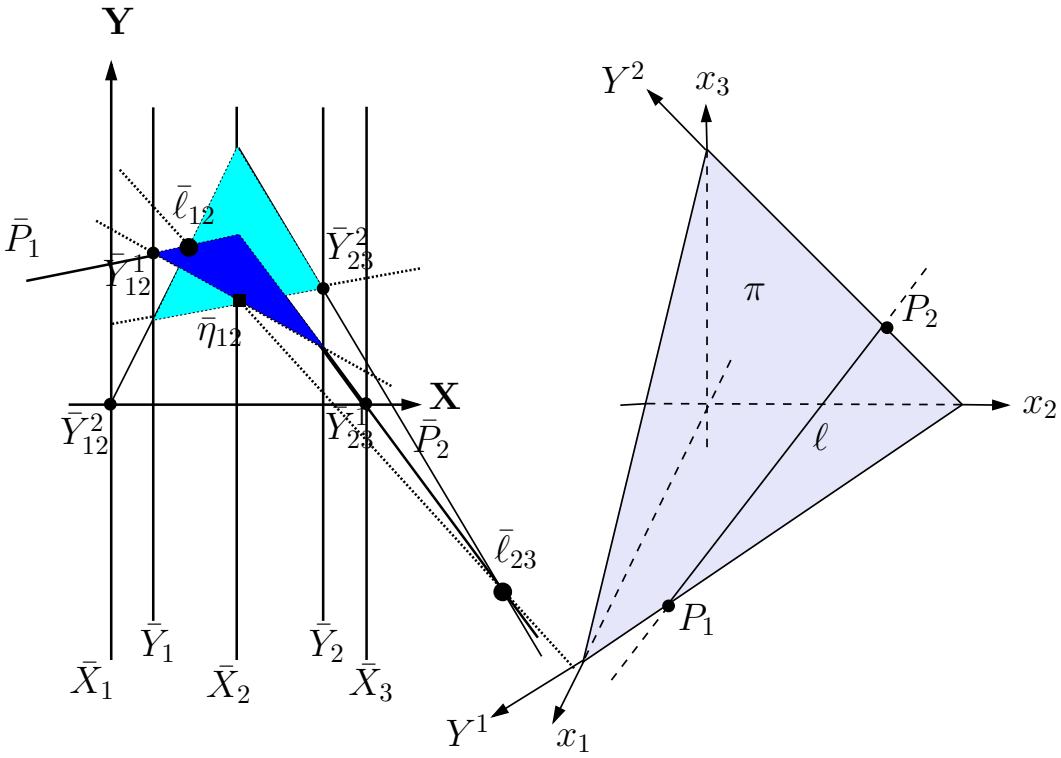

Figure 1.7: A line ℓ on a plane π is represented by one point $\bar{\eta}_{12}$.

This is in terms of the planar coordinates $\bar{Y}_1$ and $\bar{Y}_2$. The point $\bar{\eta}_{12}$ collinear with the two points $\bar{\ell}_{12}$ and $\bar{\ell}_{23}$.

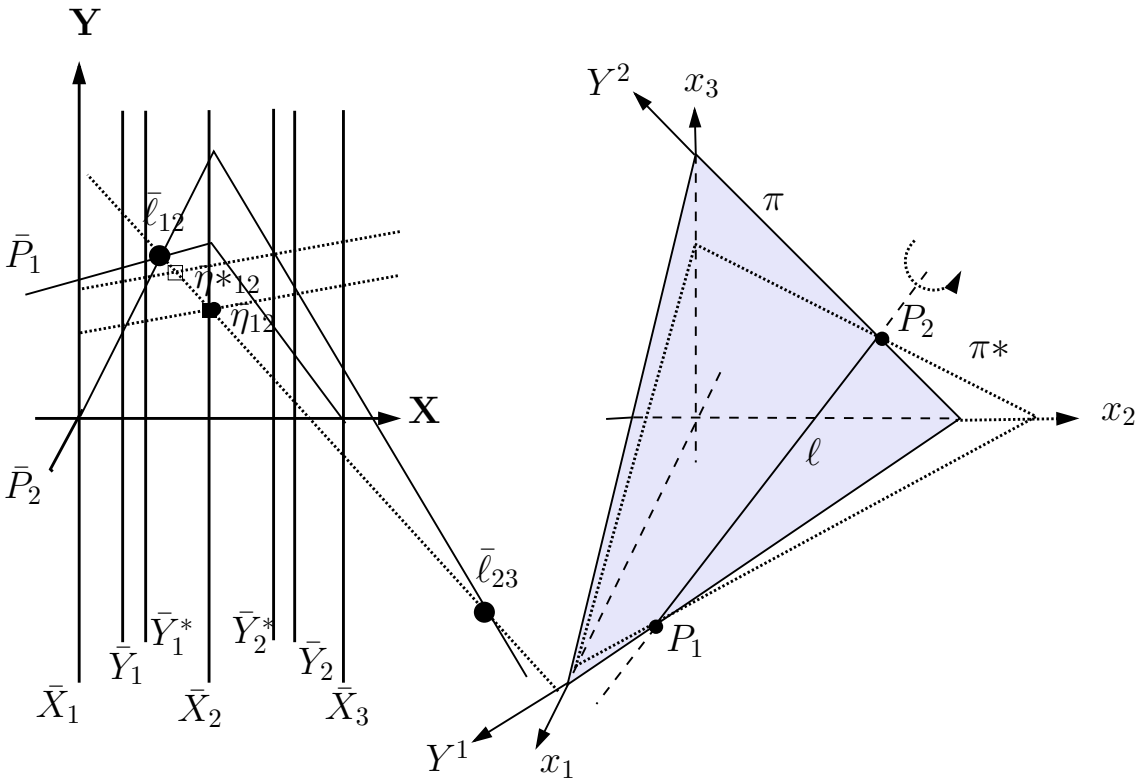

Figure 1.8: Rotation of a plane about a line ↔ Translation of a point along a line.

computation involved where ℓ is given by:

$$\ell : \begin{cases} \ell_{12} & : \quad x_2 = m_2 x_1 + b_2 \\ \ell_{23} & : \quad x_3 = m_3 x_2 + b_3 \end{cases} . \tag{1.4}$$

There exists a one parameter, say k, family[1] of planes containing ℓ. In fact, the equation of any one of the planes in the family is given by:

$$\pi : (x_3 - m_3 x_2 - b_3) + k(x_2 - m_2 x_1 - b_2) = 0 \; . \tag{1.5}$$

It can be verified that in Cartesian coordinates :

$$\bar{\eta}_{12} = (\frac{m_3^2 - 2m_3 - k^2}{m_3^2 - m_3 + k^2(m_2 - 1)} \;\; , \;\; - \frac{b_2 k^2 + m_3 b_3}{m_3^2 - m_3 + k^2(m_2 - 1)}) \tag{1.6}$$

Every value of k corresponds to a position (of the rotated plane) π and, in turn, about a position (of the translated point) η along the line formed by the points $\bar{\ell}_{12}$ and $\bar{\ell}_{23}$.

The generalization for $\mathbb{R}^N$ being straight-forward is not covered here (see [3]).

[1] In the language of Projective Geometry this is called a *pencil* of planes on the line.

Fun & Games with the ILM

Open the ILM2, the plane and line in Cartesian coords are on the right and its representation by two vertical axes $\bar{Y}_1, \bar{Y}_2$ on the left
The line is specified by P_1, P_2 and represented by $\bar{\ell}_{12}, \bar{\ell}_{23}$ in $\mathbb{R}^3$ are on a line $\bar{L}$ with the point representing $\bar{\eta}_{12}$ respect to $\bar{Y}_1, \bar{Y}_2$ axes for the plane.

For some experimentation: slide the point $\bar{\pi}_{123}$ along $\bar{L}$
notice the translation of $\bar{\eta}_{12}$ and corresponding rotation of the plane
Change the line and/or plane and repeat.
Click other buttons and experiment.

Exercises

1. The pattern between the R111 & R112 axes in figures. 1.3 and 1.4 begs a question. What if a different permutation of the axes was chosen? Whereas the coplanarity information would still be preserved the the "vertical line pattern" would not be seen. Was it fortuitous that the "right" axes permutation was chosen to plot the data? It is not difficult to show that for N variables, there are $O(N/2)$ "cleverly" chosen permutations that provide all possible *adjacent pair* of axes. For example, for $N = 6$ three such permutations are (just showing the subscripts of the $\bar{X}_i$: 126354 , 231465 , 342516 [6]). Returning to the example are 4 such permutations one of which has the coplanarity pattern.

   (a) Prove this permutation result – Hint construct an undirected graph whose vertices are variables, and edges between a pair of vertices designate that the corresponding vertices are adjacent in a particular permutation.

   (b) Find an algorithm for computing these special $O(N/2)$ permutations

   (c) Generalize this result for adjacent *triples*

   (d) Generalize this result for adjacent *p-tuples*

2. Given 3 non-collinear points in $\mathbb{R}^3$ find an algorithm for constructing in ∥-coords a set of planar coordinates for the plane determined by the 3 points.

3. Construct a set of planar coordinates for a plane π perpendicular to one of the principal 2-planes (i.e. π being parallel to one of the orthogonal axes).

4. Given a set of planar coordinates for a plane π find an algorithm for constructing a plane π' perpendicular to it.

5. In ∥-coords find an algorithm for determing the intersection of 2 planes.

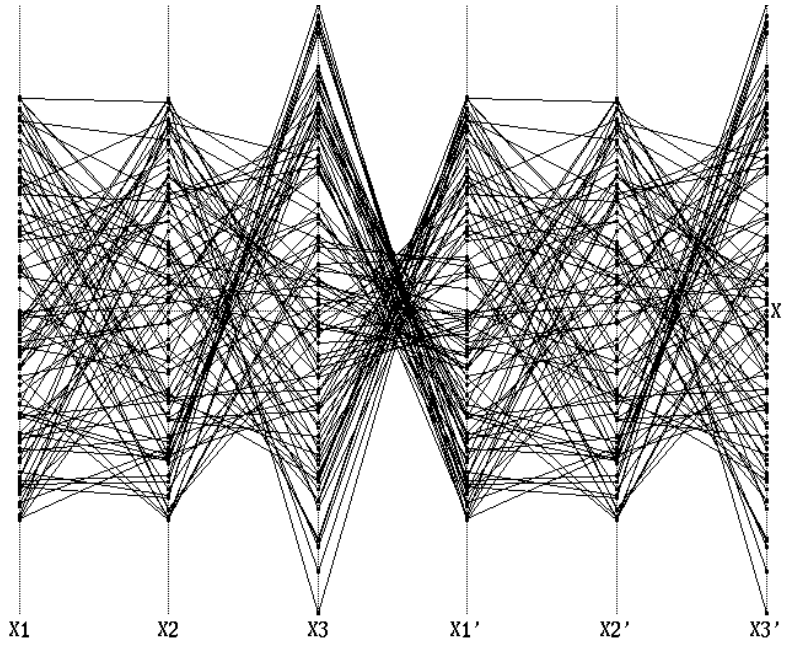

Figure 1.9: Randomly selected coplanar points in $\mathbb{R}^3$.

It is represented by the polygonal lines on the first 3 axes.

6. Given a plane π and a line ℓ, provide an algorithm which in ||-coords determines whether or not $\ell \subset \pi$.

7. Given a plane π and a point P, provide an algorithm for determining whether P is below, on or above the plane. For the notion of above/below consider π partitioning $\mathbb{R}^3$ in two half-spaces which need to be distinguished. All points in one half-space are "above" etc.

8. Provide an algorithm in ||-coords for intersecting a line with a plane.

9. Verify,

   (a) Eq. (1.5),

   (b) Eq. (1.6).

1.2 Representation by Indexed Points

$\mathcal{T}$he representation of a plane in terms of vertical lines is basically the representation of a specific coordinate system on the plane. With this representation the coplanarity of a set of points could only be checked visually if the points were on a rectangular grid as in Fig. 1.2. In Fig. 1.9 the polygonal lines on the $\bar{X}_1 \,.\, \bar{X}_2 \,.\, \bar{X}_3$ axes represent randomly sampled points on a plane π in $\mathbb{R}^3$ are shown. There is no discernible pattern. Is there a ||-coords' "pattern" associated with coplanarity of randomly selected points?

A new approach is called for [2]. Describing even a simple 3-dimensional object like a room, it in terms of its points is just not intuitive. The description it in terms of cross-sections including the boundary planes help us visualize the object. Pursuing the analogy, it is proposed to describe p-dimensional objects in terms of their (p-1)-dimensional subsets rather than their points. So the representation of a plane π is attempted in terms of the *lines* it contains. Taking pairs of polygonal lines ℓ shown in Fig. 1.9 the representation of the corresponding line $\ell \subset \pi$ is constructed. The result in Fig. 1.10 is stunning; the lines joining the pairs of points $\bar{\ell}_{12}, \bar{\ell}_{23}$ in turn determine a pencil of lines on a point and this is characteristic of coplanarity. Let us explore it.

1.2.1 The family of "Super-Planes" $\mathcal{E}$

$\mathcal{B}$ehind the striking pattern in Fig. 1.10 lurks a very special subspace of $\mathbb{R}^N$. Until now the $\|$-coords axes were taken equidistant with the y and $\bar{X}_1$ axes coincident. This was a matter of convenience which has served us well until now. The time has come to look at the general setting shown in Fig. 1.11 the position of the $\bar{X}_i$ specified by the directed (i.e. signed) distance d_i with the stipulation that for some $i \neq j$, $d_i \neq d_j$. We consider the set of points $P \in \mathbb{R}^N$ whose representation in $\|$-coords collapses to a straight line. That is, $\bar{P} \ : \ y = mx + b$ and a specific choice of (m, b) the corresponding point is :

$$P = (md_1 + b,\, md_2 + b, \ldots, md_N + b) = m(d_1,\, d_2, \ldots, d_N) + b(1, \ldots, 1)\ . \qquad (1.7)$$

For $m, b \in \mathbb{R}$ this collection of points forms the subspace of $\mathbb{R}^N$ spanned by the two N-tuples $(d_1,\, d_2, \ldots, d_N)$, $(1, \ldots, 1)$ on the vector $\mathbf{u}$ from the point $(0, 0\,, ...,\, 0)$ to $(1, 1\,, \ldots\,, 1)$ the full line denoted by u. We acknowledge the splendid role they play in our development by naming them *super-planes*. The family of super-planes generated by all the axes spacing is denoted

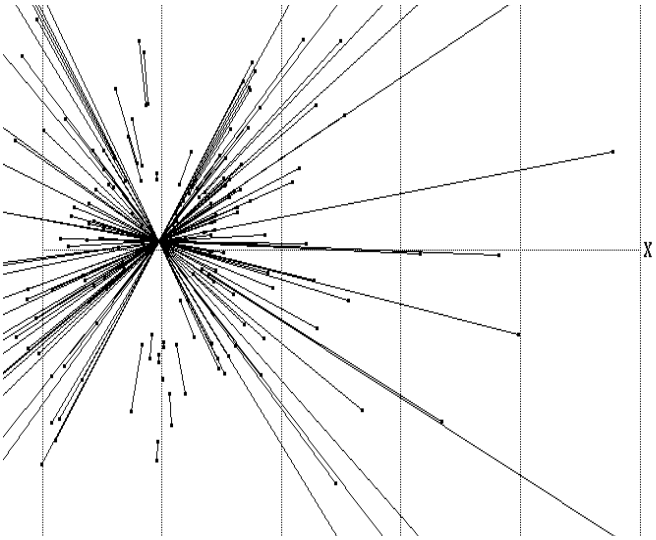

Figure 1.10: Coplanarity!

A pencil of lines on a point is formed by joining the pairs of points representing lines on a plane.

by $\mathcal{E}$. The situation is especially interesting in $\mathbb{R}^3$ where the super-planes are:

$$\pi^s = \{m(d_1,\, d_2,\, d_3) + b(1,\, 1,\, 1) \mid m,\, b \in R\}\ ,$$

and whose equation

$$\pi^s\ :\ (d_3 - d_2)x_1 + (d_1 - d_3)x_2 + (d_2 - d_1)x_3 = 0. \tag{1.8}$$

can be obtained by using numerically convenient values (i.e. $m = b = 0$, $m = 0\,, b = 1$, $m = 1, b = 0$). It describes the *pencil* on the line u of planes each specified by the axes spacing. As for eq. (1.5), it can be re-written as a one parameter family :

$$\pi^s\ :\ (x_3 - x_2) + k(x_2 - x_1) = 0,\ \ k = \frac{d_2 - d_3}{d_2 - d_1} \tag{1.9}$$

with the ratio k determining the particular plane. With the y and $\bar{X}_1$ axes coincident and the standard axes spacing $d_1 = 0\,,\, d_2 = 1\,,\, d_3 = 2$ the super-plane (sometimes referred as the "first super-plane") is:

$$\pi^s_1 : x_1 - 2x_2 + x_3 = 0\ , \tag{1.10}$$

the subscript 1 distinguishes it from the others formed with different axes spacing. The important property from Chapter **??** can now be restated in terms of π^s_1.

Theorem 1.2.1 (3 point-collinearity) *For any line $\ell \subset \mathbb{R}^N$ the points $\bar{\ell}_{ij}$, $\bar{\ell}_{jk}$, $\bar{\ell}_{ik}$, where the i, j, k are distinct integers $\in [1, 2, \ldots, N]$, are on a line $\bar{L}$ where $L = \ell \cap \pi^s_1$.*

This is the backbone of the recursive (in the dimension) construction algorithm which follows.

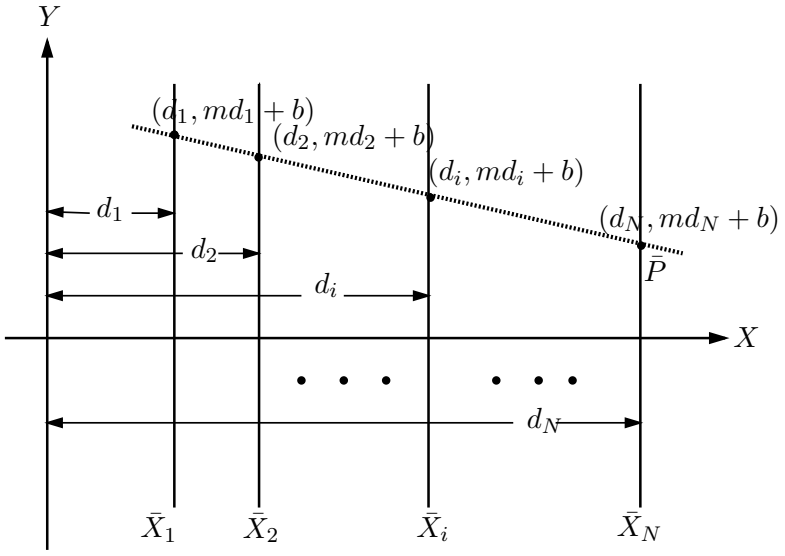

Figure 1.11: Points in $\mathbb{R}^N$ represented by lines.

1.2.2 The Triply Indexed Points

$\mathcal{L}$et us now review the construction leading to the single intersection in Fig. 1.10. For any line $\ell \subset \pi$ the 3 points $\bar{\ell}_{12}$, $\bar{\ell}_{23}$, $\bar{\ell}_{13}$ are :

- on a line $\bar{L}$ by the 3-point-collinearity property, and conversely since $\bar{L}$ lies on the 3 points the point $L \in \ell$.
- Further, since $\bar{L}$ is a straight-line L must also be a point of the "super-plane" π_1^s.

Therefore

$$\ell \cap \pi_1^s = L \ . \tag{1.11}$$

This is true for *every* line $\ell \subset \pi$. Specifically for a line

$$\ell' \subset \pi \quad \exists L' \in \ell' \quad \ni \ \ell' \cap \pi^s = L' \ .$$

Now L and L' specify a line $\ell_\pi \subset \pi_1^s$ represented by a single point $\bar{\ell}_\pi$. Altogether,

$$\left.\begin{array}{rcl} L\,, L' \in \pi & \Rightarrow & \ell_\pi \subset \pi \\ L\,, L' \in \pi_1^s & \Rightarrow & \ell_\pi \subset \pi_1^s \end{array}\right\} \ \Rightarrow \ \ for\ \pi \neq \pi_1^s \ , \ \pi \cap \pi_1^s = \ell_\pi \quad ,$$

showing that the point where all the lines intersect in Fig. 1.10 is $\bar{\ell}_\pi$. For reasons which are clarified shortly we refer to $\bar{\ell}_\pi$ by $\bar{\pi}_{123}$.

A plane $\pi \subset \mathbb{R}^3$ is determined by two intersecting lines. It is advantageous to use two lines belonging to "super-planes" for their representation requires only one point. One such line is $\ell_\pi = \pi \cap \pi_1^s$. To determine the second line we revisit eq. (1.8) and chose another convenient axes-spacing. As indicated in Fig. 1.9, the $\bar{X}_1$ axis is translated (recall that this corresponds to a rotation) to $\bar{X}_1'$, one unit to the right of $\bar{X}_3$, as shown in Fig. 1.12 with $d_2 = 1,\ d_3 = 2,\ d_1' = 3$. The new super-plane is given by

$$\pi_{1'}^s : x_1 + x_2 - 2x_3 = 0 \tag{1.12}$$

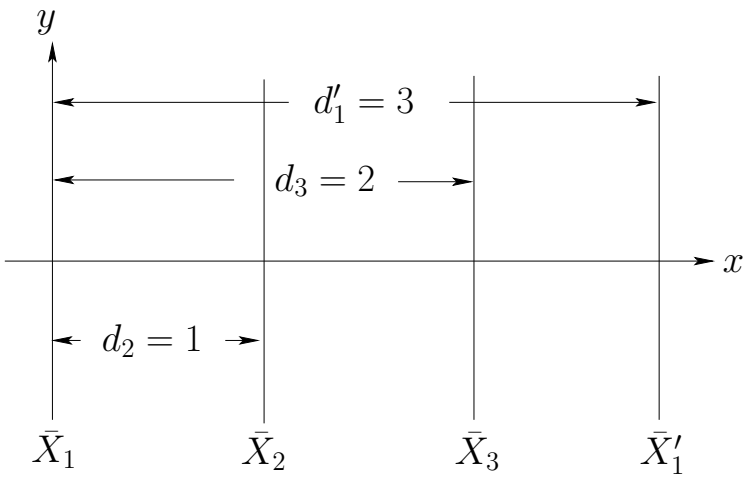

Figure 1.12: The axes spacing for the second super-plane $\pi_{1'}^s$.

Transferring the x_1 coordinate of each point P to the $\bar{X}_1'$-axis as shown in Fig. 1.13 and repeating the construction we obtain the second point, denoted by $\bar{\pi}_{231'}$ and shown in Fig. 1.15. The corresponding line is none other than the intersection $\ell_\pi' = \pi \cap \pi_{1'}^s$. What about the line $\bar{H}$ joining the points $\bar{\pi}_{123}$ and $\bar{\pi}_{231'}$? Clearly $H \in \ell_\pi$ since $\bar{\pi}_{123}$ represents ℓ_π and similarly $H \in \ell_\pi'$. Further, since $\bar{H}$ is a line in the $\bar{X}_1,\ \bar{X}_2,\ \bar{X}_3$ coordinate system and also in the $\bar{X}_2,\ \bar{X}_3,\ \bar{X}_1'$ system,

$$H = \ell_\pi \cap \ell_\pi' = \pi_1^s \cap \pi_{1'}^s \cap \pi \tag{1.13}$$

as illustrated in Fig. 1.14. So the intersecting lines ℓ_π, ℓ_π' determine the plane π and therefore the plane can be represented by the *two points* $\bar{\pi}_{123}$ and $\bar{\pi}_{231'}$. But what is going on? In Chapter **??** we saw that a *line* in $\mathbb{R}^3$ is also represented by two points. To distinguish the two points representing a plane, *three* indices are attached while only two indices are used for the point representation of a line. The deeper reason is, of course, that the linear relations specifying lines involve (or can be reduced to) two variables, whereas those involving planes necessarily involve 3 variables. Specifically, for the plane

$$\pi \ : \ c_1 x_1 + c_2 x_2 + c_3 x_3 = c_0 \ , \tag{1.14}$$

$$\ell_\pi = \pi \cap \pi_1^s \ : \ \begin{cases} \ell_{\pi_{12}} : & x_2 = -\frac{c_1 - c_3}{c_2 + 2c_3} x_1 + \frac{c_0}{c_2 + 2c_3} \\ \\ \ell_{\pi_{23}} : & x_3 = -\frac{2c_1 + c_2}{c_3 - c_1} x_2 + \frac{c_0}{c_3 - c_1}. \end{cases} \ , \tag{1.15}$$

Therefore, in homogeneous coordinates recalling that 1, the distance of $\bar{X}_2$ from the y-axis, must be added to the to the first coordinate of $\bar{\ell}'_{\pi_{23}}$

$$\bar{\pi}_{123} = \bar{\ell}_{\pi_{12}} = \bar{\ell}_{\pi_{23}} = (c_2 + 2c_3,\ c_0,\ c_1 + c_2 + c_3) \ . \tag{1.16}$$

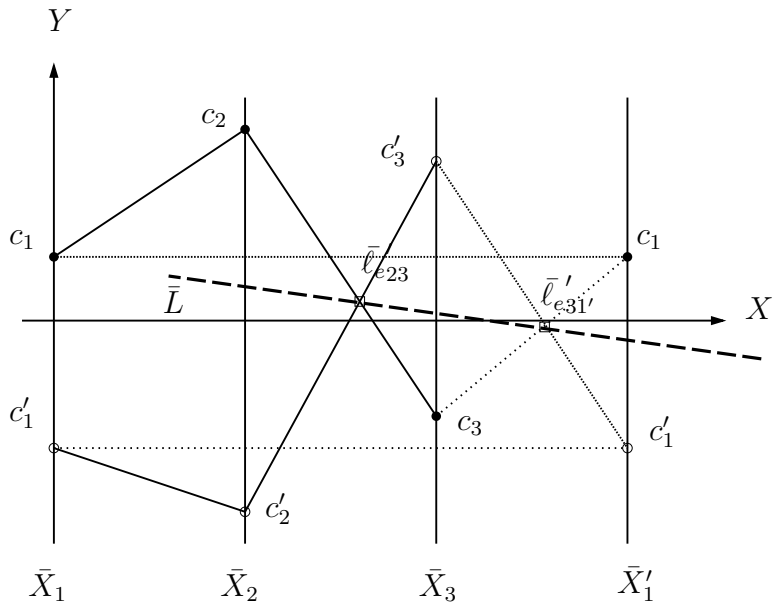

Figure 1.13: Transferring the values from the $\bar{X}_1$ to the $\bar{X}_{1'}$-axis.

Continuing

$$\ell'_\pi = \pi \cap \pi^s_{1'} \;:\; \begin{cases} {\ell'}_{\pi_{12}}: & x_2 = -\frac{2c_1+c_3}{2c_2+c_3}x_1 + \frac{2c_0}{2c_2+c_3} \\ {\ell'}_{\pi_{23}}: & x_3 = -\frac{c_2-c_1}{2c_1+c_3}x_2 + \frac{c_0}{2c_1+c_3}. \end{cases} , \tag{1.17}$$

and from the 2nd equation it is immediate that

$$\bar{\ell}'_{\pi_{23}} = (3c_1 + c_2 + 2c_3,\, c_0,\, c_1 + c_2 + c_3). \tag{1.18}$$

Since ℓ'_π is a line in the super-plane $\pi^s_{1'}$ it must that $\bar{\ell}'_{\pi_{12}} = \bar{\ell}'_{\pi_{23}}$. Yet a direct computation from the first equation of 1.17 yields

$$\bar{\ell}'_{\pi_{12}} = (2c_2 + c_3,\, c_0,\, 2(c_1 + c_2 + c_3)) \;, \tag{1.19}$$

what is going on? Figure 1.16 explains the "riddle" reminding us that $\pi^s_{1'}$ is a super-plane in the $\bar{X}_2, \bar{X}_3, \bar{X}_{1'}$ coordinate system where its points such as P, Q are represented by straight lines intersecting at $\bar{\ell}'_{\pi_{1'2}} = \bar{\ell}'_{\pi_{23}}$. To obtain $\bar{\ell}'_{\pi_{12}}$ the x_1 values must be transferred to the $\bar{X}_1$ axis and then constructing the corresponding *polygonal lines* to obtain their intersection

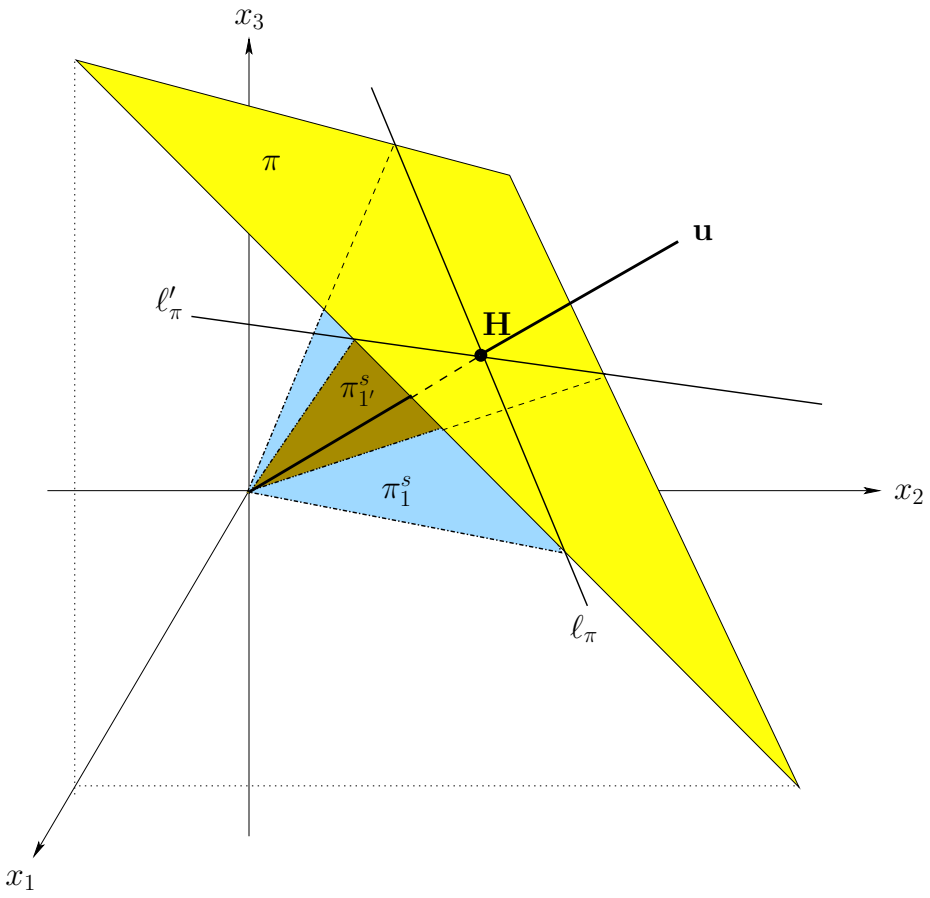

Figure 1.14: The intersections of a plane π with the two super-planes ${\pi^s}_1$ and $\pi^s_{1'}$.

These are the two lines ℓ_π , ℓ'_π which specify the plane and provide its representation.

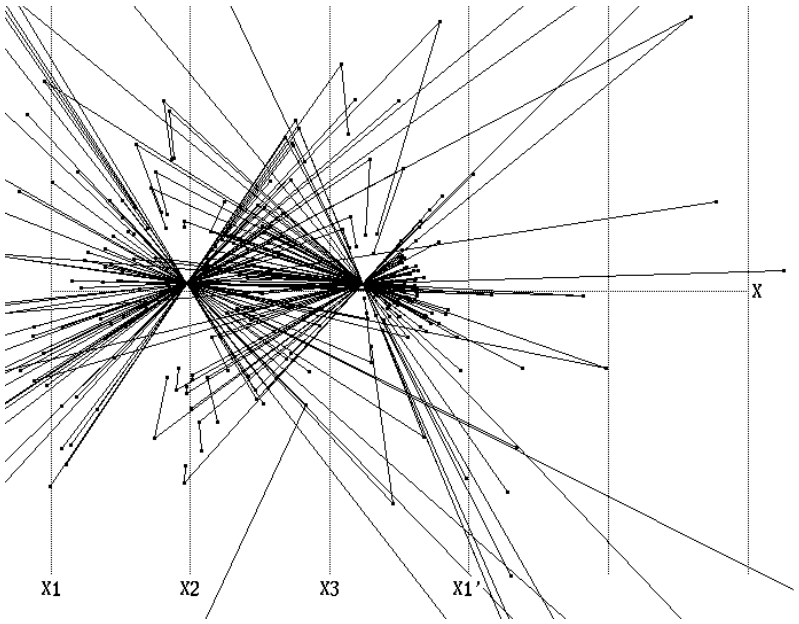

Figure 1.15: The plane π represented by two points

at $\bar{\ell}'_{\pi_{12}} \neq \bar{\ell}'_{\pi_{1'2}}$. Recall from Chapter **??** the line $\ell \rightarrow \bar{\ell}$ point correspondence

$$\ell : x_2 = mx_1 + b \;\rightarrow\; \bar{\ell} : (\frac{d}{1-m}\;,\; \frac{b}{1-m}) \quad m \neq 1 \tag{1.20}$$

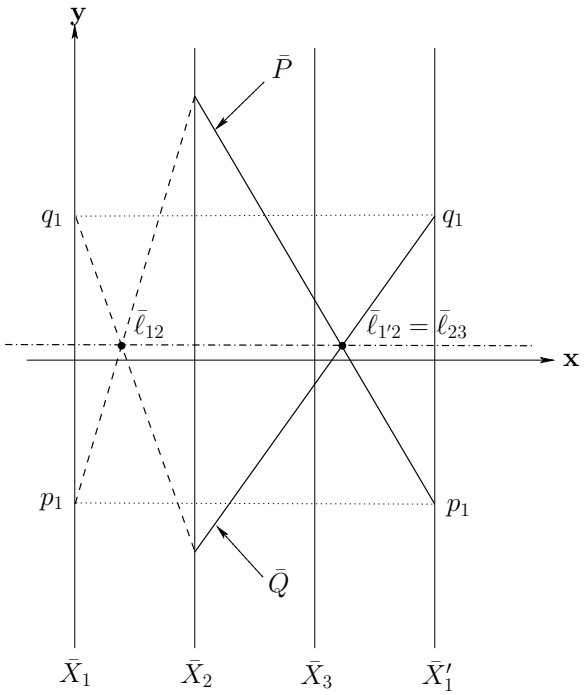

Figure 1.16: The location of the $\bar{\ell}_{12}$ and $\bar{\ell}_{1'2}$ points.

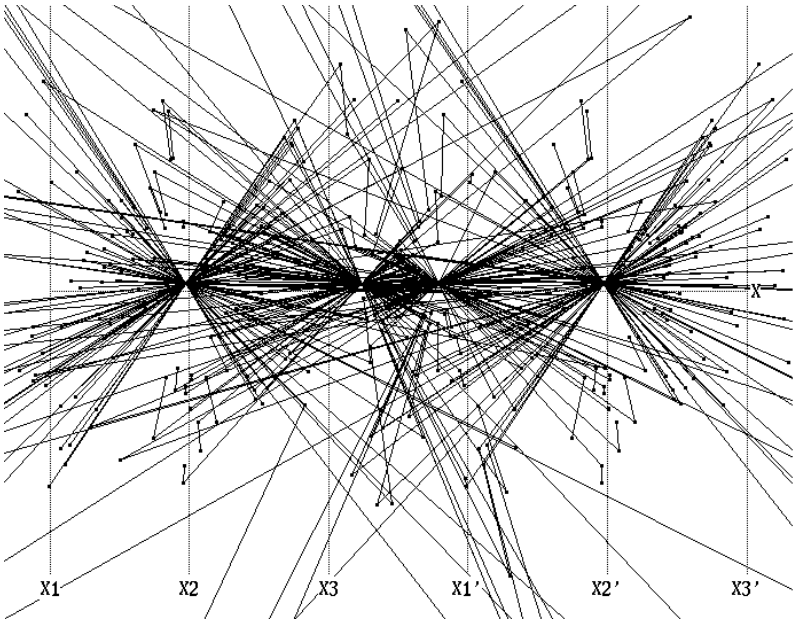

Figure 1.17: The plane π intersected with four super-planes.

Each point represents one of the resulting lines.

where d is the *directed* inter-axis distance. The distances from $\bar{X}_{1'}$ to $\bar{X}_2$ and the y-axis are 2 and 3 units respectively. Then together with the first equation in (1.17)

$$\bar{\ell'}_{\pi_{1'2}} = \left(\frac{-2}{1+\frac{2c_1+c_3}{2c_2+c_3}} + 3 \, , \, \frac{c_0}{1+\frac{2c_1+c_3}{2c_2+c_3}} \right) , \tag{1.21}$$

which in homogeneous coordinates matches eq. (1.19) and analogous to eq. 1.16 we record[2] the result as

$$\bar{\pi}_{231'} = \bar{\ell'}_{\pi_{1'2}} = \bar{\ell'}_{\pi_{23}} = (3c_1 + c_2 + 2c_3, \, c_0, \, c_1 + c_2 + c_3). \tag{1.22}$$

To simplify the notation we also write $\bar{\pi}_{1'} = \bar{\pi}_{1'23} = \bar{\pi}_{231'}$ and $\bar{\pi}_{0'} = \bar{\pi}_{123}$. The coordinates of the two points $\bar{\pi}_{0'}$ and $\bar{\pi}_{1'}$ contain 3 independent parameters and suffice to determine the coefficients of π. Let $S = c_1 + c_2 + c_3$ and denote by $x_{0'}, x_{1'}$ the x Cartesian coordinates of $\bar{\pi}_{123}$ and $\bar{\pi}_{1'23}$ respectively when $S \neq 0$. Then

$$x_{1'} - x_{0'} = 3\frac{c_1}{S} = 3c_1' \, , \tag{1.23}$$

where the $c_i' = c_i/S \ , \ i = 0, 1, 2, 3$ are the *normalized* coefficients. Exploring this further the $\bar{X}_2$-axis is translated to the right by 3 units, the construction is repeated and a third point is obtained :

$$\bar{\pi}_{31'2'} = \bar{\pi}_{1'2'3} = (3c_1 + 4c_2 + 2c_3, \, c_0, \, c_1 + c_2 + c_3). \tag{1.24}$$

which is also denoted by $\bar{\pi}_{2'}$ and its x coordinate by $x_{2'}$. Then

$$x_{2'} - x_{1'} = 3c_2' \, . \tag{1.25}$$

[2]Another detailed example is computed later for the principal 2-planes.

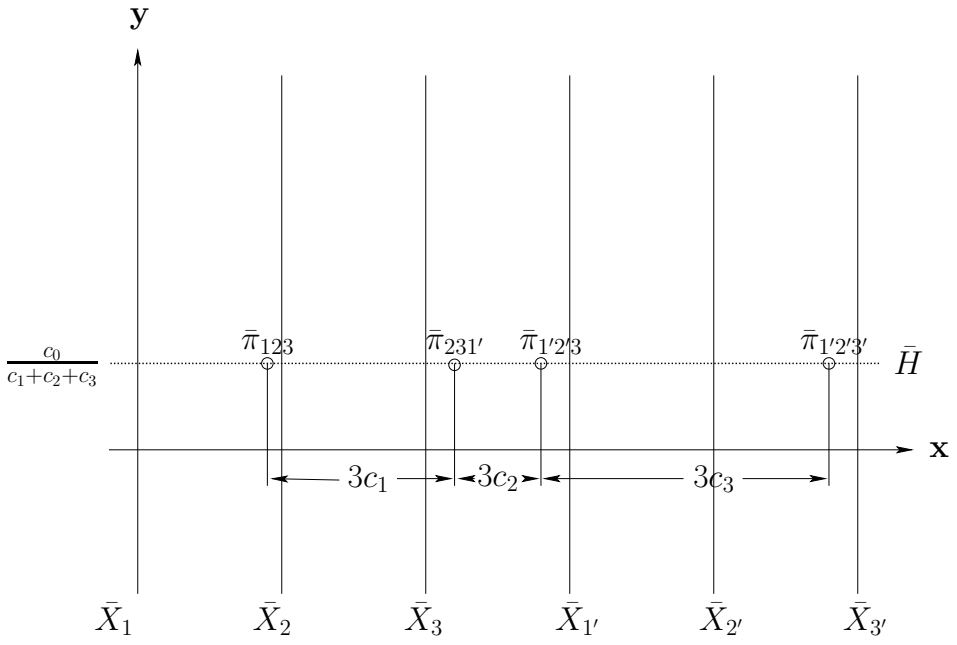

Figure 1.18: The distances between adjacent points are proportional to the coefficients.

For $\pi\ :\ c_1x_1+c_2x_2+c_3x_3=c_0$ with the normalization $c_1+c_2+c_3=1$. The proportionality constant is the dimensionality of the space. The plane's equation can be read from the picture!

Finally, translating the $\bar{X}_3$-axis 3 units to the right and repeating the construction as shown in Fig. 1.17 a fourth point is obtained

$$\bar{\pi}_{1'2'3'}=\bar{\pi}_{3'}=(3c_1+4c_2+5c_3,\ c_0,\ c_1+c_2+c_3)\ , \tag{1.26}$$

and for $x_{3'}$ its x coordinate

$$x_{3'}-x_{2'}=3c_3'\ . \tag{1.27}$$

Clearly the third and fourth points are dependent on the first two and by an easy calculation it is found that

$$x_{2'}=6-(x_{0'}+x_{1'})\ ,\quad x_{3'}=3+x_{0'}\ . \tag{1.28}$$

So with the normalization $c_1'+c_2'+c_3'=1$ the distance between adjacent (according to the indexing) points of the plane's representation is proportional to the corresponding coefficient. The proportionality constant equals the dimensionality of the space (see exercise 5). Their ordinate is the constant c_0', so the equation of the plane can effectively be read from the picture as shown in Fig. 1.18. Occasionally, we say that the distance between adjacent indexed points **is** the corresponding coefficient when the dimensionality and hence the proportionality constant are clear. When the coefficients' sum is zero the plane is an *sp* represented by ideal points. All the super-planes are on the line u so what is the angle between the four different super-planes we generated? To answer this it is convenient to introduce and work with vector notation. Letting $\mathbf{x}=(\mathbf{x_1},\mathbf{x_2},\mathbf{x_3})$, the coefficients of a plane

π^j, $\mathbf{c^j} = (\mathbf{c_1^j}, \mathbf{c_2^j}, \mathbf{c_3^j})$ so plane's equation is $\pi^j : \mathbf{c^j} \cdot \mathbf{x} = c_0^j$ where "$\cdot$" stands for the inner (or dot) product. From analytic geometry the angle ϕ between two planes π^1, π^2 is found by

$$cos\ \phi = \pm\ \frac{\mathbf{c^1} \cdot \mathbf{c^2}}{[(\mathbf{c^1} \cdot \mathbf{c^1})(\mathbf{c^2} \cdot \mathbf{c^2})]^{\frac{1}{2}}}\ . \tag{1.29}$$

Fixing the angle by adopting the + sign above we find that $\pi^s_{1'}$ is obtained from π^s_1 by a clock-wise rotation of 120^o about u. Checking for the third super-plane

$$\pi^s_{1'2'3} : -2x_1 + x_2 + x_3 = 0\ , \tag{1.30}$$

resulting from the translation of the $\bar{X}_2$ axis, the dihedral angle with $\pi^s_{1'}$ is also 120^o. Not surprisingly then the fourth super-plane $\pi^s_{1'2'3'}$, generated by the translation of the $\bar{X}_3$ axis, coincides with π^s_1.

To clarify, the rotations about u and the super-planes they generate do not effect the plane π which remains *stationary* intersecting u at H given in eq. (1.13) and shown in Fig. 1.14. This is the reason that all points $\bar{\pi}_{123}$, $\bar{\pi}_{1'23}$, $\bar{\pi}_{1'2'3}$, $\bar{\pi}_{1'2'3'}$ have the same y-coordinate $c_0/(c_1 + c_2 + c_3)$ being on horizontal line $\bar{H}$. This useful property is also true for the points representing lines and is put to good use in the construction algorithms discussed next. For consistency with this chapter's format a line ℓ equations' are re-written as

$$\ell\ :\ \begin{cases} \ell_{1,2}\ :\ c_{11}x_1 + c_{12}x_2 &= c_{10}\ , \\ \ell_{2,3}\ :\ c_{22}x_2 + c_{23}x_3 &= c_{20}\ , \end{cases} \tag{1.31}$$

emphasizing that each of the $\ell_{1,2}$, $\ell_{2,3}$ is a *projecting plane* in $\mathbb{R}^3$ orthogonal to the x_1x_2, x_2x_3 planes respectively with $c_{13} = c_{21} = 0$. It is clear then that the points $\bar{\ell}_{12}$, $\bar{\ell}_{1'2}, \bar{\ell}_{1'2'}$ all have the same y-coordinate and are on a horizontal line let's call it **12**. Similarly the triple $\bar{\ell}_{23}$, $\bar{\ell}_{2'3}, \bar{\ell}_{2'3'}$ are on a horizontal line **23** and $\bar{\ell}_{13}$, $\bar{\ell}_{1'3}$, $\bar{\ell}_{1'3'}$ are on another horizontal line **13**. All this is seen in Fig. 1.25 of the next section.

Exercises

1. Derive the equation equivalent to eq. (1.8) for $\mathbb{R}^N$ and state it's properties.

2. What planes are represented when the points $\bar{\pi}_{123}$ and $\bar{\pi}_{231'}$ are ideal?

3. How are the planes in class $\mathcal{E}$ represented?

4. Is the line intersection shown in Fig. 1.10 necessary and sufficient condition for coplanarity? Prove or give a counter-example.

5. Show that in $\mathbb{R}^N$ the distance between adjacent indexed points is N times the corresponding coefficient as in $\mathbb{R}^3$ it is 3 – equations (1.23), (1.25) and 1.27).

6. (a) Find the equations of the three super-planes containing the x_1, x_2 and x_3-axis respectively.

   (b) What are the three dihedral angles between pairs of these super-planes.

7. Provide an affine transformation resulting in the four points $\bar{\pi}_{123}$, $\bar{\pi}_{231'}$, $\bar{\pi}_{31'2'}$, $\bar{\pi}_{1'2'3'}$ being collinear and with distance c_i in between pairs rather than $3c_i$.

8. The vertical line representation of planes actually requires 4 rather than the two vertical lines shown. Explore the case where none of the 4 vertical lines coincides with the coordinate axis $\bar{X}_i$.

9. Provide algorithms based on the indexed-points representation for finding the intersection between:

   (a) a pair of 2-flats, and

   (b) a line and a 2-flat.

   Delimit carefully the special cases where the algorithms fail.

10. Given the representation of a plane in terms of vertical lines,

    (a) how would one check if the vertical lines represent two *orthogonal* families of parallel lines?

    (b) How could the vertical axes be trasformed to vertical axes representing *orthogonal* families of parallel lines?

11. Construct a vertical line representation $\bar{Y}_i$ for a plane $\pi \subset \mathbb{R}^3$ with $\bar{\pi}_{123} \in \bar{Y}_1$, and $\bar{\pi}_{231'} \in \bar{Y}_2$.

12. Given a point $P \in \mathbb{R}^3$ and a plane $\pi \subset R^3$, provide an algorithm for determining whether $P \in \pi$ or which of the half-spaces ("sides") of π (partitions $\mathbb{R}^3$) P lies.

13. Generalize the 3-point-collinearity property for $N = 4$ and more.

1.3 Construction Algorithms

$\mathcal{A}$ dream mentioned at the outset is to do *multidimensional* synthetic constructions with this new coordinate system as already done for lines and now with planes and flats starting in $\mathbb{R}^3$. Also this is an additional opportunity to better understand the properties of the indexed points by indulging in the easy constructions they enable.

1.3.1 Planes and Lines

subsec:planes-lines

Half-Spaces

$\mathcal{W}$ith reference to Fig. 1.14, a plane ρ parallel to π intersects each of the two super-planes $\pi^s_1,\ \pi^s_{1'}$ at lines ℓ_ρ, ℓ'_ρ parallel to ℓ_π and $\ell_{\pi'}$ respectively. Hence the points $\bar{\pi}_{123},\ \bar{\rho}_{123}$ are on a vertical line and similarly the points $\bar{\rho}_{231'},\ \bar{\pi}_{231'}$ are also on a vertical line. Of course this is entirely analogous to the conditions for parallel lines as it should be for after all the triply indexed points represent lines (i.e. ℓ_π, ℓ_ρ and ℓ'_π, ℓ'_ρ). From the representation of two parallel planes π, ρ we agree that the $\bar{H}$ ($H \in \mathbf{u}$) with the higher y-coordinate identifies the higher (above) plane. This clarifies how to distinguish and recognize half-spaces as illustrated in Fig. 1.19 which is the cornestone for the study of convexity. The two vertical lines together with $\bar{H}$ also provide a coordinate system of planar coordinates as described in section 1.1.1 based on the intersecting lines ℓ_π and $\ell_{\pi'}$. Usually there is no reason to distinguish between index permutations like $231'$ and $1'23$ which are henceforth considered the same unless indicated otherwise.

Line contained in a Plane

Recognition that a line ℓ is contained in a plane π is immediate from the construction of the points $\bar{\pi}_{123}$. Specifically, a line $\ell \subset \pi \Leftrightarrow \bar{\ell}_{12}, \bar{\ell}_{23}, \bar{\pi}_{123}$ are collinear. This propery is the equivalent of the collinearity in Fig. 1.7 for the two-vertical-lines planar representation As illustrated in Fig. 1.20, the line $\ell \subset \pi$ intersects the super-planes at the two points $P = \ell \cap \ell_\pi\ ,\ P' = \ell \cap \ell'_\pi$ with $\bar{P},\ \bar{P'}$ on $\bar{\pi}_{123},\ \bar{\pi}_{231'}$ respectively since these triply indexed

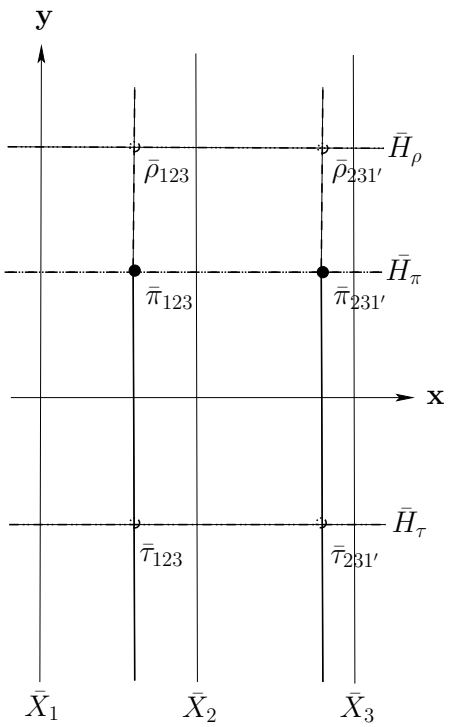

Figure 1.19: The parallel planes $\rho,\ \tau$ are above and below respectively the plane π.

The upper half-space of π is marked by the two dashed half-lines.

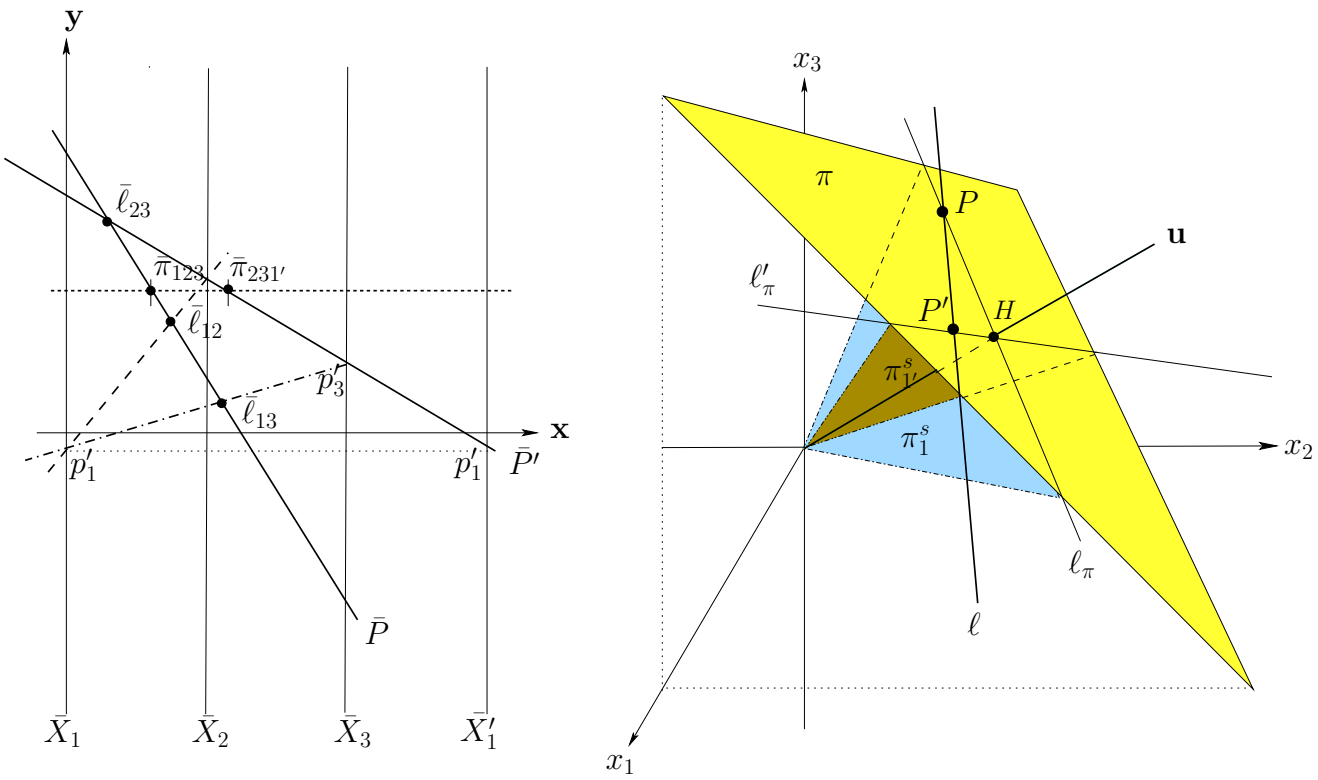

Figure 1.20: A line ℓ is contained in a plane $\pi \Leftrightarrow$ the points $\bar{\ell}_{12}, \bar{\ell}_{13}, \bar{\ell}_{23}, \bar{\pi}_{123}$ are on a line $\bar{P}$. Alternatively if $\bar{\ell}_{1'2}, \bar{\ell}_{1'3}, \bar{\ell}_{23}, \bar{\pi}_{231'}$ are on a line $\bar{P}'$ then $P = \ell_\pi \cap \pi$ and $P' = \ell_{\pi'} \cap \pi$.

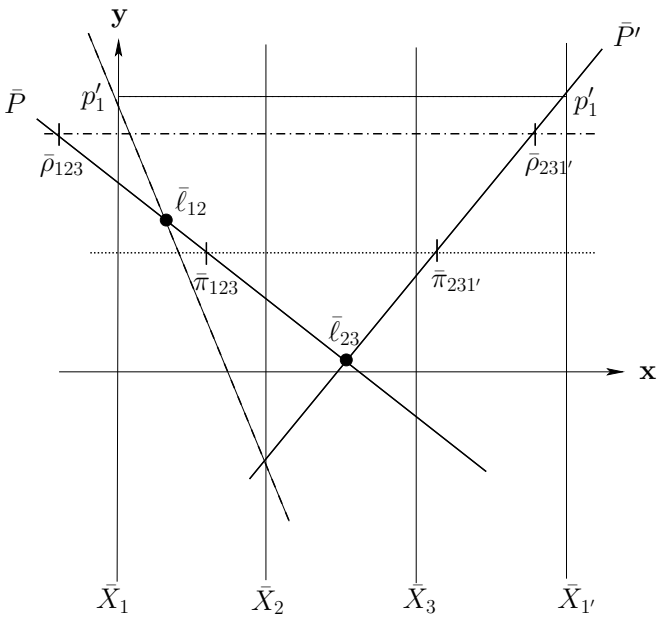

Figure 1.21: Two intersecting planes

points are actually $\bar{\ell}_\pi$ and $\bar{\ell}'_\pi$. Hence $\bar{\ell}_{23} = \bar{P} \cap \bar{P}'$ as the line $\bar{P}'$ represents P' on the $\bar{X}_2, \bar{X}_3, \bar{X}'_1$ axes. By tranfering the value of its first coordinate p'_1 to the $\bar{X}_1$ axis we obtain the $\bar{P}'_{12}$ portion of the *polygonal* line $\bar{P}'$ in the $\bar{X}_1, \bar{X}_2, \bar{X}_3$ axes with $\bar{\ell}_{12} = \bar{P} \cap \bar{P}'_{12}$. Therefore

$$\ell \subset \pi \;\Leftrightarrow\; \bar{\ell}_{12}, \bar{\ell}_{13}, \bar{\ell}_{23}, \bar{\pi}_{123} \;\in \bar{P}\,, \quad P = \ell_\pi \cap \pi. \tag{1.32}$$

The proof for the $\Rightarrow$ direction is similar. Such a collinearity must also hold for the line $\bar{P}'$ on $\bar{\ell}_{23}, \bar{\pi}_{1'23}$ for the $\bar{X}_2, \bar{X}_3, \bar{X}'_1$ axes; that is $\ell \subset \pi \;\Leftrightarrow\; \bar{\ell}_{1'2}, \bar{\ell}_{1'3}, \bar{\ell}_{23}, \bar{\pi}_{1'23}$ are on a line $\bar{P}'$ where $P' = \ell'_\pi \cap \pi$. This leads to a beautiful rotation $\leftrightarrow$ translation duality shown in Fig. 1.37 and presented shortly analogous to that obtained with the vertical lines planar representation seen in Fig. 1.8.

Intersecting Planes

To realize our goal of doing higher-dimensional constructions, that is for $N > 3$, we gradually wean the reader from the need to use 3-D pictures. In the process we discover that many constructions even for 3-D are simpler to do and certainly to draw in $\|$-coords. Such is the construction shown in Fig. 1.21 for finding the intersection of two planes $\rho \cap \pi = \ell$. Let $\ell_\rho,\ \ell_\pi$ be the line intersections of the two planes with the first super-plane π^s_1 and $\ell'_\rho,\ \ell'_\pi$ the intersections with the second super-plane $\pi^s_{1'}$. Two convenient points on ℓ are $P = \ell_\pi \cap \ell_\rho,\ P' = \ell'_\pi \cap \ell'_\rho$ since the line $\bar{P}$ is on the points with the 123 indices, and $\bar{P}'$ on the points with the $231'$ indices. The points $\bar{\ell}_{23},\ \bar{\ell}_{12}$, specifying ℓ in the $\bar{X}_1,\ \bar{X}_2,\ \bar{X}_3$ axes, (1.32) after transferring the p'_1 coordinate of P' to the $\bar{X}_1$-axis and using property (1.32). The planes' intersection is the line on the two points P, P' ... simplicity itself.

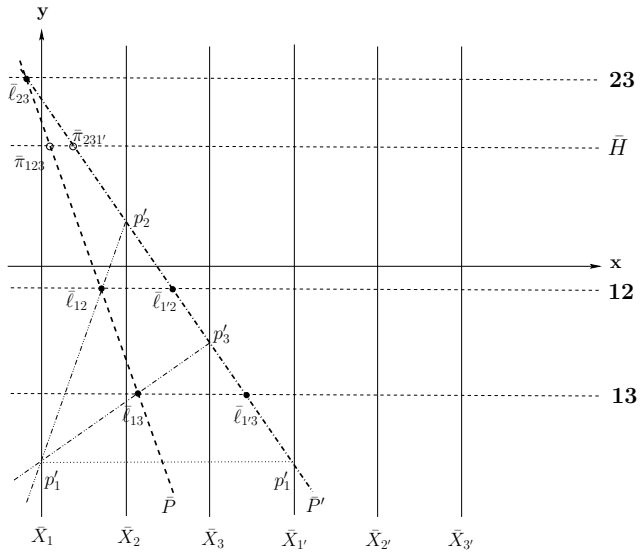

Figure 1.22: Representation of a plane $\pi \subset \mathbb{R}^3$ by two indexed points.

First step in the construction of the points $\bar{\pi}_{32'1'}, \bar{\pi}_{1'2'3'}$ from $\bar{\pi}_{123}, \bar{\pi}_{231'}$. A (any) line $\ell \subset \pi$ is constructed as in Fig. 1.20. The points $\bar{\ell}_{12}, \bar{\ell}_{13}$ are constructed and the horizontal lines $\mathbf{12}, \mathbf{13}, \mathbf{23}$ are drawn on the $\bar{\ell}$ s with the corresponding indices.

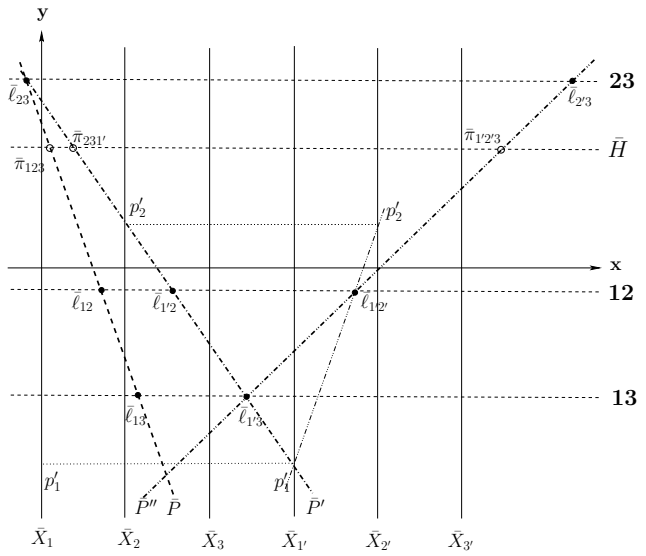

Figure 1.23: Construction of the third point $\bar{\pi}_{1'2'3}$.

1.3.2 The four Indexed Points

$\mathcal{T}$he laborious construction for the four points $\bar{\pi}_{123}, \bar{\pi}_{231'}, \bar{\pi}_{31'2'}, \bar{\pi}_{1'2'3'}$ seen in Figures 1.17 can be greatly simplified. A 2-flat is determined by *any* 3 points it contains and this is the basis in ensuing construction algorithm. On each of the points $\bar{\pi}_{123}$, $\bar{\pi}_{231'}$ any two lines $\bar{P}$ and $\bar{P}'$ respectively are chosen as shown in Fig. 1.22. We know that $P \in \pi_1^s \cap \pi$, $P' \in \pi_{1'}^s \cap \pi$ and $\bar{\ell}_{23} = \bar{P} \cap \bar{P}'$ where $\ell \subset \pi$ is the line on P and P'. The p'_1 value is transferred from the $\bar{X}_{1'}$ to the $\bar{X}_1$ axis and joined to the p'_2 coordinate intersecting $\bar{P}$ at $\bar{\ell}_{12}$; the point $\bar{\ell}_{13}$ is similarly

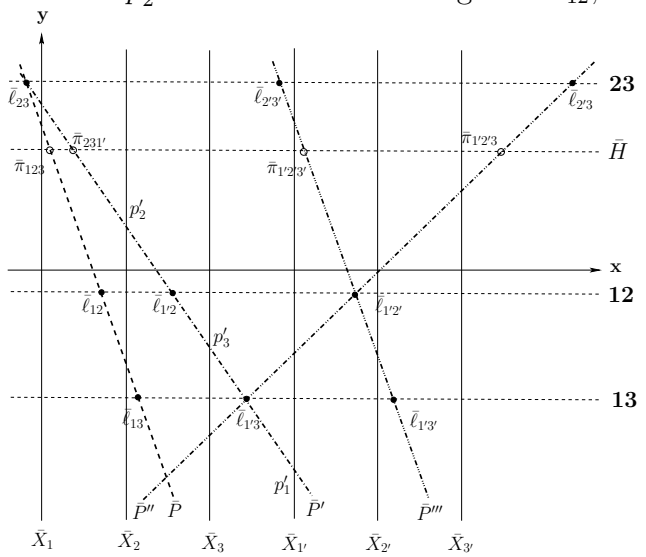

Figure 1.24: Construction of the fourth point $\bar{\pi}_{1'2'3'}$.

Note that $\bar{P}'''$ on $\bar{\ell}_{1'2'}$ is parallel to $\bar{P}$ since P''' is the point $P = \pi \cap \ell_\pi$ in the $\bar{X}_{1'}, \bar{X}_{2'}, \bar{X}_{3'}$ axes.

obtained. Horizontal lines $\mathbf{12}, \mathbf{13}, \mathbf{23}$ are drawn through the 3 $\bar{\ell}$ points as shown providing, at their intersections with the line $\bar{P}'$, the points $\bar{\ell}_{1'2}, \bar{\ell}_{1'3}$ specifying ℓ on the $\bar{X}_2, \bar{X}_3, \bar{X}_{1'}$ axes. Moving on to Fig. 1.23 the value p'_2 is transferred to the $\bar{X}_{2'}$ axis and joined to the p'_1 coordinate on $\bar{X}_{1'}$ intersecting the $\mathbf{12}$ line at point $\bar{\ell}_{1'2'}$ which together with $\bar{\ell}_{1'3}$ specifies ℓ on the $\bar{X}_3$, $\bar{X}_{1'}$, $\bar{X}_{2'}$ axes. Therefore as for P and P', the line $\bar{P}''$ on these two points represents the point $P'' \in \pi^s_{1''} \cap \pi = \ell''_\pi$ where $\pi^s_{1''}$ is the super-plane corresponding to this axes spacing (i.e. $d_{1'} = 3,\ d_{2'} = 4,\ d_3 = 2$). Hence $\bar{\pi}_{123} = \bar{P}'' \cap \bar{H}$ and $\bar{\ell}_{23} = \bar{P}'' \cap \mathbf{23}$. Proceeding as in Fig. 1.24 we place a line $\bar{P}'''$ parallel to $\bar{P}$ on the point $\bar{\ell}_{1'2'}$. In fact P''' is the image of P in the $\bar{X}_{1'}$, $\bar{X}_{2'}$, $\bar{X}_{3'}$ axes where, as we saw earlier, the super-plane $\pi^s_{1'2'3'}$ is image of π^s_{123}. The intersections of $\bar{P}'''$ with $\bar{H}, \mathbf{13}, \mathbf{23}$ complete the construction. The four points are referred to as the *augmented representation* of a plane. Use of the relations in eq. 1.28 between the x-coordinates of the four indexed points simplifies the construction. By the way, Fig. 1.25 showing the $\bar{\ell}$ points corresponding to a line ℓ in the translated $\|$-coords systems is obtained with a similar construction. The intersections of ℓ with the super-planes are the points $P = \ell \cap \pi^s_1\ ,\ P' = \ell \cap \pi^s_{1'}\ ,\ P'' = \ell \cap \pi^s_{1'2'}\ ,\ P''' = \ell \cap \pi^s_{1'2'3'}$.

1.3.3 Special Planes

$\mathcal{F}$or future reference we record the indexed points of some planes which are encountered on several occasions.

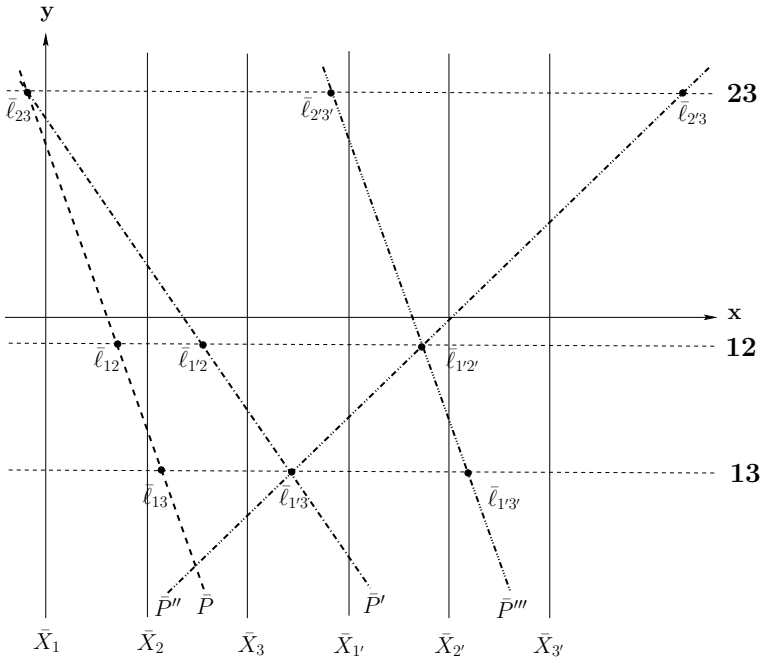

Figure 1.25: The collinear triples of points $\bar{\ell}$.

They represent a line ℓ in the four coordinate systems $\bar{X}_1, \bar{X}_2, \bar{X}_3$ through $\bar{X}_{1'}, \bar{X}_{2'}, \bar{X}_{3'}$.

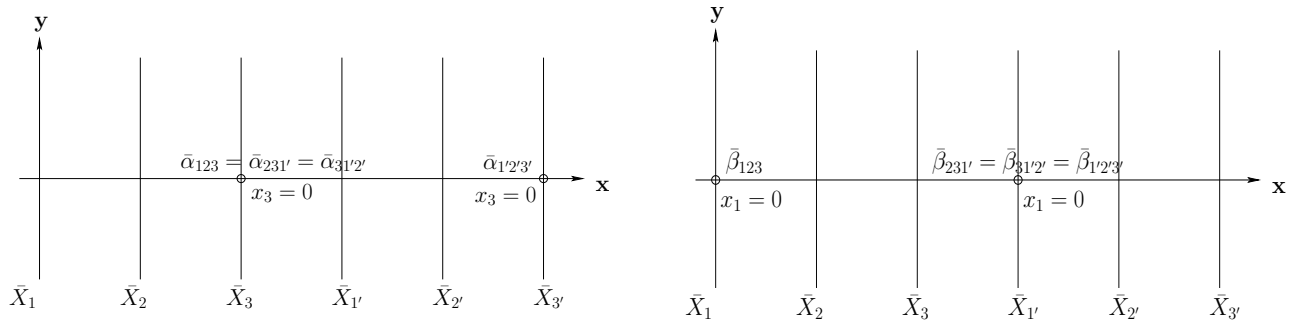

Figure 1.26: Indexed points corresponding to $\alpha : x_3 = 0$.

For the x_1x_2 principal 2-plane on the left and for the x_2x_3 principal 2-plane $\beta : x_1 = 0$ on the right.

The principal 2-planes

Our first examples are for the x_1x_2-plane $\alpha :\ x_3 = 0$, x_2x_3-plane $\beta :\ x_1 = 0$, and the x_1x_3 plane $\gamma :\ x_2 = 0$. To obtain further practice the indexed points of α are obtained from the fundamentals rather than from the formulae eqs. 1.16 , 1.22 , 1.24, 1.26. It is preferable to use the general eq. (**??**) in Chapter **??** rather than eq. (1.20).

$$\ell_\alpha = \alpha \cap \pi_1^s : \left\{ \begin{array}{c} \ell_{\alpha_{12}} : x_2 = \frac{1}{2}x_1 \\ \\ \ell_{\alpha_{23}} : x_3 = 0 \end{array} \right| \Rightarrow \left. \begin{array}{c} \bar{\ell}_{\alpha_{12}} = (\frac{1}{1-\frac{1}{2}}, 0, 1) \\ \\ \bar{\ell}_{\alpha_{23}} = (1+1, 0, 1) \end{array} \right\} = (2, 0, 1) = \bar{\alpha}_{123}\,.$$

Proceeding as for eq. (1.21) substituting the inter-axis distance $d = -2$ between $\bar{X}_1'$ and $\bar{X}_2$ and a translation by 3 from the y-axis,

$$\ell'_\alpha = \alpha \cap \pi_{1'}^s : \left\{ \begin{array}{c} \ell'_{\alpha_{1'2}} : x_2 = -x_1 \\ \\ \ell'_{\alpha_{23}} : x_3 = 0 \end{array} \right| \Rightarrow \left. \begin{array}{c} \bar{\ell}'_{\alpha_{1'2}} = (\frac{-2}{1+1} + 3, 0, 1) \\ \\ \bar{\ell}'_{\alpha_{23}} = (1+1, 0, 1) \end{array} \right\} = (2, 0, 1) = \bar{\alpha_{231'}}\,.$$

For the third point using the super-plane given in eq. (1.30),

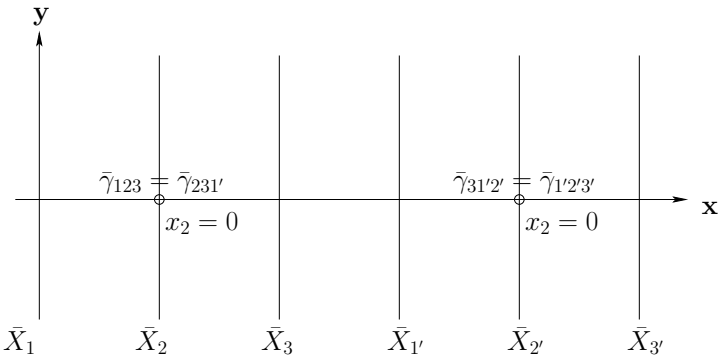

Figure 1.27: Indexed points corresponding to $\gamma : x_2 = 0$ the principal 2-plane x_1x_3.

$$\ell''_{\alpha} = \alpha \cap \pi^s_{1'2'} : \left\{ \begin{array}{l} {\ell''}_{\alpha_{1'2'}} : x_2 = 2x_1 \\ \\ {\ell''}_{\alpha_{2'3}} : x_3 = 0 \end{array} \right| \Rightarrow \left. \begin{array}{l} {\bar{\ell}''}_{\alpha_{1'2'}} = (\frac{1}{1-2} + 3, 0, 1) \\ \\ {\bar{\ell}''}_{\alpha_{2'3}} = (-2 + 4, 0, 1) \end{array} \right\} = (2, 0, 1) = \bar{\alpha}_{31'2'} \, .$$

Hence the first 3 points are congruent as they should be due to the zero coefficients of x_1 and x_2 in α's equation. As has already been pointed out the fourth super-plane $\pi^s_{1'2'3'}$ coincides with the first π^s_1 though for the computation of of the corresponding indexed point the values based on the the $\bar{X}'_1, \bar{X}'_2, \bar{X}'_3$ coordinate system are used yielding

$$\ell'''_{\alpha} = \alpha \cap \pi^s_{1'2'3'} : \left\{ \begin{array}{l} {\ell'''}_{\alpha_{1'2'}} : x_2 = \frac{1}{2}x_1 \\ \\ {\ell'''}_{\alpha_{2'3'}} : x_3 = 0 \end{array} \right| \Rightarrow \left. \begin{array}{l} {\bar{\ell}'''}_{\alpha_{1'2'}} = (\frac{1}{1-\frac{1}{2}} + 3, 0, 1) \\ \\ {\bar{\ell}'''}_{\alpha_{2'3'}} = (1 + 4, 0, 1) \end{array} \right\} = (5, 0, 1) = \bar{\alpha}_{1'2'3'} \, ,$$

This point's distance of 3 from the others is, of course, due to the only non-zero coefficient in α's equation. The representation is shown in Fig. 1.26 (left).

Alternatively, the location of the indexed points can be found graphically; by the intersection of two lines representing two points in the plane. The representations of β and γ are shown in Fig. 1.26 (right) and Fig. 1.27 respectively.

The constant planes

Next are the more general planes $\kappa : x_i = k_0 \, , i = 1, 2, 3$ with k_0 a constant. For

$$\kappa : x_1 = k_0 \tag{1.33}$$

via eqs. (1.16) , (1.22) , (1.24), (1.26) we obtain :

$$\bar{\kappa}_{123} = (0, k_0, 1) \, , \quad \bar{\kappa}_{231'} = \bar{\kappa}_{31'2'} = \bar{\kappa}_{1'2'3'} = (3, k_0, 1) \tag{1.34}$$

providing the representation shown in Fig. 1.28 (left). For

$$\kappa : x_2 = k_0 \tag{1.35}$$

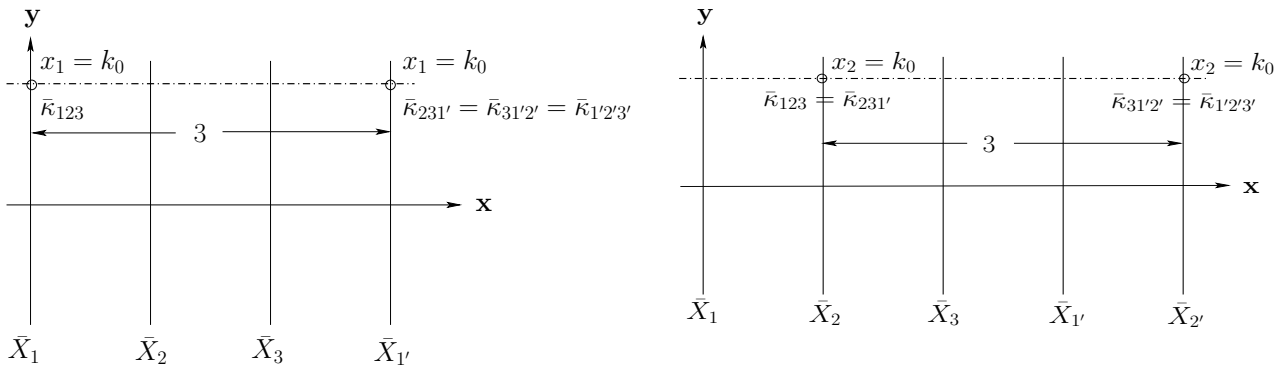

Figure 1.28: Indexed points representing constant planes.

For $\kappa : x_1 = k_0$ (left) and $\kappa : x_2 = k_0$ (right).

the indexed points are :

$$\bar{\kappa}_{123} = \bar{\kappa}_{231'} = (1, k_0, 1) \ , \quad \bar{\kappa}_{31'2'} = \bar{\kappa}_{1'2'3'} = (4, k_0, 1) \tag{1.36}$$

for the representation in Fig. 1.28 (right). Continuing

$$\kappa : x_2 = k_0 \tag{1.37}$$

has the indexed points

$$\bar{\kappa}_{123} = \bar{\kappa}_{231'} = \bar{\kappa}_{31'2'} = (2, k_0, 1) \ , \quad \bar{\kappa}_{1'2'3'} = (5, k_0, 1) \tag{1.38}$$

with the representation in Fig. 1.29. Observe that the distance between adjacent points is 3 times the value of the corresponding coefficient.

Projecting Planes and Lines

An important class are the *projecting planes* which are perpendicular to one of the principal 2-planes. Our first encounter with them was in Chapter **??** where in $\mathbb{R}^N$ a line is defined as the intersection of $N-1$ projecting planes. In general, the equation ℓ_{lj} for the pairwise linear relation between x_l and x_j describes a projecting plane perpendicular to principal 2-plane $x_l x_j$. In Fig. 1.30 we see two projecting planes in $\mathbb{R}^3$ intersecting at a line ℓ. Where it is important to avoid an inconsistency the projecting planes on α, β and γ of a line ℓ are denoted by $\ell\alpha, \ell\beta$ instead of ℓ_{12}, ℓ_{23} respectively. Fig. 1.31 is in fact Fig. 1.25 reincarnated in terms of the projecting planes of ℓ whose representation is directly discerned from the $\bar{\ell}$s. For example $\overline{\ell\alpha}_{31'2'} = \overline{\ell\alpha}_{1'2'3'}$ and also coincide with $\ell_{1'2'}$ since $\ell\alpha$'s x_3 coefficient is zero.

1.3.4 Intersecting a Plane with a Line

$\mathcal{A}$ line's ℓ description in terms of projecting planes points to an easy and intuitive algorithm, shown in Fig. 1.32, for finding the intersection with a plane π. The line $r = \ell\alpha \cap \pi$ is found and then $R = r \cap \ell = \pi \cap \ell$. This is how it works. The algorithm's input are the initial data consisting of the point pairs $\bar{\pi}_{123}, \bar{\pi}_{231'}$ and $\bar{\ell}_1 2, \bar{\ell}_{23}$ specifying the a plane π and line ℓ respectively. The construction of the point $\bar{\ell}_{1'2}$ is easily constructed as in Fig. 1.22

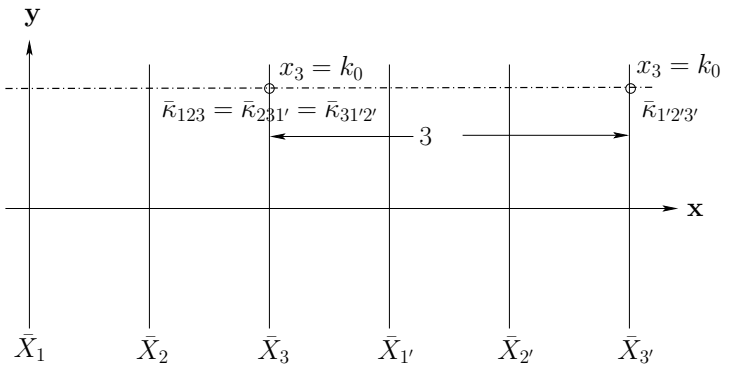

Figure 1.29: Representation of the plane $\kappa : x_3 = k_0$.

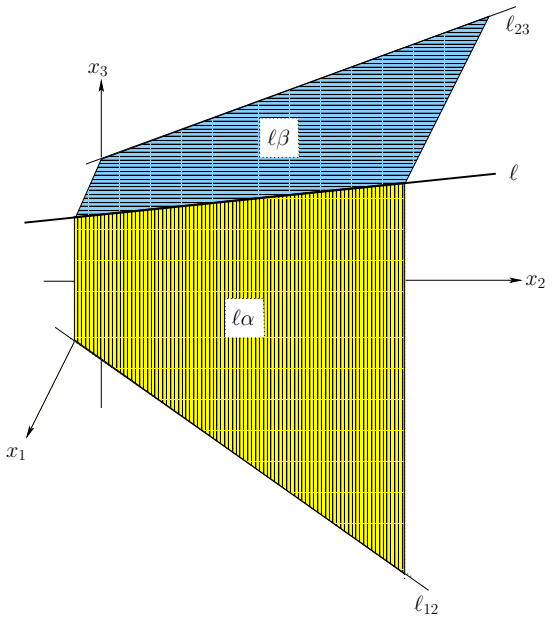

Figure 1.30: A line ℓ as the intersection of the projecting planes $\ell\alpha \perp \alpha$ and $\ell\beta \perp \beta$.

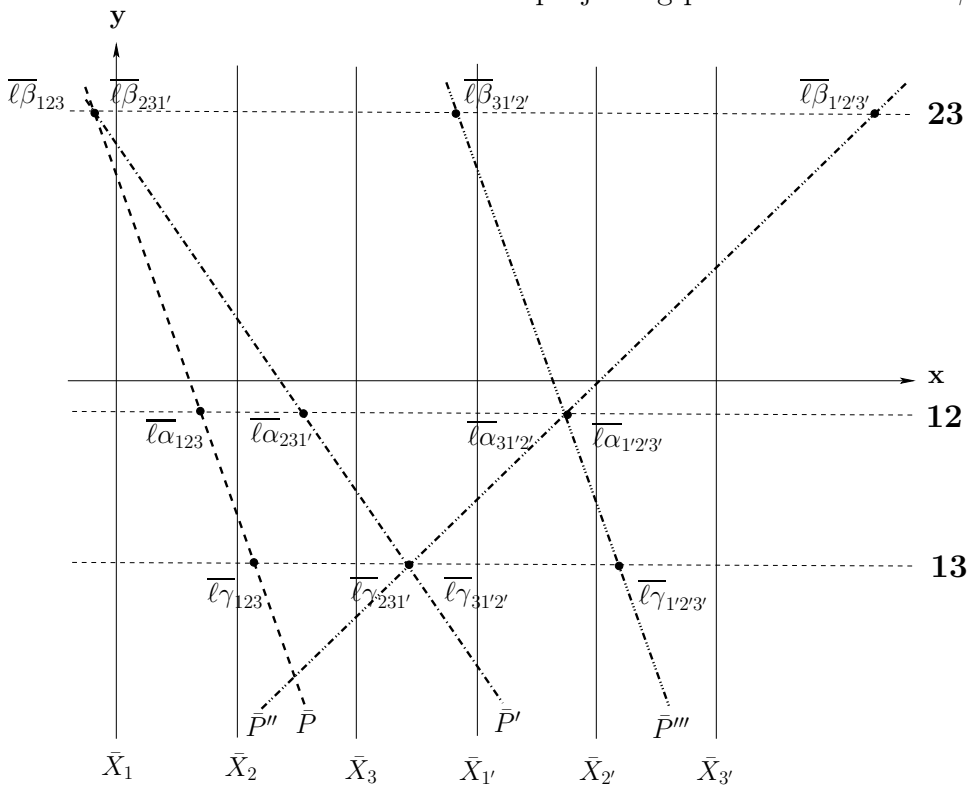

Figure 1.31: The projecting planes $\ell\alpha,\ \ell\beta,\ \ell\gamma$.

This is the line ℓ whose $\bar{\ell}$ points are shown in Fig. 1.25.

from the coordinates x_1, x_2 of *any* point on ℓ and tranferring the x_1 value to the $\bar{X}_1'$ axis. The formality of writing $\overline{\ell\alpha}_{123} = \bar{\ell}_{12}$ and $\overline{\ell\alpha}_{231'} = \bar{\ell}_{1'2}$ clarifies use of the *planes* intersection

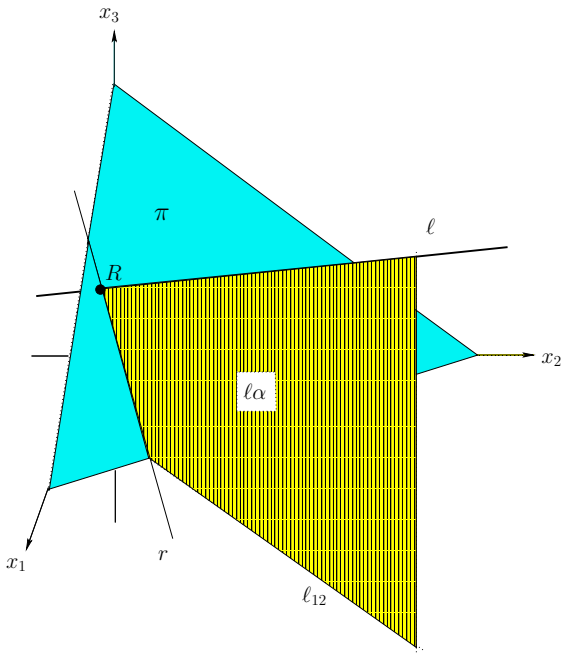

Figure 1.32: Finding $\ell \cap \pi$ using the projecting plane $\ell\alpha$.

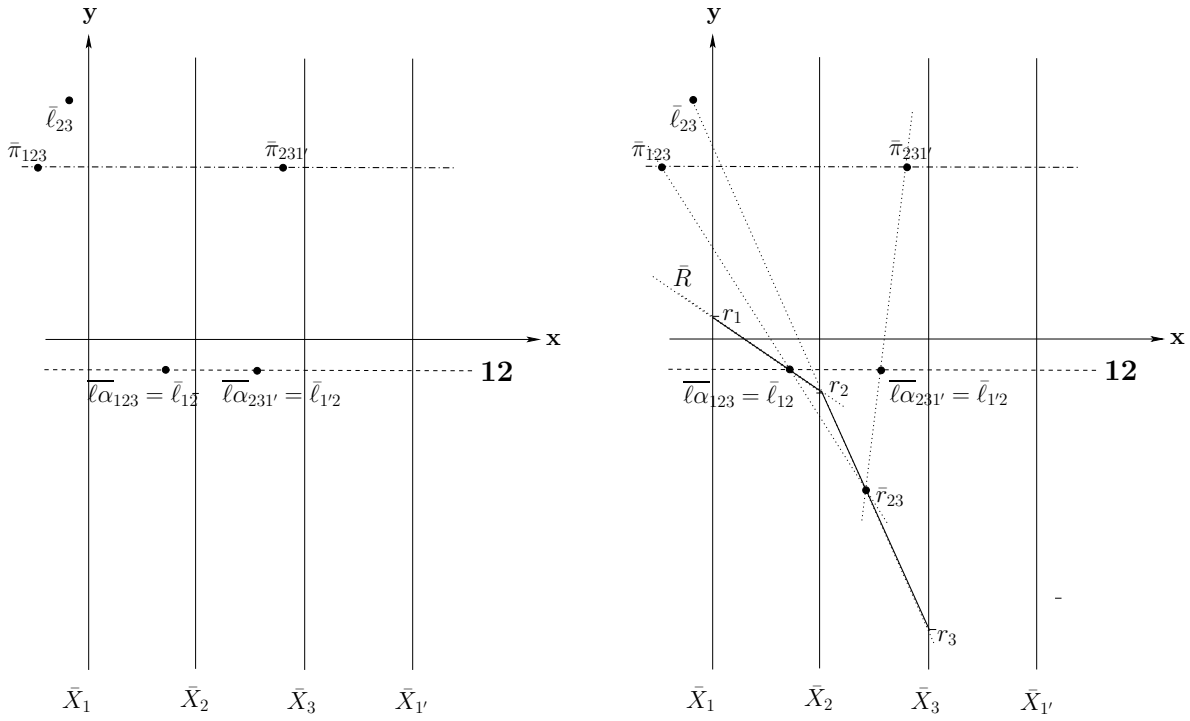

Figure 1.33: Initial data

On the left are the initial data. They are points specifying the plane π and line ℓ, for intersection construction on the right. First $r = \pi \cap \ell\alpha$ is constructed (need only $\bar{r}_{23}$ since $\bar{r}_{12} = \bar{\ell}_{12}$). Then $R = (r_1, r_2, r_3) = r \cap \ell = \pi \cap \ell$.

construction in section 1.2.2 to obtain $r = \pi \cap \ell\alpha$, actually $\bar{r}_{23}$, as in Fig. 1.3.3 with $\bar{r}_{12} = \bar{\ell}_{12}$ since $r \subset \ell\alpha$. Then $R = \ell \cap r = \ell \cap \pi$. In effect the system of linear equations

$$\left\{ \begin{array}{lcll} \pi & : & c_1x_1 + c_2x_2 + c_3x_3 & = c_0 \\ \ell_{1,2} & : & c_{11}x_1 + c_{12}x_2 & = c_{10} \\ \ell_{2,3} & : & c_{22}x_2 + c_{23}x_3 & = c_{20} \end{array} \right. . \tag{1.39}$$

is solved geometrically. The construction is simple, and is easier to draw than in cartesian coordinates. Also it generalizes nicely to N-dimensions.

1.3.5 Separation in $\mathbb{R}^3$ – Points and Planes

$\mathcal{F}$or many applications it is useful to introduce *orientation* and discuss oriented half-spaces as shown in Fig. 1.34 (left) with respect to lines. A point $P : (p_1, p_2)$ is on, above or below the line $\ell : x_2 = mx_1 + b$ if the expression $(p_2 - p_1m) =, <, > b$ as shown on the right-hand part of Fig. 1.34. Since we are working in the projective plane $\mathbb{P}^2$ we consider any regular (i.e. Euclidean) point as being below the ideal line ℓ_∞. This situation is more "fun" in ∥-coords for there the separation criterion "flips" at $m = 1$. Correspondingly, $\bar{P}$ is the line $y = (p_2 - p_1)x + p_1$ where to simplify matters we set $d = 1$. This is due to the *non-orientability* of $\mathbb{P}^2$ as already mentioned in the beginning (chapter on Geometry). For horizontal lines "+" is the positive y direction and for vertical lines the positive x direction. The various cases for $\ell \neq \ell_\infty$ are summarized in :

Lemma 1.3.1 *P is on, below, above a line ℓ whose slope $m < 1 (m \geq 1) \Longleftrightarrow \bar{P}$ is on, below(above), above(below) $\bar{\ell}$.*

In $\mathbb{R}^3$ for a plane π and a point P, for any plane ρ not parallel to π with $P \in \rho$ the intersection $\ell = \pi \cap \rho$ is found. *Within* the plane ρ Lemma 1.3.1 is applied to determine

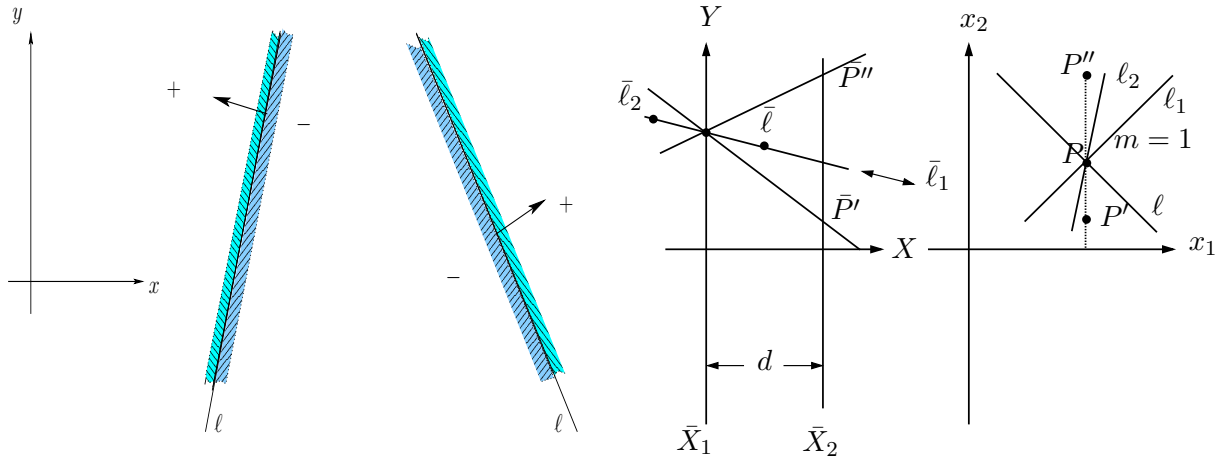

Figure 1.34: Oriented half-spaces and orientation in ∥-coords.

(left)Orienting half-spaces on each side of a line $\ell : ax + by = c$ for $c \geq 0$. Points in " $-$ " : $ax + by < c$ are "below" ℓ and "above" with the reverse inequality.(right) In ∥-coords the above-below relation "flips" for lines with $m = 1$ due to the non-orientability of $\mathbb{P}^2$.

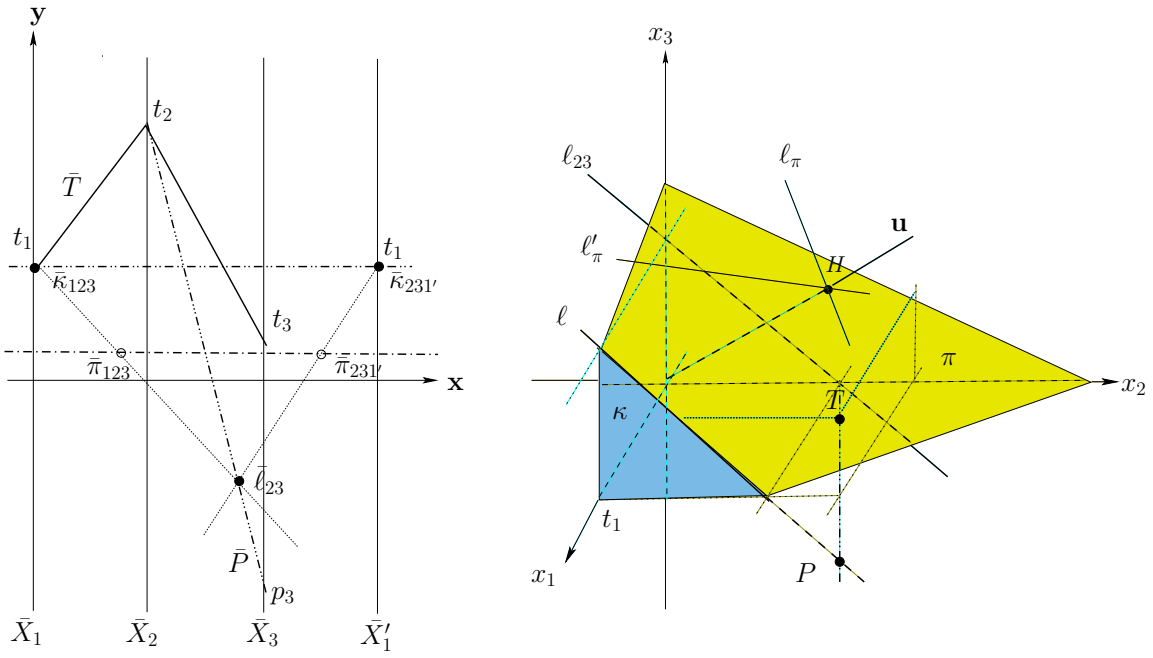

Figure 1.35: Point $T = (t_1, t_2, t_3)$ is above the plane π.

Line $\ell = \pi \cap \kappa$ where $\kappa : x_1 = t_1$ with $P = (t_1, t_2, p_3) \in \ell \cap \pi$. With $\bar{\ell}_{23}$ between the $\bar{X}_2, \bar{X}_1$, i.e. the slope of ℓ_{23} is negative, and *below* the portion $\bar{T}_{23}$ of the polygonal line $\bar{T}$, T is *above* ℓ in the plane κ and also π. This is also clear from the picture since T, $P \in \kappa$ have the same x_1, x_2 coords and $p_3 < t_3$.

whether P is on, below or above $\pi \Leftrightarrow$ it is on, below or above the line ℓ. The construction for this determination is shown in Fig. 1.35 where a point $T = (t_1, t_2, t_3)$ and plane π are shown. The constant plane $\kappa : x_1 = t_1$ which contains T and $\ell = \kappa \cap \pi$ is chosen as well as the point $P = (t_1, t_2, p_3) \in \ell$ (and hence in π). Viewing the picture in $\|$-coords ℓ is found as the intersection of the two planes κ, π (by the construction in Fig. 1.21). Actually only $\bar{\ell}_{23}$ is needed since $\bar{\ell}_{12}$ coincides with $\bar{\kappa}_{123}$ so that κ is ℓ's projecting plane. The $\bar{T}_{12}$ and $\bar{P}_{12}$ portions of $\bar{T}, \bar{P}$ coincide, $\bar{\ell}_{23}$ is below $\bar{T}_{23}$ and in between the $\bar{X}_2$ and $\bar{X}_3$ axes so the slope of ℓ_{23} is negative so by Lemma 1.3.1 T is *above* π.

While we are at it we might as well find the plane ρ parallel to π and containing the point T. Through T the line r parallel to ℓ is determined, see Fig. 1.36, by the point $\bar{r}_{23}$ at the intersection of the vertical line on $\bar{\ell}_{23}$ and $\bar{T}_{23}$. The line $\bar{R}$ on $\bar{r}_{23}$ and $\bar{r}_{12} = \bar{\ell}_{12}$ represents the point $R = r \cap \pi_1^s$ by theorem 1.2.1 and is on the sought after plane ρ since $r \subset \rho$. The point $\bar{\rho}_{123}$ must be on $\bar{R}$ at the intersection of the vertical line through $\bar{\pi}_{123}$ for ρ is to be parallel to π. All the rest is now determined, $\bar{H}_\rho$ is the horizontal line through $\bar{\rho}_{123}$; it intersects the vertical line through $\bar{\pi}_{231'}$ at $\bar{\rho}_{231'}$.

With $\|$-coords then we have the means to do easy synthetic constructions, like those we enjoyed doing in elementary geometry, the lower dimensional ones honing our intuition for their multidimensional counterparts which we shortly meet.

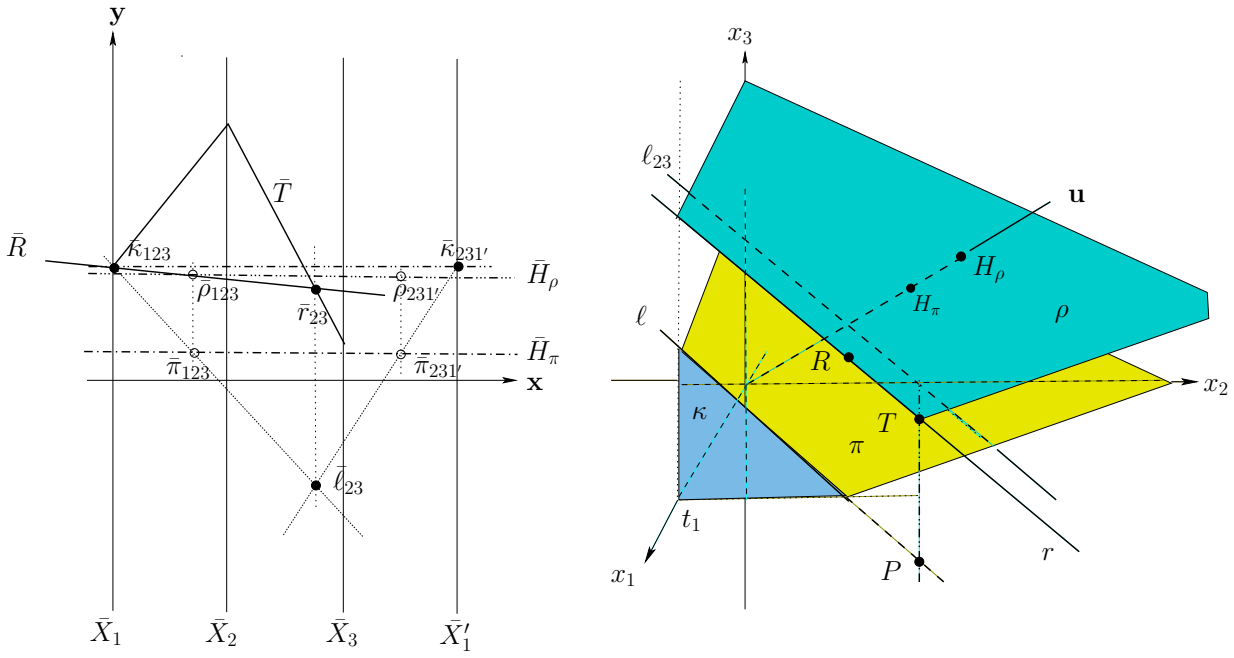

Figure 1.36: Point $T = (t_1, t_2, t_3)$ is above the plane π.

Line $\ell = \pi \cap \kappa$ where $\kappa : x_1 = t_1$ with $P = (t_1, t_2, p_3) \in \ell \cap \pi$.

1.3.6 Rotation of a Plane about a Line and the Dual Translation

The analogue to the translation $\leftrightarrow$ rotation duality in Fig. 1.8, based on the index-point representation, brings into play many of the constructions we just learned. Starting with

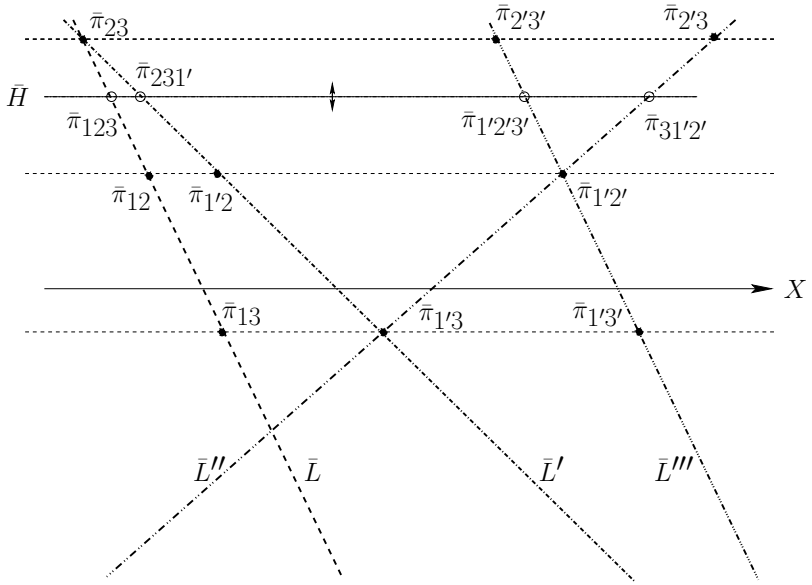

Figure 1.37: Rotation of a 2-flat (plane) about a 1-flat(line) in $\mathbb{R}^3$.

It corresponds to a translation of the points with 3 indices on the horizontal line $\bar{H}$ along the lines $\bar{L}$, $\bar{L}'$, $\bar{L}''$, $\bar{L}'''$ joining the points with 2 indices.

augmented representation of a 2-flat with 4 rather than 2 points, as derived in Fig. 1.22, 1.23 and 1.24, the intent is to show the rotation of a plane $\pi^2 : c_1x_1 + c_2x_2 + c_3x_3 = c_0$ about a line π^1. With only one line and plane appearing the superscripts denoting the flats' dimensionality are not needed for the flat's dimensionality can be determined from the number of subscripts. In reference to Fig. 1.37 a position of π^2 is shown by the points $\bar{\pi}_{123}\,, \bar{\pi}_{231'}, , \bar{\pi}_{31'2'}\,, \bar{\pi}_{1'2'3'}$ representing π^2 on the horizontal line $\bar{H}$, while the line's π^1 3 points $\bar{\pi}_{12}\ ,\ \bar{\pi}_{13}\ ,\ \bar{\pi}_{23}$ on the line $\bar{L}$ which, as in Fig 1.25, also appears in terms of the other triples of axes with $L = \pi^1 \cap \pi^s_1$ and similarly L', L'', L''' being the line's intersections with the 2nd, 3rd and 4th super-planes. To clarify

$$\bar{\pi}_{1'2}\,\bar{\pi}_{1'3}\,\bar{\pi}_{2'3}\ \textit{on line}\ \bar{L}' \quad , \bar{\pi}_{12'}\,\bar{\pi}_{13'}\,\bar{\pi}_{2'3'}\ \textit{on line}\ \bar{L}'' \quad , \bar{\pi}_{12'}\,\bar{\pi}_{13'}\,\bar{\pi}_{2'3'}\ \textit{on line}\ \bar{L}'''.$$

With $\pi^1 \subset \pi^2$ the picture is that shown in Fig. 1.20 where the point $\bar{\pi}_{123}$ is on the intersection of $\bar{H}$ with the line $\bar{L}$ and similarly

$$\bar{\pi}_{231'} \ = \bar{H} \cap \bar{L}'\,, \bar{\pi}_{31'2'} \ = \bar{H} \cap \bar{L}''\,, \bar{\pi}_{1'2'3'} = \bar{H} \cap \bar{L}'''\ . \tag{1.40}$$

The distance between adjacent points being proportional to the coefficient of the plane's equation, see Fig 1.18, the intersections of the $\bar{L}$-lines mark the positions where coefficients are zero. There, the plane π^2 is perpendicular to the corresponding principal 2-plane. Specifically at

$$\begin{array}{ll} \bar{H} \cap \bar{L} \cap \bar{L}'\,, & c_1 = 0\ \ \&\ \ \pi^2 \perp x_2x_3 - \textit{plane}\ , \\ \bar{H} \cap \bar{L}' \cap \bar{L}''\,, & c_2 = 0\ \ \&\ \ \pi^2 \perp x_1x_3 - \textit{plane}\ , \\ \bar{H} \cap \bar{L}'' \cap \bar{L}'''\,, & c_3 = 0\ \ \&\ \ \pi^2 \perp x_1x_2 - \textit{plane}\ . \end{array} \tag{1.41}$$

Now translate $\bar{H}$ vertically with the 4 triply indexed $\bar{\pi}$ points moving along the four lines $\bar{L}, ..., \bar{L}'''$. The conditions (1.40) hold so that at *any* such translated position of $\bar{H}$ the containment property of Fig. 1.20 holds. Hence, the corresponding transformation must be the rotation of π^2 about π^1 passing along the way through the positions specified by (1.41) with all points on π^1 being invariant under the transformation. The variation of the coefficients can be followed thoughout the transit.

Let us look at all this in "reverse" for the axis of rotation given by

$$\pi^1 : \left\{ \begin{array}{l} \pi^1_{12} : x_2 = m_2x_1 + b_2\ , \\ \pi^1_{23} : x_3 = m_3x_2 + b_3\ . \end{array} \right. \tag{1.42}$$

properly read then Fig. 1.37 exhibits the full pencil of planes

$$\pi^2 : (x_3 - m_3x_2 - b_3) + k(x_2 - m_2x_1 - b_2) = 0 \tag{1.43}$$

on the line π^1, the parameter's k value being determined by the corresponding y-coordinate of $\bar{H}$. With some reflection aided by Fig. 1.7 it is becomes clear that rotation of the line $\bar{L}$ about the point $\bar{\pi}_{123}$, inducing rotations of $\bar{L}', \bar{L}'', \bar{L}'''$ about the points $\bar{\pi}_{1'23}, \bar{\pi}_{1'2'3}, \bar{\pi}_{1'2'3'}$ respectively, corresponds to a translation of the line π^1 on π^2 (Exercise 5).

Fun & Games with the ILM

Open ILM2 and *click the 5th button with the ∥-coords icon*
The plane and line in Cartesian coords are on the right
A picture similar to Fig. 1.37 appears on the left

For some experimentation:
translate vertically the horizontal line $\bar{H}$ on the 4 $\bar{\pi}$ points and observe
that the $\bar{\pi}$ slide along the $\bar{L}\ldots\bar{L}'''$ lines.
Note the distance between the adjacent $\bar{\pi}$
and the coefficients of the plane's equation at the bottom.

In preparation for the next discussion
place the line $\bar{H}$ on each of the line intersections i.e. $\bar{L}\cap\bar{L}'$ etc.
Note that then the plane is perpendicular to a principal 2-plane

Change the line and/or plane and repeat.

An important phenomenon occurs when the horizontal line $\bar{H}$ crosses the intersection points of the $\bar{L}^i$ lines with $i=0,1,2$ denoting the number of primes. The coefficients $c_i\neq 0$, and in this case are all positive, for $\bar{H}$ in the position shown in 1.38. When $\bar{H}$ is on the point $\bar{L}'\cap\bar{L}''$ the $\bar{\pi}_{231'},\bar{\pi}_{31'2'}$ coincide. Hence $c_2=0$ (see Fig. 1.18) and the plane π being

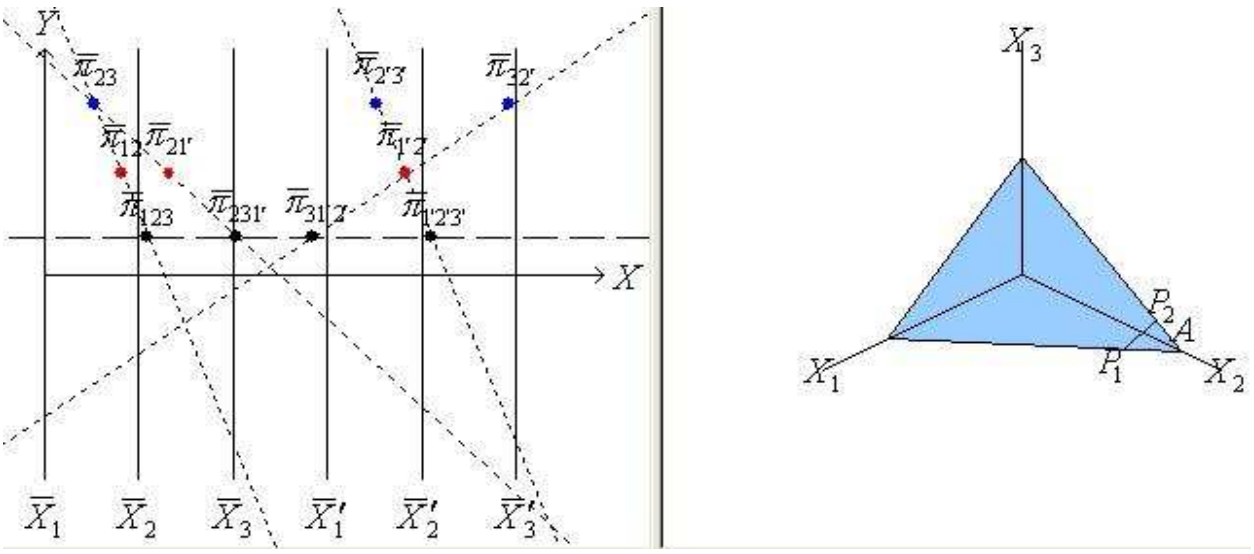

Figure 1.38: Rotation of a plane about a line in Cartesian and ∥-coords.

In this instance all the coefficients of the plane's equation $c_i\not>0$.

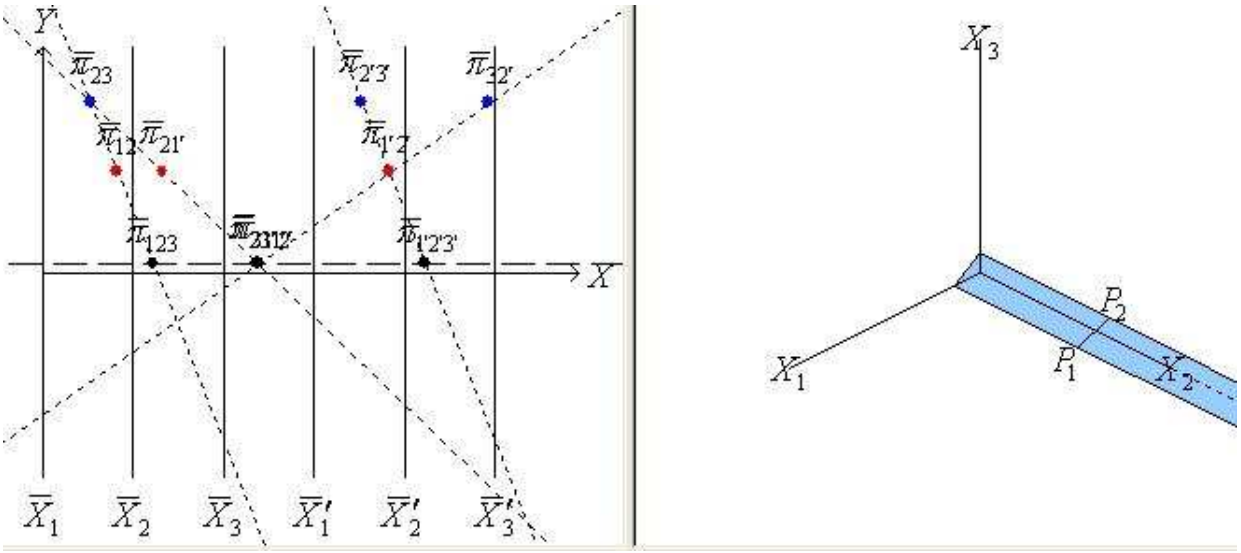

Figure 1.39: Here $c_2 \approx 0$ and positive.

The line $\bar{H}$ being just *above* the point $\bar{L}' \cap \bar{L}''$ indicates the plane is nearly perpendicular to the 2-plane x_1x_3.

perpendicular to the x_1x_3 plane. Pursuing this closely, in Fig. 1.39 $\bar{H}$ is just above this point and Fig. 1.40 just below the point significantly showing that that π has *flipped*. Consider the *oriented* plane together with its normal vector $\vec{N}$, whose components are the coefficients

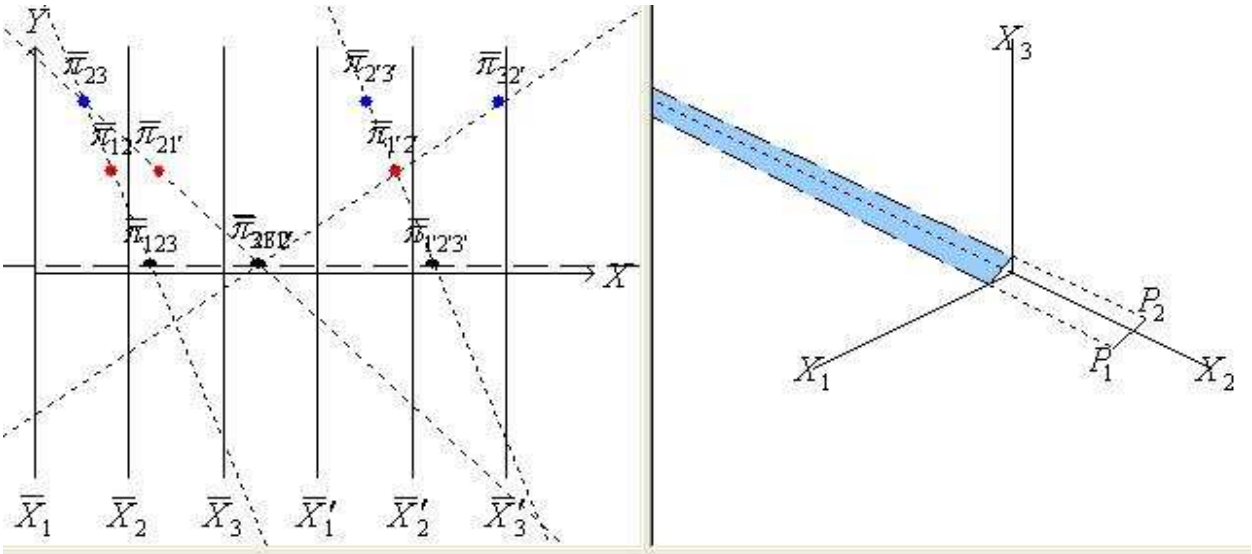

Figure 1.40: Here $c_2 \approx 0$ and negative the.

The line $\bar{H}$ being just *below* the point $\bar{L}' \cap \bar{L}''$. The plane is nearly perpendicular to the principal plane x_1x_3 but has "flipped" compared to the previous figure.

c_i, we show next that $\bar{H}$ that just traversing *all 3* the points $\bar{L}^i \cap \bar{L}^{i+1}$ corresponds to the plane making a 180^0 rotation about its axis resulting in the normal $\vec{N} \to -\vec{N}$.

Let

$$\bar{L}^i \ : \ y = m_i x + b_i \ , \ i = 0, 1, 2, 3 \ , \tag{1.44}$$

$$(x_I, y_I) = \bar{L}' \cap \bar{L}'' = \left(-\frac{(b_2 - b_1)}{(m_2 - m_1)} \ , \ \frac{(m_2 b_1 - m_1 b_2)}{(m_2 - m_1)} \right) \tag{1.45}$$

For a value $\epsilon > 0$ with the superscripts $+$, $-$ denoting values above or below y_I respectively,

$$y^+ = y_I + \epsilon = m_i x_i^+ + b_i \ , \ y^- = y_I + \epsilon = m_i x_i^- + b_i \ ,$$
$$x_i^+ = x_I + \epsilon/m_i \ , \ x_i^- = x_I - \epsilon/m_i \ .$$

Then

$$c_2^+ = k(x_2^+ - x_1^+) = \epsilon(m_1 - m_2)/m_1 m_2 \ , \ c_2^- = k(x_2^- - x_1^-) = -\epsilon(m_1 - m_2)/m_1 m_2 \ ,$$

$$\Rightarrow \quad c_2^+/c_2^- = -1 \ , \tag{1.46}$$

where k is a proportionality constant. It is clear from Fig. 1.38 or from an easy calculation that $c_1^+/c_1^- \approx 1 \approx c_3^+/c_3^-$ for ϵ small. Therefore, as

$$\epsilon \to 0 \ \Rightarrow \ c_1^+/c_1^- \to 1 \ , \ c_3^+/c_3^- \to 1 \quad \textbf{and} \quad c_2^+/c_2^- \to -1 \ . \tag{1.47}$$

As $\bar{H}$ traverses the point $\bar{L}' \cap \bar{L}''$, the plane π remains perpendicular to the x_1x_3-plane with *the x_2 component of the normal $\vec{N}$ flipping its orientation by* 180^0. With c_1 and c_3 unchanged this amounts to the plane π "flipping" *with respect to the principal plane x_1x_3*. That is what is seen in Fig. 1.39, 1.40. Of course, a similar flip occurs when $\bar{H}$ traverses either $\bar{L} \cap \bar{L}'$ or $\bar{L}'' \cap \bar{L}'''$ as stated below, the superscripts $+, -$ referring to above/below position of $\bar{H}$ with respect to the intersection point.

Corollary 1.3.2 *(***Flip***) For an oriented plane π, having normal vector $\vec{N} = (c_1, c_2, c_3)$, rotating about a line ℓ, the traversal of the point $\bar{L}^i \cap \bar{L}^{i+1}$, $i = 0, 1, 2$ by $\bar{H}$ corresponds to $c_i^+/c_i^- \to -1$, $c_j^+/c_j^- \to 1$, $j \neq i$.*

This observation is useful in the study of non-orientability as for the Möbius strip in Chapter **??** on surfaces.

Specializations and Generalizations

We have seen that the rotation of a plane about an axis is completely determined by the translation of $\bar{H}$ with the $\bar{\pi}_{123}, \bar{\pi}_{231'}$ along the two lines $\bar{L}, \bar{L}'$. Pictorializing the rotation facilitates its customization to specific cases. For example, what rotation leaves the coefficient c_1 of the plane's equation invariant? The geometric requirement is for $\bar{L}$ and $\bar{L}'$ to be parallel, that is their point of intersection $\bar{\pi}_{23}$ is ideal, which occurs when the slope $m_3 = 1$ in eq. 1.42. The rotation then leaves the first coefficient c_1 invariant, the direction of $\bar{L}$ and hence of $\bar{\pi}_{23}$ is determined by b_3. All that is seen in Fig. 1.41 with the corresponding translation of $\bar{H}$ the $\bar{\pi}_{123}, \bar{\pi}_{231'}, \bar{\pi}_{31'2'}, \bar{\pi}_{1'2'3'}$ rolling along $\bar{L}, \bar{L}', \bar{L}'', \bar{L}'''$ respectively show the variation of

the plane's equation other coefficients. The construction starts by chosing $\bar{L}$ and $\bar{L}'$ in the direction given by b_3 while the horizontal distance is $3c_1$. As in Fig. 1.22 the coordinates of $\bar{L}'$ determine the points $\bar{\pi}_{12}, \bar{\pi}_{13}$ and the lines **12, 13**. Or conversely these are obtained from the line's equation either way proceeding as outlined in section 1.3.2 where only $\bar{L}''$ is not parallel to $\bar{L}$. The pencil of planes obtained by the vertical translation of $\bar{H}$ is now

$$\pi^2 : (x_3 - x_2 - b_3) + k(x_2 - m_2 x_1 - b_2) = 0 \, . \tag{1.48}$$

Here it is assumed that the axis of rotation π^1 lies on the plane π^2 (see exercise 7) . Then for $\pi^2 : c_1x_1 + c_2x_2 + c_3x_3 = c_0$,

$$\begin{array}{l} \pi^1_{23} : x_3 = x_2 + b_3 \\ \pi^2_{12} : x_2 = \frac{c_1}{c_2+c_3} x_1 + \frac{c_0 - c_3 b_3}{c_2+c_3} \, . \end{array} \tag{1.49}$$

The translation of $\bar{H}$ is not the essential "ingredient" for there is no vertical movement when the axis of a plane's rotation is on the point H. For our purposes this means that the lines $\bar{L}, \bar{L}'$ are on $\bar{H}$ and the points $\bar{\pi}_{123}, \bar{\pi}_{231'}$ move only horizontally, and there are some interesting sub-cases. For example rotation of a plane π about its ℓ_π results in $\bar{\pi}_{123}$ being stationary (since it is ℓ_π) while $\bar{\pi}_{231'}$ is tranlated along $\bar{H}$ together, of course, with the other

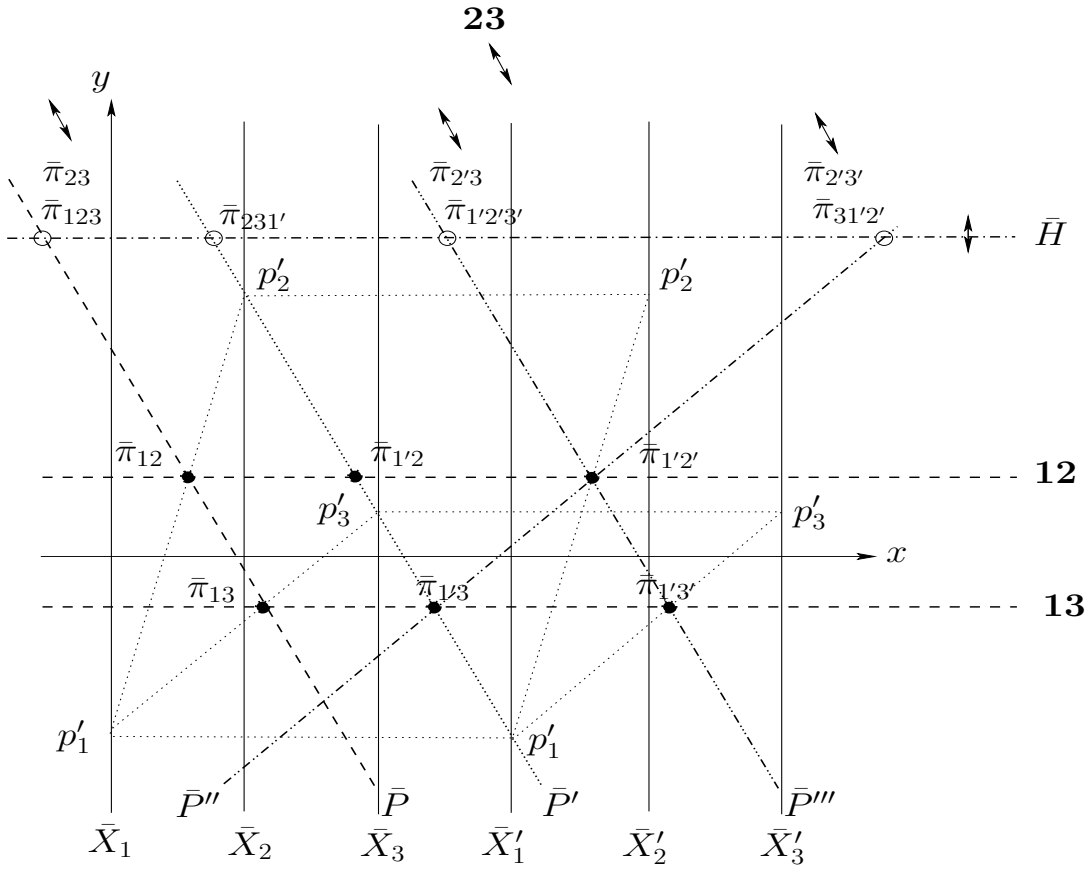

Figure 1.41: Rotation of a plane π^2 about a line π^1 with c_1 constant.

two points. Similarly rotation about ℓ'_π leaves $\bar{\pi}_{231'}$ stationary. Rotation about a general axis $\pi^1 \subset \pi^2$ on H results in all triply indexed points moving simultaneously along $\bar{H}$.

The rotation of a plane π viewed in ‖-coords as the movement of points opens up new vistas for generalizations. For parallel translations of π the corresponding movement in ‖-coords is vertical with the "pencil" of planes so generated being the family represented in Fig. 1.19. It is didactic to design the transformation of planes defining the corresponding pair of loci of the points $\bar{\pi}_{123}, \bar{\pi}_{231'}$ on the plane. For example, in chapter **??** it is shown that any developable surface σ is represented by a pair of curves with the same minimum and maximum y-coordinate, σ being the envelope of a one parameter family of tangent planes (exercise 8). So in $\mathbb{R}^N$ a developable hypersurface is represented by $N-1$ such curves.

With some care the composition of transformations can be specified and visualized as the union of the corresponding loci. Consider for example the representation of "wobbling", as in the motion of a spinning-top, as the composition of a rotation about an axis rotating about its tip while moving along a path on a plane (exercise 9). The interesting generalizations to $\mathbb{R}^N$ are an excellent research topic, see for example ([1] pp. 403-409) and sections **??**, **??** in Chapter **??**.

Exercises

1. Given three non-collinear points $P \in \pi^s_1, P' \in \pi^s_{1'}, P'' \in \pi^s_{1'2'}$ provide an algorithm which finds the representation of the 2-flat π^2 which contains the three points. Even though a plane is uniquely specified by 3 non-collinear points, in this case the algorithm should take advantage of the fact that 3 given points belong to the 3 principal *sp*.

2. For the construction of the four indexed points in section 1.3.2 prove that any choice of the three lines $\bar{L}, \bar{L}', \bar{L}''$ gives the same result.

3. Draw the figures corresponding to Fig. 1.41 but for rotations leaving the second and separately the third coefficients of the plane's equation invariant.

4. Find k in eq. 1.48 as a function of the corresponding y-coordinate of $\bar{H}$ and then specialize it to the subcases given.

5. Draw the figure corresponding to Fig. 1.37 for an axis of rotation through the point H of the plane. In this case $\bar{L}$ and $\bar{H}$ coincide.

6. Find the angle of rotation of a 2-flat π about a 1-flat π^1 as a function of the motion of the triply indexed $\bar{\pi}$ points. Specialize for the case when π^1 is on the point H.

7. Draw the figure showing the rotation of a plane π^2 about a line π^1 *not* on π^2 and include the $\pi^2 \cap \pi^1$.

8. Describe the transformation of a plane where the points $\bar{\pi}_{123}$ and $\bar{\pi}_{1'23}$ each trace two different ellipses having the same minimum and maximum y-coordinate.

9. Provide the geometric locus for the representation of a plane's wobbling (last sentence of this section).

10. Construct the constant planes representation in higher dimensions.

11. Prove the correctness of the algorithm for

    (a) The intersection of 2 planes.

    (b) The intersection of a line with a plane.

    This means to show that for any input the algorithm terminates with the correct output.

1.4 Hyperplanes and p-flats in $\mathbb{R}^N$

1.4.1 The Higher Dimensional Super-Planes

$\mathcal{J}$ust as for $\mathbb{R}^3$ we expect the super-planes in $\mathbb{R}^N$ consisting of points of the form eq. (1.7) to play a fundamental role. They are denoted by π^{Ns} to mark their dimensionality and abbreviated to *sp*. We use the general the axes spacing $\mathbf{d} = (d_1, d_2, ..., d_i, ..., d_N)$ this notation designating that the axis $\bar{X}_i$ is at $x_i = d_i$ and recall that the *sp* are on the line

$$u : x_2 = x_1 \ , \ x_3 = x_2 \ , \ \ldots \ , \ x_i = x_{i-1} \ , \ \ldots \ , \ x_N = x_{N-1} \ . \tag{1.50}$$

Being 2-flats the *sp* are described by $N-2$ linearly independent equations which after some matrix manipulations can be given with 2 variables each as :

$$\pi^{Ns} : \left\{ \begin{array}{lll} \pi^{Ns}_{123} & : & (x_2 - x_1) + k_1(x_3 - x_2) = 0 \ , \\ \pi^{Ns}_{234} & : & (x_3 - x_2) + k_2(x_4 - x_3) = 0 \ , \\ & \ldots & \\ \pi^{Ns}_{i(i+1)(i+2)} & : & (x_{i+i} - x_i) + k_i(x_{i+2} - x_{i+1}) = 0 \ , \\ & \ldots & \\ \pi^{Ns}_{(N-2)(N-1)N} & : & (x_{N-i} - x_{N-i-1}) + k_{N-1}(x_N - x_{N-1}) = 0 \ . \end{array} \right. \tag{1.51}$$

The form of the equations stems from the fact that in the 3-dimensional subspace $x_{i-2}x_{i-1}x_i$, $\pi^{Ns}_{(i-2)(i-1)i}$ is the pencil of 2-flats on the 1-flat (line) $x_{i-1} = x_{i-2}, \ x_i = x_{i-1}$. Pointing out that each such 2-flat contains the points $(1,1,1)$, (d_{i-2}, d_{i-1}, d_i) enables the elimination of the parameter k_i in the equations π^{Ns} which are rewritten in terms of the axes spacing as :

$$\begin{array}{rcl} \pi^{Ns}(d_1, d_2, d_3) & : & (d_3 - d_2)x_1 + (d_1 - d_3)x_2 + (d_2 - d_1)x_3 = 0 \ , \\ \pi^{Ns}(d_2, d_3, d_4) & : & (d_4 - d_3)x_2 + (d_2 - d_4)x_3 + (d_3 - d_2)x_4 = 0 \ , \\ & \ldots & \\ \pi^{Ns}(d_i, d_{i+1}, d_{i+2}) & : & (d_{i+2} - d_{i+1})x_i + (d_i - d_{i+2})x_{i+1} + (d_{i+3} - d_i)x_{i+2} = 0 \ , \\ & \ldots & \\ \pi^{Ns}(d_{N-2}, d_{N-1}, d_N) & : & (d_N - d_{N-1})x_{N-2} + (d_{N-2} - d_N)x_{N-1} + (d_{N-1} - d_{N-2})x_N = 0 \ . \end{array} \tag{1.52}$$

For example in $\mathbb{R}^4$ the *sp* are given by

$$\pi^{4s} : \left\{ \begin{array}{ll} \pi^{4s}_{123} & : (d_3 - d_2)x_1 + (d_1 - d_3)x_2 + (d_2 - d_1)x_3 = 0 \\ \pi^{4s}_{234} & : (d_4 - d_3)x_2 + (d_2 - d_4)x_3 + (d_3 - d_2)x_4 = 0 \end{array} \right. \ . \tag{1.53}$$

This is a good time to make a recursive notational convention[3] for the axes spacing obtained by the successive translations of the $\bar{X}_i$ to the new positions $\bar{X}_{i'}$. For the initial N axes system $\bar{X}_1, \bar{X}_2, \ldots, \bar{X}_N$ we write

$$\mathbf{d_N^0} = \overbrace{(0, 1, 2, \ldots, i-1}^{i}, \ldots, N-1) \; .$$

This states that the first axis $\bar{X}_1$ is placed at $x = 0$, $\bar{X}_2$ is placed at $x = 2$ ... and $x = N-1$ for $\bar{X}_N$. After translating the $\bar{X}_1$ axis one unit to the right of $\bar{X}_N$, renaming it $\bar{X}_{1'}$, the axes spacing N-tuple is

$$\mathbf{d_N^1} = \mathbf{d_N^0} + (N, 0, \ldots, 0) = \overbrace{(N, 1, 2, \ldots, i-1}^{i}, \ldots, N-1) \; .$$

And after i such successive unit translations with the $\bar{X}_i$ axis in position $\bar{X}_{i'}$ the axes spacing for $i = 0, \ldots, N$, $k = 1, \ \ldots, \ N$ is given by

$$\mathbf{d_N^i} = \mathbf{d_N^0} + \overbrace{(N, \ldots, N}^{i}, 0, \ldots, 0) = \overbrace{(N, N+1, \ldots, i-1+N}^{i}, i, ..., N-1) = (d_{ik}) \; . \quad (1.54)$$

To clarify the indices, i refers to the number of the axes translations and k is the position (component) within the vector $\mathbf{d_N^i}$. Using the step function

$$S_i(k) = \begin{cases} 1 & i \geq k \\ 0 & i < k \end{cases} \; , \quad (1.55)$$

the axes-spacing after the ith translation can be conveniently written as

$$\mathbf{d_N^i} = (d_{ik}) = (k - 1 + NS_i(k)) \; . \quad (1.56)$$

When the dimensionality is clear from the context the subscript N can be omitted. For a flat π^p expressed in terms of the $\mathbf{d_N^i}$ spacing, the points $\bar{\pi}^p_{1',\ldots,i',i+1,\ldots,N}$ of its representation are denoted compactly by $\bar{\pi}^p_{i'}$ and it is consistent to write $\pi^p = \pi^p_{0'}$, that is π^p described in terms of the axis spacing $\mathbf{d_N^0}$.

Returning now to the higher dimensional *sp*, in $\mathbb{R}^4$ for the standard spacing $\mathbf{d^0}$

$$\pi^{4s}_{0'} : \begin{cases} \pi^s_{123} & : x_1 - 2x_2 + x_3 = 0 \\ \pi^s_{234} & : x_2 - 2x_3 + x_4 = 0 \end{cases} \; . \quad (1.57)$$

The axes are translated, as in $\mathbb{R}^3$, to generate different *sp* corresponding to rotations about u which are summarized in Fig 1.42. First, the axis $\bar{X}_1$ is translated to position $\bar{X}_{1'}$ one unit to the right of $\bar{X}_4$ with the resulting axes spacing $\mathbf{d^1} = (4, 1, 2, 3)$ yielding

$$\pi^{4s}_{1'} : \begin{cases} \pi^s_{1'23} & : x_1 + 2x_2 - 3x_3 = 0 \\ \pi^s_{234} & : x_2 - 2x_3 + x_4 = 0 \end{cases} \; . \quad (1.58)$$

The angle of rotation between π^{4s}_{123} and $\pi^{4s}_{1'23}$ computed via eq. (1.29) is $cos^{-1}\left(-\sqrt{3/7}\right) = 180^o - \phi \; , \quad \phi = cos^{-1}\left(\sqrt{3/7}\right) \approx 49.1^o$. Note that since π^s_{234} remains unchanged this is not

[3] I am indebted to Liat Cohen for proposing this notation.

a complete rotation of π^{4s}_{1234} about the line u. Proceeding, with the translation of $\bar{X}_2$ to position $\bar{X}'_2$ one unit to the right of $\bar{X}_{1'}$ provides the axes spacing $\mathbf{d^2} = (4, 5, 2, 3)$ and the *sp*

$$\pi^{4s}_{2'} : \begin{cases} \pi^s_{1'2'3} & : 3x_1 - 2x_2 - x_3 = 0 \\ \pi^s_{2'34} & : x_2 + 2x_3 - 3x_4 = 0 \end{cases} . \tag{1.59}$$

The angle between $\pi^s_{1'23}$ and $\pi^s_{1'2'3}$ is $cos^{-1}(-1/7) = 2\phi$ while the angle between π^s_{234} and $\pi^s_{2'34}$ is $180^o - \phi$. With the translation of $\bar{X}_3$ to position $\bar{X}_{3'}$ one unit to the right of $\bar{X}'_2$, $\mathbf{d^3} = (4, 5, 6, 3)$ and

$$\pi^{4s}_{3'} : \begin{cases} \pi^s_{1'2'3'} & : x_1 - 2x_2 + x_3 = 0 \\ \pi^s_{2'3'4} & : 3x_2 - 2x_3 - x_4 = 0 \end{cases} . \tag{1.60}$$

returning $\pi^s_{1'2'3'}$ to its original position π^s_{123} while bringing $\pi^s_{2'3'4}$ to an angle 2ϕ from $\pi^s_{2'34}$. Again this is not a complete rotation of the whole *sp* about the line u. The final translation of $\bar{X}_4$ to $\bar{X}_{4'}$ one unit to the right of $\bar{X}_3$ provides $\mathbf{d^4} = (4, 5, 6, 7)$ and

$$\pi^{4s}_{4'} : \begin{cases} \pi^s_{1'2'3'} & : x_1 - 2x_2 + x_3 = 0 \\ \pi^s_{2'3'4'} & : x_2 - 2x_3 + x_4 = 0 \end{cases} . \tag{1.61}$$

which is identical to π^s_{1234}. Unlike $\mathbb{R}^3$ the rotations angles are not all equal though the sum is a full circle. The "anomaly" suggest that $\phi(N)$ is a function of the dimensionality N with $\phi(3) = 60^o$ and $\phi(4) \approx 49.1^o$ and it is interesting to investigate. For $\mathbb{R}^N$ we look at π^{Ns}_{123} with $\mathbf{d}^0 = (0, 1, 2, ..., N-2, N-1)$ and after the translation of $\bar{X}_1$ to position $\bar{X}_{1'}$ with the axes spacing is $\mathbf{d}^1 = (N, 1, 2, ..., N-2, N-1)$ yielding respectively the two corresponding $\pi^{Ns}(d_1, d_2, d_3)$ in eq. (1.52) :

$$\begin{cases} \pi^{Ns}_{123} & : x_1 - 2x_2 + x_3 = 0 \ , \\ \pi^{Ns}_{1'23} & : x_1 + (N-2)x_2 + (1-N)x_3 = 0 \ . \end{cases} \tag{1.62}$$

The angle function is

$$\phi(N) = cos^{-1}\left(\tfrac{\sqrt{3}(N-2)}{2\sqrt{3-3N+N^2}} \right) , \tag{1.63}$$

some of whose values are $\phi(5) \approx 47.88^o$, $\phi(6) = 45^o$ and the $\lim_{N\to\infty} \phi(N) = 30^o$.

Next let us compute the 1-flat (line) intersection $\ell_\pi = \pi^{4s} \cap \pi$ where the plane $\pi \subset \mathbb{R}^4$ to find the index points representationt for π first for a general axes spacing $\mathbf{d} = (d_1, d_2, d_3, d_4)$ described by :

$$\begin{cases} \pi & : c_1x_1 + c_2x_2 + c_3x_3 + c_4x_4 = c_0 \ , \\ \pi^{4s}_{123} & : (d_3 - d_2)x_1 + (d_1 - d_3)x_2 + (d_2 - d_1)x_3 = 0 \\ \pi^{4s}_{234} & : (d_4 - d_3)x_2 + (d_2 - d_4)x_3 + (d_3 - d_2)x_4 = 0. \end{cases} \tag{1.64}$$

With the notation

$$\begin{cases} a = c_1(d_2 - d_1) + c_3(d_2 - d_3) + c_4(d_2 - d_4) \ , \\ b = c_2(d_2 - d_1) + c_3(d_3 - d_1) + c_4(d_4 - d_1) \ , \end{cases} \tag{1.65}$$

the line intersection is given by

$$\ell_\pi : x_2 = -\frac{a}{b}x_1 + \frac{(d_2 - d_1)}{b}c_0 \ . \tag{1.66}$$

Since $\ell_\pi \subset \pi^{4s}_{1234}$, $\bar{\ell}_{\pi_{ij}} = \bar{\ell}_{\pi_{kr}}$ for distinct indices $i,j,k,r \in (1,2,3,4)$ so that in homogeneous coordinates

$$\bar{\ell}_{\pi_{12}} = \big(\ (d_2-d_1)b + d_1\textstyle\sum_{i=1}^4 c_i\ , (d_2-d_1)c_0\ , \sum_{i=1}^4 c_i)\ \big) = (\sum_{i=1}^4 c_i d_i\ , c_0\ , \sum_{i=1}^4 c_i)\ . \quad (1.67)$$

Substituting the axes spacing $\mathbf{d^i_N}$ in the above the indexed points for the representation of π are obtained below where $S = \sum_{i=1}^4 c_i$:

$$\begin{cases} \bar{\pi}_{0'} = \bar{\pi}_{1234} & = (c_2 + 2c_3 + 3c_4\ , c_0\ , S)\ , \\ \bar{\pi}_{1'} = \bar{\pi}_{1'234} & = (4c_1 + c_2 + 2c_3 + 3c_4\ , c_0\ , S) \\ \bar{\pi}_{2'} = \bar{\pi}_{1'2'34} & = (4c_1 + 5c_2 + 2c_3 + 3c_4\ , c_0\ , S)\ , \\ \bar{\pi}_{3'} = \bar{\pi}_{1'2'3'4} & = (4c_1 + 5c_2 + 6c_3 + 3c_4\ , c_0\ , S)\ , \\ \bar{\pi}_{4'} = \bar{\pi}_{1'2'3'4'} & = (4c_1 + 5c_2 + 6c_3 + 7c_4\ , c_0\ , S)\ . \end{cases} \quad (1.68)$$

We wrote this out in full detail to show that again the distance between adjacently indexed points, appearing on the left above in simplified notation, is as for $\mathbb{R}^3$ proportional (equal to the dimension) to the corresponding coefficient. Specifically,

$$\begin{cases} \bar{\pi}_{1'} - \bar{\pi}_{0'} & = (4c_1\ , 0\ , 0)\ , \\ \bar{\pi}_{2'} - \bar{\pi}_{1'} & = (4c_2\ , 0\ , 0)\ , \\ \bar{\pi}_{3'} - \bar{\pi}_{2'} & = (4c_3\ , 0\ , 0)\ , \\ \bar{\pi}_{4'} - \bar{\pi}_{3'} & = (4c_4\ , 0\ , 0)\ . \end{cases} \quad (1.69)$$

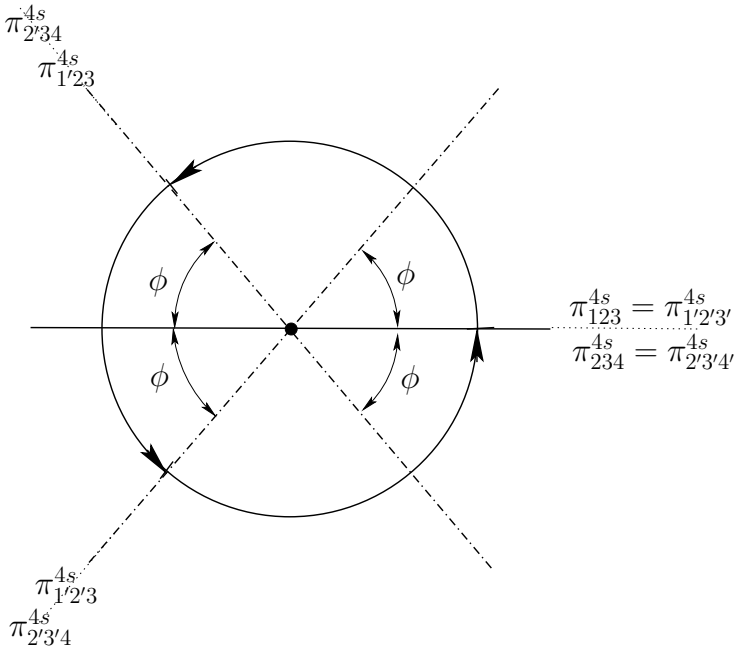

Figure 1.42: The rotations of $\pi^4 s$ about the line u.

This is a projection on a plane perpendicular to u and so that projections of the 3-flats π^{4s}_{123} , π^{4s}_{234} are lines.

From which the relations analogous to eq. (1.28) are immediately found i.e.

$$x(\bar{\pi}_{3'}) = 12 - [x(\bar{\pi}_{0'}) + x(\bar{\pi}_{1'}) + x(\bar{\pi}_{2'})] \ , \quad x(\bar{\pi}_{4'}) = 4 + x(\bar{\pi}_{0'}) \ . \tag{1.70}$$

To reduce the cumbersome notation the *sp* eqs. (1.57) , (1.58) , (1.59) , (1.60) , (1.61) are referred to by $\pi^{4s}_{0'}, \pi^{4s}_{1'}, \pi^{4s}_{2'}, \pi^{4s}_{3'}, \pi^{4s}_{4'}$ respectively. Next we show that the indexed points can be easily obtained in general and the property in eq. (1.69) holds for all N.

Exercises

1. State explicitly the equations for the first *sp* in $\mathbb{R}^5$.
2. Perform the standard translations of the 5 coordinate axes in $\mathbb{R}^5$ to obtain explicitly the corresponding rotated 5 *sp*.
3. Obtain the coordinates of the 6 points arising in the representation of a 4-flat in $\mathbb{R}^5$. This is the generalization of eq. 1.68.

1.4.2 Indexed Points in $\mathbb{R}^N$

$\mathcal{R}$emarkably, the collinearity property (as in theorem 1.2.1) generalizes to higher dimensions enabling the recursive (on the dimensionality) construction of the representation of p-flats for $2 \leq p \leq N-1$. To achieve this some intermediate steps are needed. The indexed point corresponding to the axes spacing $\mathbf{d^i_N}$ (i.e. obtained from the translation of the axes $\bar{X}_1, \ldots, \bar{X}_i$ to the positions $\bar{X}_{1'}, \ldots, \bar{X}_{i'}$ see eq. (1.54) is denoted by $\bar{\pi}_{i'}$.

Theorem 1.4.1 (B.Dimsdale) *The 1-flat $\pi \cap \pi^{Ns}_{i'}$, where $i = 0, 1, \ldots, N$ and*

$$\pi : \ \sum_{k=1}^{N} c_k x_k = c_0 \ , \tag{1.71}$$

is a hyperplane in $\mathbb{R}^N$ an $(N-1)$-flat, is represented by the point :

$$\bar{\pi}_{i'} = (\sum_{k=1}^{N} d_{ik} c_k \ , \ c_0 \ , \ \sum_{k=1}^{N} c_k) \tag{1.72}$$

where the d_{ik} are the inter-axes distances for the spacing $\mathbf{d^i_N}$ as given in eq. (1.54). Explicitly using eq. 1.56

$$\bar{\pi}_{i'} = (\sum_{k=1}^{N} (k - 1 + NS_i(k)) c_k \ , \ c_0 \ , \ \sum_{k=1}^{N} c_k) \ . \tag{1.73}$$

Proof: To determine the 1-flat and obtain its representation it suffices to find two points in the intersection $\pi \cap \pi^{Ns}_{i'}$.

Step 1 Points $P_j = (p_{1j}, p_{2j}, \ldots, p_{Nj}) \in \pi^{Ns}_{i'}$ are such that :

$$\exists m_j \ , \ b_j \in R \ni \ p_{kj} = m_j d_k + b_j \quad . \tag{1.74}$$

Step 2 So for $P_j \in \pi \cap \pi_{i'}^{Ns}$, in addition to eq. (1.74), the coordinates of P_j must also satisfy eq. (1.71) i.e.

$$\sum_{k=1}^{N} c_k(m_j d_k + b_j) = c_0 \ .$$

Step 3 By Step 1 $\bar{P}_j$ is the straight line $y = m_j x + b_j$ in the xy-plane and together with Step 2 we have ,

$$\sum_{k=1}^{N} c_k\{m_j d_k + (y - m_j x)\} = c_0 \ ,$$

or

$$-m_j \,(\sum_{k=1}^{N} c_k)\, x + (\sum_{k=1}^{N} c_k)\, y = -m_j \,(\sum_{k=1}^{N} d_k c_k) + c_0 \ , \tag{1.75}$$

this is an alternate form of the equation for the line $\bar{P}_j$.

Step 4 Since xy is the projective plane $\mathbb{P}^2$, for *any* two distinct points P_1, P_2 the corresponding lines $\bar{P}_1$ and $\bar{P}_2$, intersect at :

$$(-m_1 + m_2)\,(\sum_{k=1}^{N} c_k)\, x = (-m_1 + m_2)\,(\sum_{k=1}^{N} d_k c_k) \quad \Rightarrow$$

$$(\sum_{k=1}^{N} c_k)\, x = (\sum_{k=1}^{N} d_k c_k)$$

Substitution in eq. (1.75) provides the remaining coordinate :

$$(\sum_{k=1}^{N} c_k)\, y = c_0 \ .$$

The point $(x,\, y)$ is independent of the particular lines $\bar{P}_1$ and $\bar{P}_2$ used, so all the lines $\bar{P}_j$ for the $\bar{P}_j$ in Step 2 must all intersect at the same $(x,\, y)$. Converting to homogeneous coordinates yields eq. (1.72). ∎

Corollary 1.4.2 (Hyperplane Representation – J. Eickemeyer) *The hyperplane π given by eq. (1.71) is represented by the $N-1$ points $\bar{\pi}_{i'}$ with N indices given by eq. (1.73), for $i = 0, 1, 2, \ldots, (N-2)$.*

Specifically

$$\begin{cases} \bar{\pi}_{0'} = \bar{\pi}_{12\ldots N} = (c_2 + 2c_3 + ... + (k-1)c_k + ... + (N-1)c_N \ ,\ c_0 \ ,\ S) \ , \\ \bar{\pi}_{1'} = (Nc_1 + c_2 + \ldots + (k-1)c_k + \ldots (N-1)c_N \ ,\ c_0 \ ,\ S) \ , \\ \bar{\pi}_{2'} = (Nc_1 + (N+1)c_2 + \ldots + (k-1)c_k + \ldots + (N-1)c_N \ ,\ c_0 \ ,\ S) \ , \\ \quad . \quad . \quad . \\ \bar{\pi}_{i'} = (Nc_1 + \ldots + (N+i-1)c_i + ic_{i+1} + \ldots + (N-1)c_N \ ,\ c_0 \ ,\ S) \ , \quad i \geq 1 \\ \quad . \quad . \quad . \\ \bar{\pi}_{(N-2)'} = (Nc_1 + \ldots + (2N-3)c_{N-2} + (N-2)c_{N-1} + (N-1)c_N \ ,\ c_0 \ ,\ S) \\ \bar{\pi}_{(N-1)'} = (Nc_1 + \ldots + (2N-3)c_{N-2} + (2N-2)c_{N-1} + (N-1)c_N \ ,\ c_0 \ ,\ S) \\ \bar{\pi}_{N'} = (Nc_1 + \ldots + (2N-3)c_{N-2} + (2N-2)c_{N-1} + (2N-1)c_N \ ,\ c_0 \ ,\ S) \ . \end{cases} \tag{1.76}$$

where $S = \sum_{k=1}^{N} c_k$. The first $N-1$ points suffice for the representation. As for $\mathbb{R}^3$ and $\mathbb{R}^4$ it is useful to generate two additional points $\bar{\pi}'_{N-1}, \bar{\pi}'_N$ here based on the axes-spacing $\mathbf{d_N^{N-1}}, \mathbf{d_N^N}$ providing also the of eqs. analogous to (1.70)

$$x_{N'} = N(N-1) - \sum_{i=0}^{N-1} x_{i'} \quad , \quad x'_{N+1} = N + x'_0 \tag{1.77}$$

with the compact notation $x_{i'} = x(\bar{\pi}_{i'})$.

A p-flat in $\mathbb{R}^N$ is specified by $N-p$ linearly independent linear equations which, without loss of generality, can be of the form:

$$\pi^p : \begin{cases} \pi^p_{12\cdots(p+1)} \ : \ c_{11}x_1 & +\ldots+ \ c_{(p-1)1}x_p + c_{p1}x_{p+1} = c_{10} \\ \pi^p_{23\cdots(p+2)} \ : \ c_{22}x_2 & +\ldots+ \ c_{p2}x_{p+1} + c_{(p+1)2}x_{p+2} = c_{20} \\ & \cdots \\ \pi^p_{j\cdots(p+j)} \ : \ c_{jj}x_j & +\ldots+ \ c_{(p+j-1)j}x_{p+j-1} + c_{(p+j)j}x_{p+j} = c_{j0} \\ & \cdots \\ \pi^p_{(N-p)\cdots N} \ : \ c_{(N-p)(N-p)}x_{N-p} & +\ldots+ \ c_{(N-1)(N-p)}x_{N-1} + c_{N(N-p)}x_N = c_{(N-p)0} \end{cases}$$

and is rewritten compactly as

$$\pi^p \ : \ \{\pi^p_{j\ldots(p+j)} \ : \ \sum_{k=i}^{p+j} c_{jk}x_k = c_{j0} \ , \ j = 1, 2, \ldots, (N-p)\}. \tag{1.78}$$

A p-flat $\pi^p \subset \mathbb{R}^N$ is the intersection of $N-p$ hyperplanes and eq. 1.78 is the analogue of the "adjacent-variable" description for lines in Chapter **??** with analogous indexing. Unless otherwise specified, a p-flat is described by eq. (1.78) with the standard spacing $\mathbf{d_N^0}$.

Theorem 1.4.3 (J. Eickemeyer) *A p-flat in $\mathbb{R}^N$ given by eq. (1.78) is represented by the $(N-p)p$ points with $p+1$ indices :*

$$\bar{\pi}^p_{\{j\ldots(p+j)\}_{i'}} = (\sum_{k=1}^{p+1} d_{ik}c_{jk}, \ c_{j0}, \ \sum_{k=1}^{p+1} c_{jk}), \tag{1.79}$$

where $j = 1, 2, \ldots, N-p, \quad i = 1, 2, \ldots, p$ and the d_{ik} are the distances specified by the axes spacing $\mathbf{d_N^i}$.

Proof: Each $\pi^p_{j\cdots(p+j)}$ in eq. (1.78) can be considered as a hyperplane in $\mathbb{R}^{(p+1)}$: $x_j \ldots x_{j+p+1}$, whose representation, according to corollary 1.4.2 consists of the represented by p points $\bar{\pi}^p_{\{j\ldots(p+j)\}_{i'}}, \quad i = 1, \ldots p$. They are prescribed by the axes spacing $\mathbf{d_N^i} = (d_{i1}, \ldots, d_{i(p+1)}, \ldots, N)$ as per Theorem 1.4.1. There are $(N-p)$ hyperplanes described by eq. (1.78), therefore there are $(N-p)p$ such points altogether. ∎

To clarify, a hyperplane π in $\mathbb{R}^4$ π (i.e. 3-flat) can be represented by the three points

$$\bar{\pi}_{1234}, \ \bar{\pi}_{1'234}, \ \bar{\pi}_{1'2'34} \ , \tag{1.80}$$

while for a 2-flat $\pi^2,\ p=2,\ N=4,\ p(N-p)=4$ and is represented by the four points :

$$\pi^2_{123} : \bar{\pi}^2_{123},\ \bar{\pi}^2_{1'23}\ ; \quad \pi^2_{234} : \bar{\pi}^2_{234},\ \bar{\pi}^2_{2'34}. \tag{1.81}$$

Similarly in $\mathbb{R}^5$, a hyperplane π is represented by the four, a 3-flat π^3 and a 2-flat π^2 by six points each i.e.

$$\begin{cases} \pi \quad : \bar{\pi}_{12345}\ ,\ \bar{\pi}_{1'2345}\ ,\ \bar{\pi}_{1'2'345}\ ,\ \bar{\pi}_{1'2'3'45} \\ \pi^3 \ : \begin{cases} \pi^3_{1234} \ : \bar{\pi}^3_{1234}\ ,\ \bar{\pi}^3_{1'234}\ ,\ \bar{\pi}^3_{1'2'34} \\ \pi^3_{2345} \ : \bar{\pi}^3_{2345}\ ,\ \bar{\pi}^3_{2'345}\ ,\ \bar{\pi}^3_{2'3'45} \end{cases} \\ \pi^2 \ : \begin{cases} \pi^2_{123} \ : \bar{\pi}^2_{123}\ ,\ \bar{\pi}^2_{1'23} \\ \pi^2_{234} \ : \bar{\pi}^2_{234}\ ,\ \bar{\pi}^2_{2'34} \\ \pi^2_{345} \ : \bar{\pi}^2_{345}\ ,\ \bar{\pi}^2_{3'45}\ . \end{cases} \end{cases} \tag{1.82}$$

In many instances it is possible to use simplified notation by just retaining the subscripts so that the three points in eq. (1.80) are referred by $1234, 1'234, 1'2'34$. The dimensionality is one less than the number of indices. Continuing, the points representing pi^3 in eq. (1.82) denoted simply by $1234, 1'234, 1'2'34$; $2345, 2'345, 2'3'45$; since there 2 sets of 3 points with 5 different indices altogether we can conclude that this is a 2-flat in $\mathbb{R}^5$. The simplified and the more formal notation are used interchangeably as in section 1.5. This theorem unifies all previous results for p-flats π^p where $0 \leq p < N$.

1.4.3 Collinearity Property

$\mathcal{T}$he underpining of the construction algorithm for the point representation of a 2-flat $\pi^2 \subset \mathbb{R}^3$, as we saw, is the collinearity property. Namely for *any* $\pi^1 \subset \pi^2$ the points $\bar{\pi}^1_{12},\ \bar{\pi}^1_{13},\ \bar{\pi}^1_{23}$ are collinear with $\bar{\pi}_{123}$. For the generalization to p-flats let

$$\bar{L}^{p_k}_j = \bar{\pi}^{p_k}_{j\cdots(p+j)} \bullet \bar{\pi}^{p_k}_{(j+1)\cdots(p+j+1)} \tag{1.83}$$

denote the line $\bar{L}^{p_k}_j$ on the indicated two points. The gist of this section is the proof that $\pi^{(p-1)_1},\ \pi^{(p-1)_2} \subset \pi^p \subset \mathbb{R}^N$

$$\bar{\pi}^p_{j\cdots(p+j+1)} = \bar{L}^{(p-1)_1}_j \cap \bar{L}^{(p-1)_2}_j\ . \tag{1.84}$$

As an example for $j=1, p=2, N=3$ recasts our old friend from section 1.2.2 as :

$$\bar{L}_1^{\pi^{1_k}} = \bar{\pi}^{1_k}_{12} \bullet \bar{\pi}^{1_k}_{23}, \quad k=1,2, \quad \bar{\pi}^2_{123} = \bar{L}_1^{\pi^{1_1}} \cap \bar{L}_1^{\pi^{1_2}}\ .$$

The pair (1.83) and (1.84) state the basic recursive construction implied in the *Representation Mapping* stated formally below. The recursion is on the dimensionality, increased by one at each stage, of the flat whose representative points are constructed. Though the notation may seem intimidating the idea is straight forward and to clarify it we illustrate it for a hyperplane $\pi^3 \subset \mathbb{R}^4$ in Figs. 1.43 and 1.45 starting from the 4 points $\pi^{0_1}, \pi^{0_2}, \pi^{0_3}, \pi^{0_4}$

with $\rightarrow$ pointing to the construction result. Diagramatically the sequence of steps is :

$$\left.\begin{array}{l} \left.\begin{array}{ll} \pi^{0_1},\pi^{0_2} & \rightarrow \pi^{1_1} \\ \pi^{0_2},\pi^{0_3} & \rightarrow \pi^{1_2} \end{array}\right\} \rightarrow \pi^{2_1} \quad (\bar{\pi}^{2_1}_{123}\,,\,\bar{\pi}^{2_1}_{1'23}) \\ \\ \left.\begin{array}{ll} \pi^{0_2},\pi^{0_3} & \rightarrow \pi^{1_2} \\ \pi^{0_3},\pi^{0_4} & \rightarrow \pi^{1_3} \end{array}\right\} \rightarrow \pi 2_2 \quad (\bar{\pi}^{2_2}_{234}\,,\,\bar{\pi}^{2_2}_{2'34}) \end{array}\right\} \rightarrow \pi^3 \quad (\bar{\pi}^3_{1234}\,,\,\bar{\pi}^3_{1'234}\,,\,\bar{\pi}^3_{1'2'34}) \tag{1.85}$$

For the construction of a regular (i.e. not ideal) flat, the flats $\pi^p \subset \pi^3$ with dimensionality $3 > p \geq 1$ in the construction must have a non-empty intersection. From the the polygonal lines representing $\pi^{0_1}, \pi^{0_2}, \pi^{0_3}$, the two one 1-flats π^{1_1}, π^{1_2} are constructed with $\pi^{1_1} \cap \pi^{1_2} = \pi^{0_2}$ yielding the points $\bar{\pi}^{1_1}_{12}\,,\,\bar{\pi}^{1_1}_{23}\,,\,\bar{\pi}^{1_1}_{34}$ as shown in Fig. 1.43 (left). The portion of the construction involving x_1, x_2, x_3 is shown in cartesian coordinates in Fig. 1.44. The 3 representing points for each 1-flat are joined by **two** lines to form polygonal lines having 3 vertices (the points). From the intersection of these new polygonal lines the points $\bar{\pi}^{2_1}_{123}\,,\,\bar{\pi}^{2_1}_{234}$, representing a 2-flat contained on π^3, are constructed as shown on the right of Fig. 1.43. Similarly π^{2_2} is constructed from the 3 points $\pi^{0_2}, \pi^{0_3}, \pi^{0_4}$ in the same way.

At any stage a point representing $\bar{\pi}^r$, where the superscript is the flat's dimension, is obtained by the intersection of *any pair* of lines joining points representing flats of dimension $r-1$ contained in π^r.

The axes $\bar{X}_1, \bar{X}_2$ are each translated 4 units to the right and construction proceeds until all 3 representing points $\bar{\pi}^3_{1234}, \bar{\pi}^3_{1'234}, \bar{\pi}^3_{1'2'34}$ are obtained. The first translation is shown in Fig. 1.45 on the right. As a reminder this points represent the *lines* which are the intersections of π^3 with the first super-plane, due to the standard spacing with $d_1 = 0, d_2 = 1, d_3 = 2, d_4 = 3$, followed by by the second *sp* with $d_1' = 4$ and then third *sp* with $d_2' = 5$ in $\mathbb{R}^4$.

Theorem 1.4.4 (Collinearity Construction Algorithm) : *For any $\pi^{(p-2)} \subset \pi^{(p-1)} \subset \mathbb{R}^N$, the points $\bar{\pi}^{(p-2)}_{1\ldots(p-1)}\,,\,\bar{\pi}^{(p-2)}_{2\ldots(p-1)p}\,,\,\bar{\pi}^{(p-1)}_{1\ldots(p-1)p}$ are collinear.*

Proof: Step 1 Let the $(p-1)$ and $(p-2)$-flats be given by:

$$\left\{\begin{array}{lllll} \pi^{(p-1)} & : & \pi^{(p-1)}_{i\ldots(p+i-1)} & : & \sum_{k=i}^{p+i-1} c_{ik}x_k = c_{0i}\,, \quad i = 1,\ldots,N-p+1 \\ \pi^{(p-2)} & : & \pi^{(p-2)}_{j\ldots(p+j-2)} & : & \sum_{k=j}^{p+j-2} a_{jk}x_k = a_{0j}\,, \quad j = 1,\ldots,N-p+2 \end{array}\right. \tag{1.86}$$

Step 2 Let Consider two distinct points $A^r = (\alpha^r_1, \ldots, \alpha^r_N),\ r = 1, 2, \in \pi^{(p-2)}$ and substitute their first p-components in the equation for $\pi^{(p-1)}_{12\ldots p}$ in eq. (1.86) to obtain

$$c_{11}\alpha^r_1 + \ldots + c_{(p-1)1}\alpha^r_{(p-1)} + c_{p1}\alpha^r_p = c_{01}\,. \tag{1.87}$$

Whereas substitution in the first two equations for $\pi^{(p-2)}$, i.e. $\pi^{(p-2)}_{12\ldots(p-2)},\ \pi^{(p-2)}_{2\ldots(p-2)(p-1)}$, yields

$$\left\{\begin{array}{l} \pi^{(p-2)}_{12\ldots(p-2)} \ : \ a_{11}\alpha^r_1 + \ldots + a_{(p-2)1}\alpha^r_{(p-2)} + a_{(p-1)1}\alpha^r_{(p-1)} = a_{01} \\ \pi^{(p-2)}_{2\ldots(p-2)(p-1)} \ : \ a_{22}\alpha^r_2 + \ldots + a_{(p-1)2}\alpha^r_{(p-1)} + a_{p2}\alpha^r_p = a_{02}\,, \end{array}\right.$$

whose sum is

$$a_{11}\alpha^r_1 + (a_{21}+a_{22})\alpha^r_2 + \ldots + (a_{(p-1)1}+a_{(p-1)2})\alpha^r_{(p-1)} + a_{p2}\alpha^r_p = a_{01} + a_{02}\,. \tag{1.88}$$

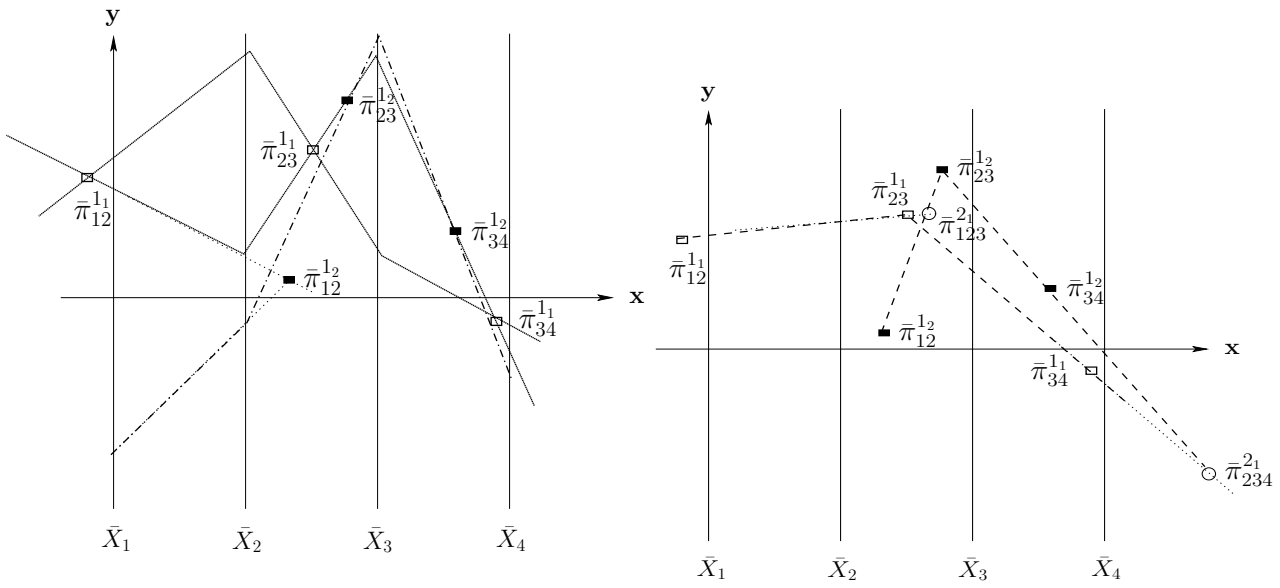

Figure 1.43: Recursive Construction in $\mathbb{R}^4$.

A pair of points π^{0_1}, π^{0_2} determines a line (1-flat) π^{1_1} represented by the 3 constructed points $\bar{\pi}^{1_1}_{i-1,i}$, $\quad i = 2, 3, 4$ (left). Another 1-flat π^{1_2} is determined by one of these points π^{0_2} and an additional point π^{0_3} as represented by the 3 black points. Since $\pi^{1_1} \cap \pi^{1_2} = \pi^{0_2}$ the 2 1-flats determine 2-flat π^{2_1} and two of its representing points $\bar{\pi}^{2_1}_{123}$, $\bar{\pi}^{2_1}_{234}$ are seen on the right. They are the intersections of the two polygonal lines joining the previously points obtained representing the 2 1-flats.

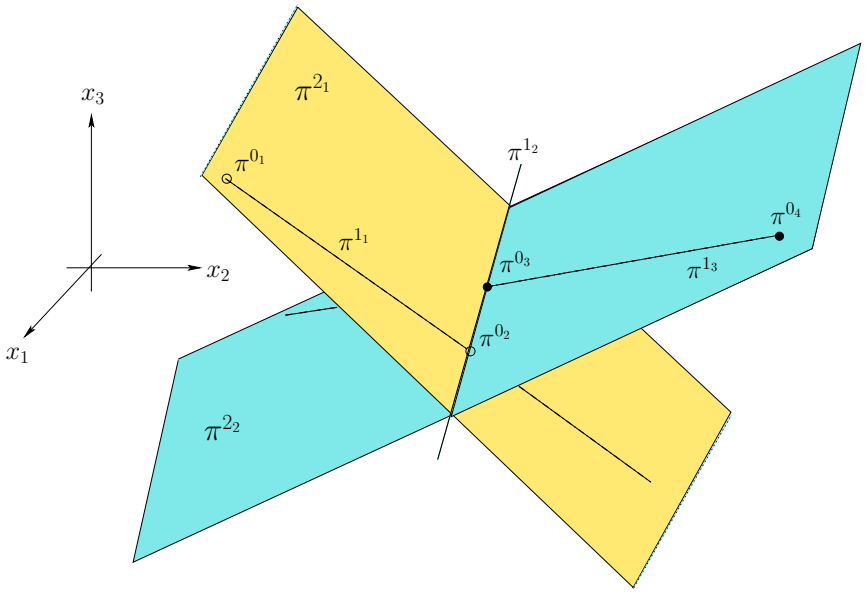

Figure 1.44: The construction of the $x_1x_2x_3$ part of the 3-flat π^3 from 4 points (0-flats).

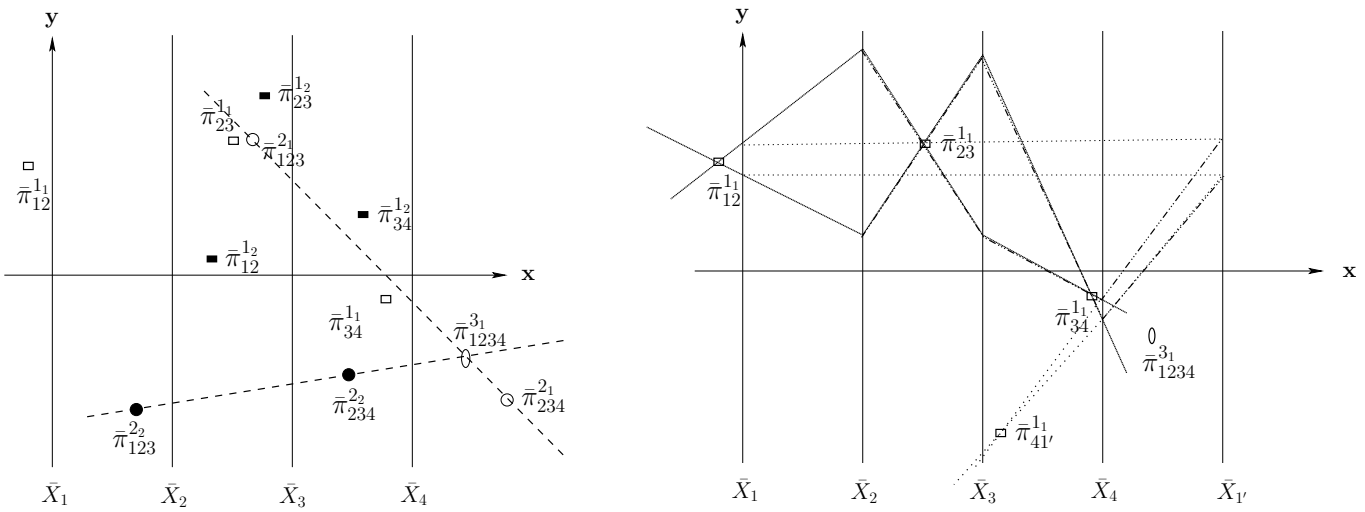

Figure 1.45: Recursive Construction in $\mathbb{R}^4$ continued.

Two 2-flats π^{2_1}, previously constructed, and another π^{2_2} represented by the 2 black points (left), determine a 3-flat π^3. Pairs of points representing the same 2-flat are joined and their intersection is the point $\bar{\pi}^3_{1234}$. This is one of the 3 points representing the 3-flat. The "debris" from the previous constructions, points with fewer than 4 indices, can now be discarded. A new axis (right) $\bar{X}_{1'}$ is placed one unit to the right of $\bar{X}_3$ and the x_1 values are transfered to it from the $\bar{X}_1$ axis. Points are now represented by new polygonal lines between the $\bar{X}_2$ and $\bar{X}_{1'}$ axes and one of the points $\bar{\pi}^{1_1}_{41'}$, representing the 1-flat π^{1_1} on the new triple of $\|$-coords axes, is constructed as in the 1st step.

Step 3. Equations (1.87) and (1.88) are the same for subtracting one from the other yields

$$\alpha^r_1(c_{11} - a_{11}) + \alpha^r_2\{c_{21} - (a_{21} + a_{22})\} + \ldots + \alpha^r_p(c_{p1} - a_{p2}) = c_{01} - (a_{01} + a_{02}). \qquad (1.89)$$

Letting $r = 1, 2$ successively in (1.89) provides two equations whose difference is

$$[\alpha^1_1 - \alpha^2_1]b_1 + [\alpha^1_2 - \alpha^2_2]b_2 \ldots + [\alpha^1_p - \alpha^2_p]b_p = 0\ , \qquad (1.90)$$

the b_i being the coefficients of eq. (1.89). This is effectively an *identity* for every pair of distinct points in $\pi^{(p-2)}$. Hence the coefficients and the right-hand-side of eq. (1.89) must vanish

$$c_{01} = (a_{01} + a_{02}),\ c_{11} = a_{11},\ c_{p1} = a_{p2},\ c_{k1} = (a_{k1} + a_{k2}),\ k = 2, \ldots, p-1. \qquad (1.91)$$

Step 4. The homogeneous coordinates of the 3 points in question as obtained from Theorem 1.4.3 are :

$$\bar{\pi}^{(p-2)}_{1\ldots(p-1)} = (\sum_{k=1}^{p-1} d_{1k}a_{1k},\ a_{01},\ \sum_{k=1}^{p-1} a_{1k}),$$

$$\bar{\pi}^{(p-2)}_{2\ldots(p-1)p} = (\sum_{k=2}^{p} d_{2k}a_{2k},\ a_{02},\ \sum_{k=2}^{p} a_{2k}),$$

and

$$\bar{\pi}^{(p-1)}_{12\ldots(p-1)p} = (\sum_{k=1}^{p} d_{1k}c_{2k},\, c_{01},\, \sum_{k=1}^{p} c_{1k})\ .$$

Note that for this portion of the construction the axes spacing is $d_{1k} = d_{2k},\ k = 1, 2, \ldots, p$. Forming the determinant from these homogeneous coordinates

$$\begin{vmatrix} \sum_{k=1}^{p-1} d_{1k}a_{1k} & a_{01} & \sum_{k=1}^{p-1} a_{1k} \\ \sum_{k=2}^{p} d_{2k}a_{2k} & a_{02} & \sum_{k=2}^{p} a_{2k} \\ \sum_{k=1}^{p} d_{1k}c_{2k} & c_{01} & \sum_{k=1}^{p} c_{2k} \end{vmatrix} \quad .$$

From Step 3 and the observation on the axes spacing the last row is the sum of the first and second rows, the value of the determinant is zero showing that the 3 points are collinear. ■

Corollary 1.4.5 *For any* $\pi^{(p-2)} \subset \pi^{(p-1)} \subset \mathbb{R}^N$, *the points* $\bar{\pi}^{(p-2)}_{\{j\ldots(p+j-2)\}_{i'}}$, $\bar{\pi}^{(p-2)}_{\{(j+1)\ldots(p+j-1)\}_{i'}}$, $\bar{\pi}^{(p-1)}_{\{(j\ldots(p+j-1)\}_{i'}}$ *are collinear.*

The proof is the same taking proper care to keep track of the indices and the corresponding axes spacing. The recursive construction is illustrated for a 5-flat in $\mathbb{R}^6$ from Fig. 1.46 through 1.48.

Exercises

1. What points represent the *sp* in $\mathbb{R}^N$?
2. State the coordinates of the five points representing a 5-flat $\pi \subset \mathbb{R}^6$.

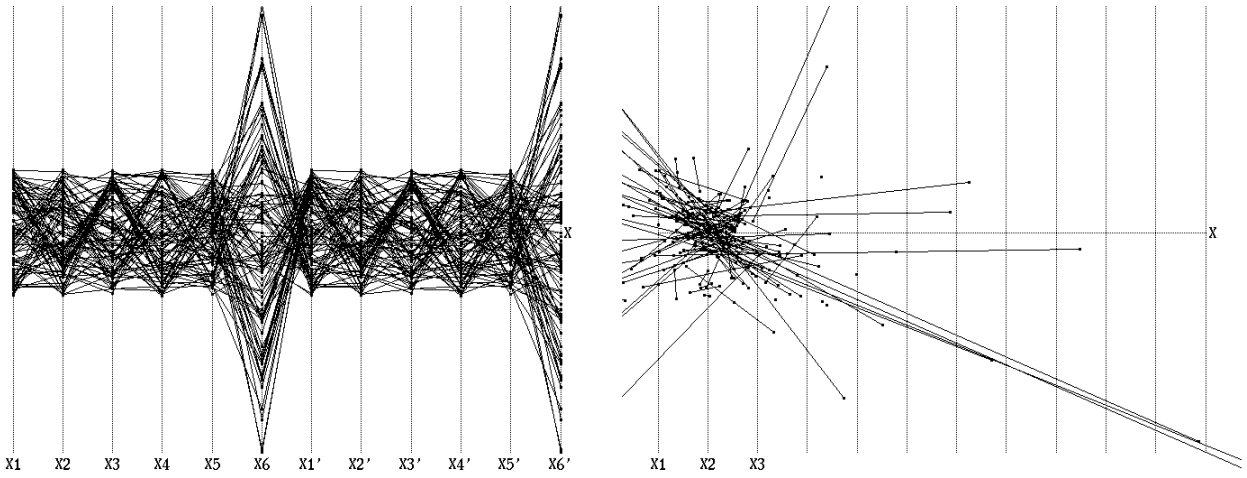

Figure 1.46: Randomly selected points on a hyperplane in $\mathbb{R}^6$.

Polygonal lines (left) on the $\bar{X}_1 \ldots \bar{X}_6$ axes representing randomly selected points on a 5-flat $\pi^5 \subset \mathbb{R}^6$. ted points on a 5-flat $\pi^5 \subset \mathbb{R}^6$ .The $\bar{\pi}^{1_i}_{12}$, $\bar{\pi}^{1_i}_{23}$ portions of the 1-flats $\subset \pi^5$ constructed (right) from the polygonal lines lines. No pattern is evident.

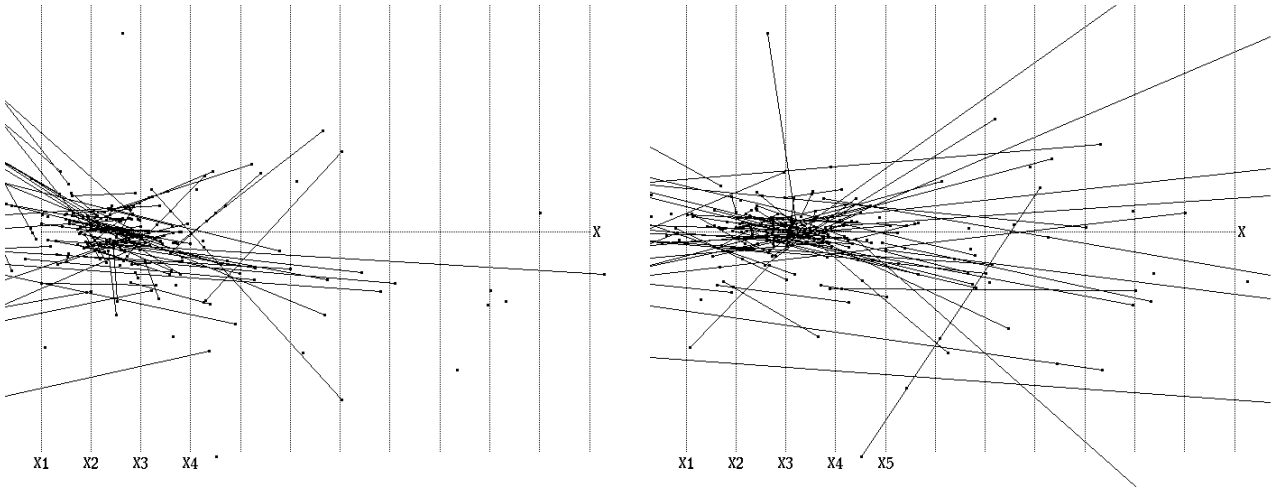

Figure 1.47: The $\bar{\pi}^{2_i}_{123}$, $\bar{\pi}^{2_i}_{234}$ (left) points for the 2-flats $\subset \pi^5$.
They are constructed from the polygonal lines joining $\bar{\pi}^{1_i}_{12}, \bar{\pi}^{1_i}_{23}$, $\bar{\pi}^{1_i}_{34}$. The $\bar{\pi}^{2_i}_{123}$, $\bar{\pi}^{2_i}_{234}$ (right) portions of the 2-flats $\subset \pi^5$ constructed from the polygonal lines joining $\bar{\pi}^{1_i}_{12}, \bar{\pi}^{1_i}_{23}$, $\bar{\pi}^{1_i}_{34}$.

3. State the points representing a 4-flat π^4, 3-flat π^3 and 2-flat π^2 in $\mathbb{R}^6$ as in eq. (1.82).

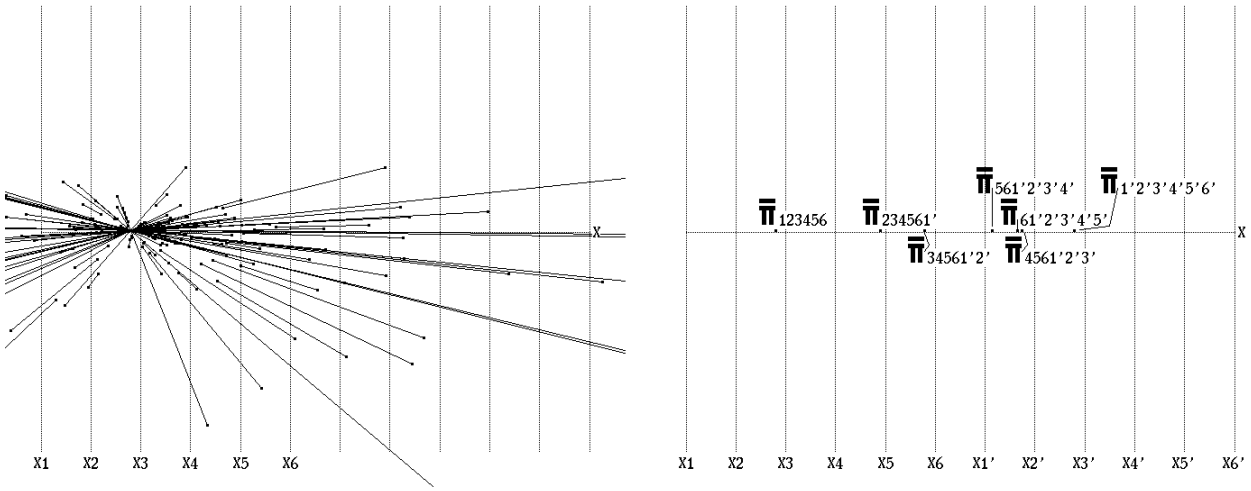

Figure 1.48: This is it!

On the left are the $\bar{\pi}^{4_i}_{12345}$, $\bar{\pi}^{4_i}_{23456}$ of the 4-flats $\subset \pi^5$ constructed from the polygonal lines joining $\bar{\pi}^{3_i}_{1234}, \bar{\pi}^{3_i}_{2345}, \bar{\pi}^{3_i}_{3456}$. This shows that the original points whose representation is in Fig. 1.46(left) are on a 5-flat in $\mathbb{R}^6$. The remaining points of the representation are obtained in the same way and all 7 points of the representation of π^5 are seen on the right. The coefficients of its equation are equal to 6 times the distance between sequentially indexed points for in Fig. **??** for $\mathbb{R}^3$.

4. Prove eq. (1.77) for $\mathbb{R}^N$.

1.5 Construction Algorithms in $\mathbb{R}^4$

The generalization of the 3-D construction algorithms to 4-D is direct and is an opportune time to introduce simplified notation which is used when the context is clear.

1.5.1 The Five Indexed Points

The first example is the equivalent of the four-indexed-point algorithm in section 1.3.2 for 4-D. That is, given three points $\bar{\pi}_{1234}, \bar{\pi}_{1'234}, \bar{\pi}_{1'2'34}$ specifying a 3-flat $\pi^3 : c_1x_1 + c_2x_2 + c_3x_3 + c_4x_4 = c_0$ in $\mathbb{P}^4$ to construct the other two $\bar{\pi}_{1'2'3'4}$ and $\bar{\pi}_{1'2'3'4'}$. We start by revisiting the last step in the recursive construction Fig. 1.45 and show it again in Fig. 1.49 (left). This is the stage where two lines $\bar{P}_1, \bar{P}_2$ each on the 123 and 234 points of a 2-flat determine the first point $\bar{\pi}_{1234}$ representing a 3-flat π^3; a situation completely analogous to that in Fig. 1.10 where here the dimensionality of the objects involved is raised by one. Of course, the lines represent points $P_1 \in \pi^4 s_1 \cap \pi^{2_1}$ and $P_2 \in \pi^4 s_1 \cap \pi^{2_2}$ for two 2-flats π^{2_1}, π^{2_2} contained in π^3. As a reminder containment is seen by the **on** relation. For example, line $\bar{P}$ **on** point $\bar{\pi}^2_{123} \Leftrightarrow P \in \pi^2$ and here in particular the point P is on the line $\pi^2_{123} = \pi^2 \cap \pi^s_1$. As for the 3-D case the point $\bar{\pi}_{1234}$ represents a line on an *sp*. Specifically $\bar{\pi}_{1234} = \pi^{4s}_1 \cap \pi^3$. From a line $\bar{P}_1$ on the points $\bar{\pi}_{234_1}$ (which we assume has been previously constructed) and $\bar{\pi}_{1'23_1}$ the second point $\bar{\pi}_{1'234}$ is determined as shown on the right of Fig. 1.49.

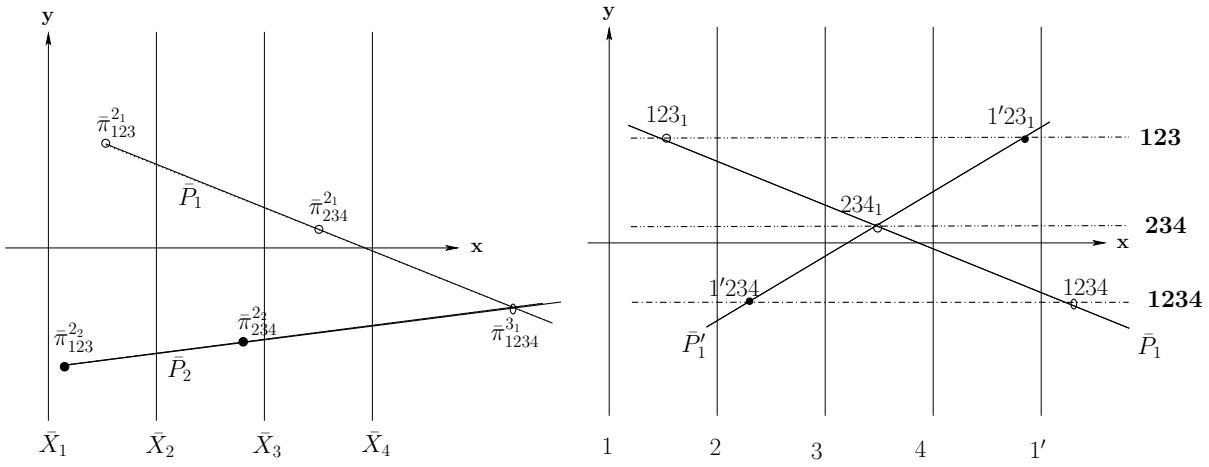

Figure 1.49: Continuing the construction of indexed points for a 3-flat π^3 in 4D.

On the left is the point $\bar{\pi}_{1234}$ previously constructed in Fig. 1.45. Using simplified notation the construction is continued on the right to obtain the point $\bar{\pi}_{1'234}$ – marked by $1'234$. The $123_1, 1'23_1, 234_1$ are points of the representation of a 2-flat π^2_1 contained in π^3. The lines $\bar{P}_1, \bar{P}'_1$ on 1234 and $1'234$ share the indices 234 and necessarily intersect at the 234_1 point.

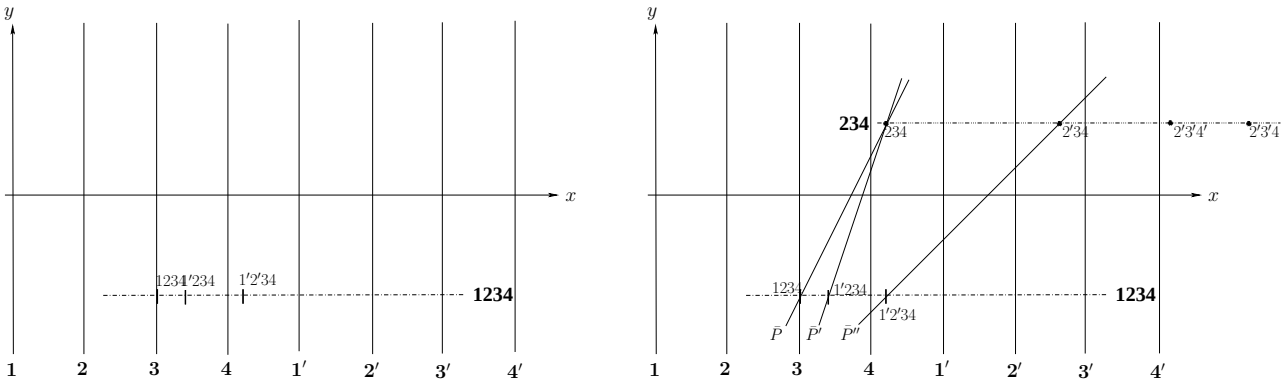

Figure 1.50: On the left are the initial data for a 3-flat π^3 in $\mathbb{R}^4$.
Three points (right) $P \in \pi^3 \cap \pi_1^{4s}, P' \in \pi^3 \cap \pi_1^{4s}, P'' \in \pi^3 \cap \pi^{4s}$ are chosen. In the $x_2x_3x_4$ subspace of $\mathbb{R}^4$ they determine a 2-flat π^2_{234}.

The algorithm's input consists of three points $\bar{\pi}^3_{1234}, \bar{\pi}^3_{1'234}, \bar{\pi}^3_{1'2'34}$ shown in simplified notation $1234, 1'234, 1'2'34$ on the left of Fig. 1.50. Four points determine a hyper-plane $\pi^3 \subset \mathbb{R}^4$. On the right, 3 lines $\bar{P}, \bar{P}', \bar{P}''$ are chosen on the points $1234, 1'234, 1'2'34$ respectively. Clearly $P \in \pi^3 \cap \pi_1^{4s}, P' \in \pi^3 \cap \pi_{1'}^{4s}, P'' \in \pi^3 \cap \pi_{1''}^{4s}$ and these 3 points determine a 2-flat $\pi^2 \subset \pi^3$ which can be described by:

$$\pi^2 : \begin{cases} \pi^2_{123} : & a_1x_1 + a_2x_2 + a_3x_3 = a_0 \\ \pi^2_{234} : & b_2x_2 + b_3x_3 + b_4x_4 = b_0 \end{cases} \tag{1.92}$$

As for a 1-flat in a 2-flat, see Fig. 1.20, also for a 2-flat in a 3-flat $\bar{P} \cap \bar{P}'$ is $\bar{\pi}^2_{234}$ one of the points representing π^2. It is denoted by 234 and is on the the horizontal line **234** so that $2'34$ is $\mathbf{234} \cap \bar{P}''$. These two points represent π^2_{234} given by eq. 1.92); a 2-flat in the $x_2x_3x_4$ subspace of $\mathbb{R}^4$. The points $\bar{\pi}^2_{2'3'4}, \bar{\pi}^2_{2'3'4'}$, denoted by $2'3'4, 2'3'4'$, are needed next and are determined from $234, 2'34$ via the construction algorithm in section 1.3.2. For the representation of the a 2-flat π^2_{123} as in eq. 1.92 **any** point $\bar{\pi}^2_{123}$ can be chosen on $\bar{P}$ such as the one denoted by 123 in Fig. 1.51. The intersections of the horizontal line **123** on 123 and $\bar{P}', \bar{P}''$ determine the points $1'23, 1'2'3$. Four points determine a hyper-plane $\pi^3 \subset \mathbb{R}^4$ and so far we have used three. Proceeding, as shown in Fig. 1.51, the line $\bar{P}'''$ is drawn on the point $2'3'4$ and *parallel* to $\bar{P}$, the point P''' is the point P in the $\bar{X}_{1'}, \bar{X}_{2'}, \bar{X}_{3'}, \bar{X}_{4'}$ axes. Just as for the 3-D case but here $P''' \in \pi^3 \cap \pi^{4s}_{1'2'3'4'}$ with $\pi^{4s}_{1'2'3'4'}$ coinciding with π^{4s}_{1234}. The intersections of $\bar{P}'''$ with the lines $\mathbf{123}, \mathbf{1234}$ determine the points $1'2'3'$ and $1'2'3'4$. The construction is completed by drawing the line $\bar{P}^{iv}$ *on the points* $2'3'4', 1'2'3'$ whose intersection with the **1234** provides the the fifth point of π^3 representation. The four independent points P, P', P'', P^{iv} determine π^3. The algorithm's output is invariant of the the choice of points as well as the selection of the π^2 (see exercise 3). Other equivalent determinations for the 3-flat are one point P and a 2-flat π^2 or 3 lines, the 3-flat's intersection with the *sp*, which provide the 3 indexed points representation.

By the way, it is immediately clear that a 2-flat $\pi^2 \subset \pi^3 \Leftrightarrow \bar{\pi^2}_{123}, \bar{\pi^2}_{234}, \bar{\pi^3}_{1234}$ are collinear and equivalently for the remaining points representing π^3. This is the generalization of the

$\ell \subset \pi^2$ condition shown in Fig. 1.20 and of course a particular instance of the recursive on the dimensionality collinearity construction.

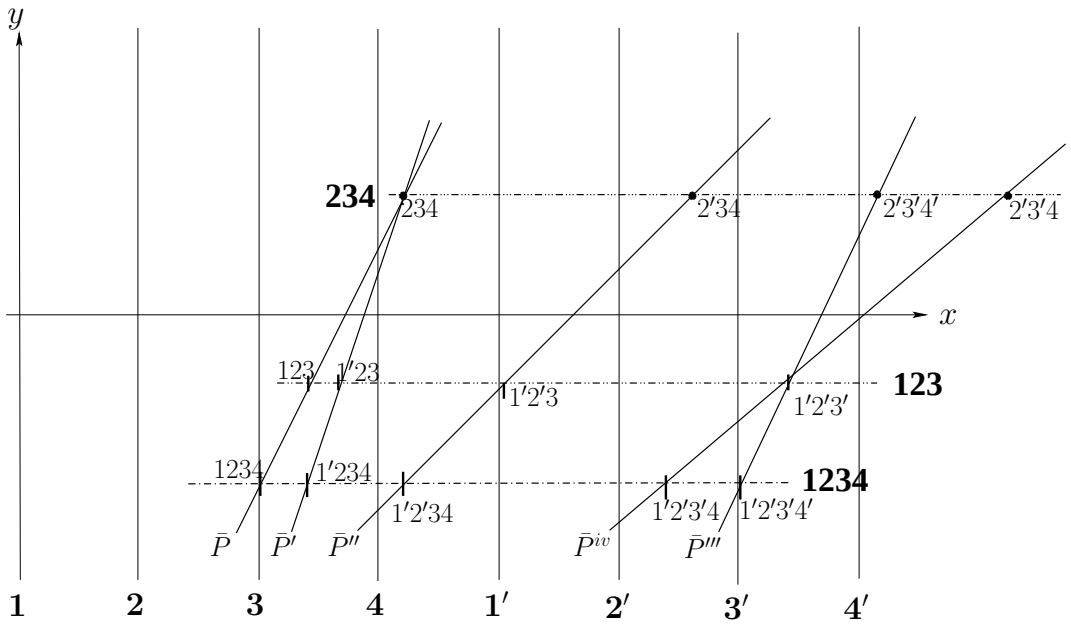

Figure 1.51: Completing the construction of the 5 points representing a hyperplane in $\mathbb{R}^4$.

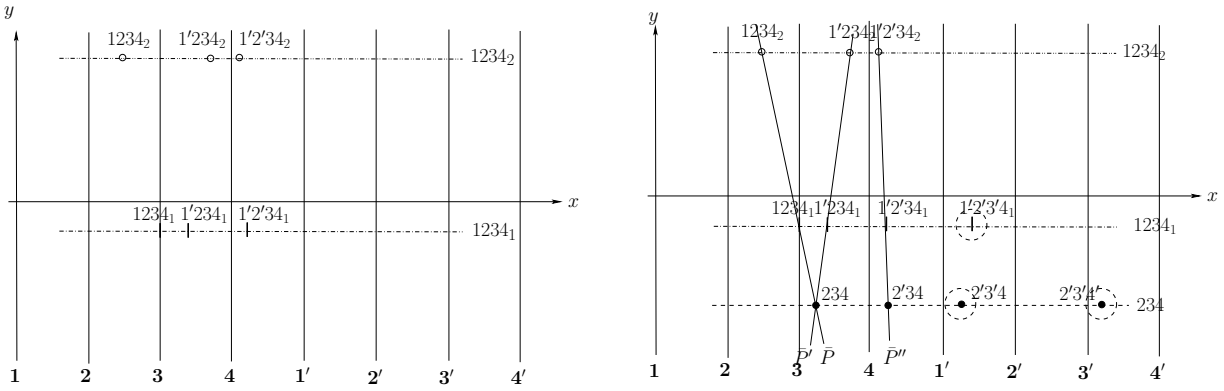

Figure 1.52: On the left are the initial data specifying two 3-flats π^{3_1}, π^{3_2} in $\mathbb{R}^4$. On the right the lines $\bar{P}, \bar{P}', \bar{P}''$ are drawn on the pair of points $1234, 1'234, 1'2'34$ respectively providing the 234 and $2'34$ points for the 2-flat $\pi^2 = \pi^{3_1} \cap \pi^{3_2}$. Then the points $2'3'4, 2'3'4'$ for π^2_{234} and $1'2'3'4_1$, shown within the dotted circles, are constructed.

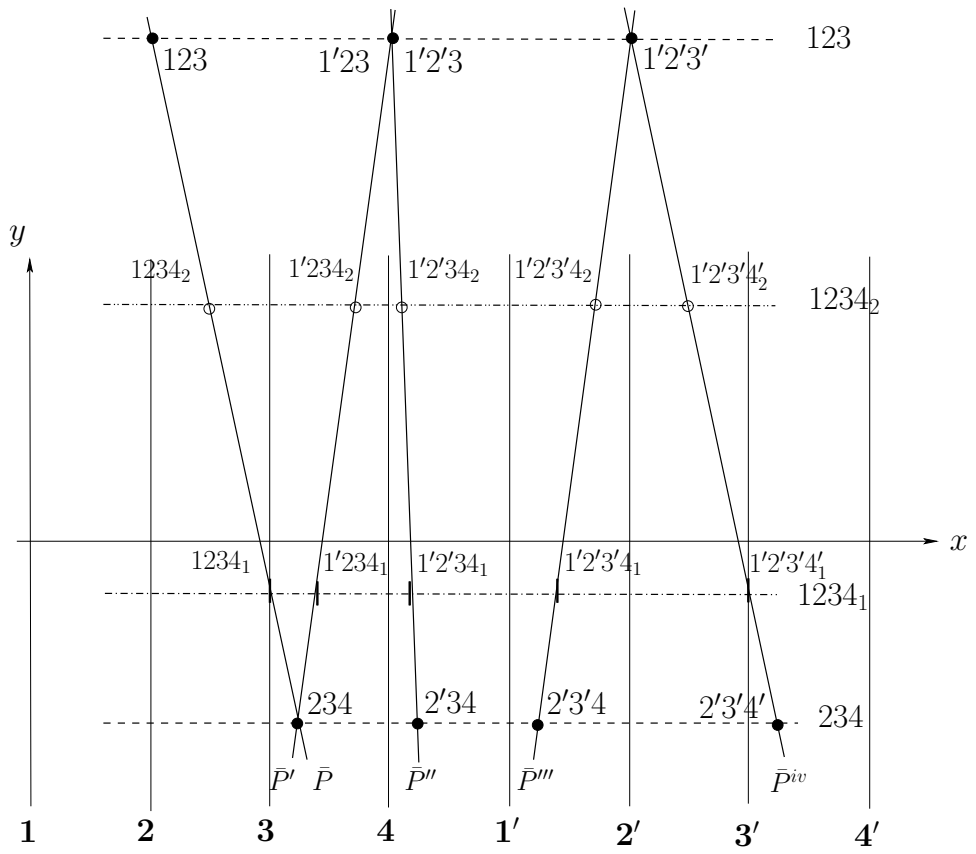

Figure 1.53: Intersection of two 3-flats in 4-D.

The result is the 2-flat π^2 given by the points $123, 1'2'3'$ etc. representing π^2_{123} and $234, 2'34$ etc for π^2_{234}.

1.5.2 Intersecting Hyperplanes in $\mathbb{R}^4$

$\mathcal{N}$ext we provide an algorithm which constructs the intersection of two 3-flats π^{3_1}, π^{3_2} the result being a 2-flat π^2 as the one given in eq. (1.92). The algorithm's input is shown on the left of Fig. 1.52 consisting of 3 points in $\|$-coords each representing the 2 3-flats. On the right the lines $\bar{P}, \bar{P}', \bar{P}''$ joining the pairs $1234, 1'234, 1'2'34$ represent 3 points which specify the 2-flat $\pi^2 = \pi^{3_1} \cap \pi^{3_2}$ whose representation is constructed in the next steps. As seen the point $\bar{\pi}^2_{234} = \bar{P} \cap \bar{P}'$, 234 also establishes the **234** horizontal line with $\bar{\pi}^2_{2'34} = \bar{P}'' \cap$ **234** marked by $2'34$. The points $2'3'4, 2'3'4'$ and, using the previous algorithm, also $1'2'3'4$ are constructed and for easy reference are marked by the dotted circles.

The remaining steps are illustrated in Fig. 1.53.

1. Draw the line $\bar{P}^{iv}$ on the point $2'3'4'$ parallel to $\bar{P}$, as in the 3-D construction, since the point P^{iv} is the pont P but in the rotated coordinates designated by $1', 2', 3', 4'$ in the simplifed notation. Necessarely $\bar{P}^{iv}$ is on the $1'2'3'4'$ on the two horizontal lines $1\bar{2}34_i, i = 1, 2$. The point $2'3'4'$ is constructed previously for this purpose. Alternatively any of the two $1'2'3'4'$ points can be used but its construction is more laborious.

2. The line $\bar{P}'''$ on the points $2'3'4, 1'2'3'4_1$ is constructed providing $1'2'3'4_2 = \bar{P}''' \cap \mathbf{1234_2}$ and $1'2'3' = \bar{P}'' \cap \bar{P}^{iv}$ which establishes the **123** horizontal line.

3. The points $123 = \bar{P} \cap \mathbf{123}, 1'23 = \bar{P}' \cap \mathbf{123}, 1'2'3 = \bar{P}'' \cap \mathbf{123}$ are now available. The coincidence of the points 123 and $1'23$ here is due to the second coefficient $a_2 = 0$ of π^2_{123} – see eq. (1.92)) – and is not true in general.

Note that π^2_{123} is a 3-flat in $\mathbb{R}^4$ parallel to the x_4 axis and hence its equation has zero coefficient for x_4. The location of the points $123, 1'23, 1'2'3, 1'2'3'$ which are now available together with the first eq. of 1.68 and equation 1.69 enable us to obtain the values of π^2_{123} coefficients. Similarly, the coefficients of π^2_{234}, a 3-flat parallel to the x_1 axis (hence zero coefficient of x_1 is zero), equation are found. The two equations describe explicitly the algorithm's output π^2 .

Further higher-dimensional constructions are not presented. They offer wonderful opportunities for exercises (below), projects and research topics.

Exercises

1. Simplify the above constructions using the relations in eq. (1.70).

2. Given four points each in a successive *sp* provide an algorithm to construct the 3-flat containing them.

3. For the algorithm in section 1.5.1 show that the result is invariant for *any* choice of points $P \in \pi^3 \cap \pi^{4s}_1, P' \in \pi^3 \cap \pi^{4s}_{1'}, P'' \in \pi^3 \cap \pi^{4s}_{1''} P^{iv} \in \pi^3 \cap \pi^{4s}_{1'2'3'4}$ and π^2_{123}.

4. Genelarize the algorithm in section 1.3.5 for a point P and 3-flat π^3 in $\mathbb{R}^4$.

5. For a given 3-flat π^3 and a 1-flat (line) ℓ provide conditions for containment $\ell \subset \pi^3$ and $\ell \cap \pi^3 = \emptyset$. What is $\ell \cap \pi^3$?

6. Generalize the algorithm of section 1.5.1 to $\mathbb{R}^5$ construct the *six* points arising in the representation of a 4-flat given the first 4 points.

7. Generalize the algorithm of section 1.5.2 to construct the intersection of two 4-flats in $\mathbb{R}^5$.

8. Generalize the rotation of a 2-flat in $\mathbb{R}^3$ to display in $\|$ the rotation of 3-flat in $\mathbb{R}^4$ about an axis (i.e. a 1-flat). If it is not possible to perform this rotation show **graphically** the constraints involved - **hard**.

1.5.3 Detecting Near Coplanarity

$\mathcal{T}$he coplanarity of a set of points $S \subset \pi$ can be visually verified. What if the points are perturbed staying close to by no longer being on the plane π, can "near-coplanarity" still detected? Let us formulate this question more specifically by perturbing the the coefficients c_i of a plane's equation by a small amount ϵ_i. This generates a family of "proximate" planes

forming a surface resembling a "multiply twisted slab". Now the experiment is performed by selecting a random set of points from such a twisted slab, and repeating the construction for the representation of planes. As shown in Fig. 1.54, 1.55 the there is a remarkable resemblance to the coplanarity pattern. The construction also works for any N. It is also possible to obtain error-bounds measuring the "near coplanarity" [4]. This topic is covered in Chapter **??**

Experiments on points selected from several twisted slabs simultaneously and performing similar construction showed that it is possible to determine the actual slabs from which the points were obtained or conversely can be fitted to. All this has important and interesting applications (USA patent # 5,631,982). Given a set of points composed of point clusters each from a different plane(or hyperplane) the determination of these planes can be made with very high accuracy and low computational complexity as shown in the second section of the last chapter on *Recent Results*.

1.5.4 Representation Mapping - Version II

$\mathcal{L}$et us revisit and update the representation mapping

$$\mathcal{J} : 2^{P^N} \rightarrow 2^{P^2} \times 2^{[1,2,\ldots,N]} , \tag{1.93}$$

in view of this chapter's results. The recursive construction starts with the **non-recursive step** for the representation of a point $P \in \mathbb{R}^N$, a 0-flat π^0, in terms of N points each with one index – the values of the coordinates p_i, $i \in [1, \ldots, N]$ of P on the $\bar{X}_i$ axes. For consistency, a point is also specified by the N equations

$$x_i = p_i \ , \ i = 1, \ldots, N \ . \tag{1.94}$$

The construction of a p-flat from its points (0-flats) to lines(1-flats) and so on proceeds according to Theorem 1.4.4 the dimensionality being raised by 1 until it reaches p providing the indexed points needed for the representation.

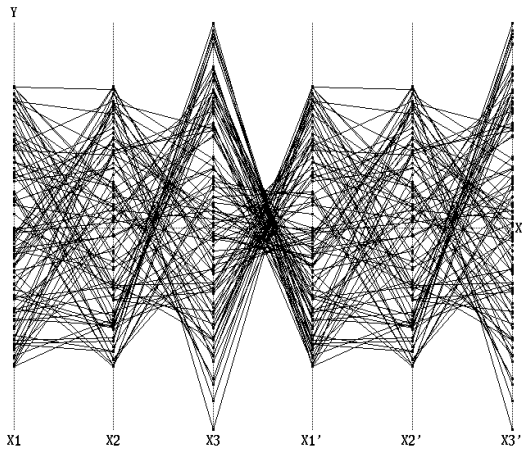

Figure 1.54: Polygonal lines representing a randomly selected set of "nearly" coplanar points.

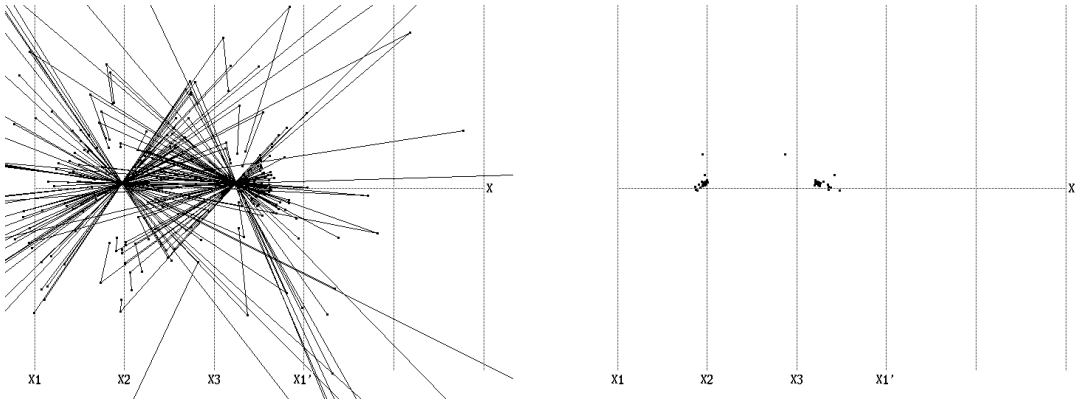

Figure 1.55: The "near-coplanarity" pattern.

On the left is very similar to that obtained for coplanarity with the points of intersection forming two clusters (right).

Let N_r be the number of points and n_r the number of indices appearing in the representation of a flat in $\mathbb{R}^N$ then for p-flat, $N_r = (N-p)p$, $n_r = p+1$ and

$$N_r + n_r = (N-p)p + (p+1) = -p^2 + p(N+1) + 1 \; . \tag{1.95}$$

In $\mathbb{R}^N$ some examples are

1. $p = 0$ — points $\pi^0 : \; N_r + n_r = N + 1$,
2. $p = 1$ — lines $\pi^1 : \; N_r + n_r = (N-1) + 2 = N + 1$,
3. $p = 2$ — 2-flats (2-planes) $\pi^2 : \; N_r + n_r = (N-2)2 + 3 = 2N - 1$,
4. $p = N-1$ — hyperplanes $N_r = N-1$, $n_r = N : \; N_r + n_r = N - 1 + N = 2N - 1$.

Note that eq. (1.95) does not include the case for $p = 0$ (points). In summary, the representation by points reveals that the object being represented is a p- flat whose dimensionality is one less than the number of indices used. The dimensionality of the space where the p-flat resides is, of course, equal to the number of parallel axes or it can also be found from the number of points $(N-p)p$ knowing the value of p.

We have seen that the image $\mathcal{I}(U) = \bar{U}$ of a $U \subset \mathbb{P}^N$ consists of several points each *indexed* by a subset of $[1, 2, ..., N]$; the indexing being an essential part of the representation. The mapping $\mathcal{I}$ provides a unique representation since it is one-to-one with $\bar{U_1} = \bar{U_2} \Leftrightarrow U_1 = U_2$. By representation is meant a *minimal* subset of points which uniquely identify the object in question for, as we have seen, there are lots of redundant points. The final version of the $\mathcal{J}$ is given in the conclusion after the representation of surfaces.

Index

References

[1] D. M. Bloom. *Linear Algebra and Geometry.* Cambridge University Press, Cambridge, 1979.

[2] J. Eickemeyer. *Visualizing p-flats in N-space using Parallel Coordinates.* Ph.D. Thesis, Dept. Comp. Sc., UCLA, 1992.

[3] A. Inselberg. *N-Dimensional Graphics, LASC Tech. Rep. G320-2711, 140 pages.* IBM, 1981.

[4] T. Matskewich, A. Inselberg, and M. Bercovier. *Approximated Planes in Parallel Coordinates.* Proc. of Geom. Model. Conf., St. Malo, Vanderbilt Univ. Press, 257-266, 2000.

[5] D. M. Y. Sommerville. *An Introduction to the Geometry of N Dimensions.* (First Publ. 1929), Dover Publications, New York, 1958.

[6] E. Wegman. Hyperdimensional data analysis using parallel coordinates. *J. Amer. Stat. Assoc.*, 85:664–675, 1990.